Hydrological simulation of the Bang Pakong River Basin using Soil and Water Assessment Tool

WITCHAYADA PRASERTSRI

A THESIS SUBMITTED IN PARTIAL FULFILLMENT OF
THE REQUIREMENTS FOR MASTER OF SCIENCE
IN GEOINFORMATICS
FACULTY OF GEOINFORMATICS
BURAPHA UNIVERSITY
2020

การศึกษาสภาพอุทกวิทยาของลุ่มน้ำบางปะกงโดยใช้แบบจำลอง Soil and Water Assessment Tool (SWAT)

วิชญาดา ประเสริฐศรี

วิทยานิพนธ์นี้เป็นส่วนหนึ่งของการศึกษาตามหลักสูตรวิทยาศาสตรมหาบัณฑิต
สาขาวิชาภูมิสารสนเทศศาสตร์
คณะภูมิสารสนเทศศาสตร์ มหาวิทยาลัยบูรพา
2563

Hydrological simulation of the Bang Pakong River Basin using Soil and Water Assessment Tool

WITCHAYADA PRASERTSRI

A THESIS SUBMITTED IN PARTIAL FULFILLMENT OF
THE REQUIREMENTS FOR MASTER OF SCIENCE
IN GEOINFORMATICS
FACULTY OF GEOINFORMATICS
BURAPHA UNIVERSITY
2020

The Thesis of Witchayada Prasertsri has been approved by the examining committee to be partial fulfillment of the requirements for the Master of Science in Geoinformatics of Burapha University

Advisory Committee

Principal advisor

.....
(Professor Xiaoling Chen)

Co-advisor

.....
(Associate Professor Jianzhong Lu)

Examining Committee

..... Principal examiner
(Professor Lingli Zhao)

..... Member
(Professor Timo Balz)

..... Member
(Lecturer Dr. Kitsanai Charoenjit)

..... Member
(Associate Professor Phattraporn Soytong)

Member
..... Dean of the Faculty of Geoinformatics
(Lecturer Dr. Kitsanai Charoenjit)
14 May 2021

This Thesis has been approved by Graduate School Burapha University to be partial fulfillment of the requirements for the Master of Science in Geoinformatics of Burapha University

..... Dean of Graduate School
(Associate Professor Dr. Nujjaree Chaimongkol)
8 June 2021

61910093: MAJOR: GEOINFORMATICS; M.Sc. (GEOINFORMATICS)

KEYWORDS: SWAT model, Hydrological model, SUFI-2, Sensitivity analysis, Streamflow simulating, Water resource management, Bang Pakong river basin

WITCHAYADA PRASERTSRI : HYDROLOGICAL SIMULATION OF THE BANG PAKONG RIVER BASIN USING SOIL AND WATER ASSESSMENT TOOL. ADVISORY COMMITTEE: XIAOLING CHEN, Ph.D., JIANZHONG LU, Ph.D. 2020.

Water is a fundamental priority in the planning and management of the resource. With the rapid economic and social development, freshwater resources have been used to fulfill the demands of socioeconomic growth without proper management. Anthropogenic activities lead to degradation and fast of the desolation of water resources. Also, it affects environmental aspects such as loss of soil fertility, soil degradation, water resources deposit of sediment, invasion, and deforestation. Increasing water demand for industrial and domestic water use in the basin increases the pressure on water resources. Abrupt and unpredictable depletion of freshwater brings the concerns of water resource management. Understanding watersheds are essential for interpreting water quality and stream health.

Bang Pakong river basin is an important river basin in Thailand located in the eastern part. It can be divided into two-part, Upper Prachinburi basin and Lower Bang Pakong basin, with drainage area 1,809,477.58 ha. Flow to the Gulf of Thailand and population 2,662,717. Bang Pakong river basin supports a large farming community, mainly involved in agroforestry, irrigated crops, livestock, fisheries, tourism, and a wide range of growing industries. It is rapidly industrializing with a high development level, and agriculture is still the most influential industry in the region. Without proper management of water resources, it will affect the economic, social, and resulting in extensive damage to properties and human lives. The watershed modelling simulating runoff is crucial for sustainable development. Because of this, the watershed is facing instant water scarcity and insufficient water management policy.

The Soil and Water assessment tools (SWAT) is a hydrological model, which has been used to simulate the runoff in the Bang Pakong river basin. SWAT is

a physically-based distributed model to predict the impact of land management practices on water, sediment, and agricultural chemical yield in the vast and complex watershed with varying soil, land use, and management condition. The objective of the research was to simulate Streamflow in the Bang Pakong river basin and to compare the model result and field observation (measure station) in the watershed.

SWAT model was used to test the performance of the model on Streamflow simulating using calibration and validation with daily observed data in the Bang Pakong river basin. All related data for the SWAT model are Digital Elevation Model (DEM) with 25 meters resolution, Land use map, soil map, river network, and historical of meteorological data: Precipitation, Maximum and minimum temperature, Wind speed, and Relative humidity. Combined with the input data, SWAT can estimate the surface runoff from HRUs by using the Soil Conservation Service (SCS) curve number method on the Green and Ampt infiltration method, which comprised of unique land use land cover, soil and slope, and estimating evapotranspiration with The Penman-Monteith method.

SWAT model was set up with a study period from 2009–2018. With a warm-up period from 2009-2010, the calibration period from 2011-2015. Model performance is adjudged base on visual comparison of the observed and simulated model as well as on statistical by using a coefficient of determination (R^2), the Nash-Sutcliffe efficiency (NSE), and percent BIAS (PBIAS). Additionally, ArcSWAT2012 and ArcGIS10.5, combined with Sequential Uncertainty Fitting-2(SUFI-2) algorithms in SWAT Calibration and Uncertainty Procedures (SWAT-CUP) programs was used for sensitivity analysis.

The result from the SWAT model indicates that the Bang Pakong river basin was divided into 17 sub-basins, with 99 Hydrological response units (HRUs), 16 Types of land use, 9 types of soil series, and 5 different range of percentage slope. For sensitivity analysis in SWAT-CUP showed that the most five parameters were sensitive to the simulation of Streamflow were: the Initial Soil Conservation Series runoff curve number for moisture condition II (CN2), the Effective hydraulic conductivity in main channel alluvium (CH_K2), the saturated hydraulic conductivity

(SOL_K), the Manning ‘n’ value for the main channel (CH_N2) and the soil evaporation compensation factor (ESCO), respectively.

The statistical comparison of calibration results with the observed data in KGT3 and KGT9 indicated that there is a reasonable agreement for both daily and monthly determination by using coefficient (R^2), the Nash-Sutcliffe coefficient (NSE), and PBIAS with the range: R^2 = 0.72 and 0.44, NSE = 0.72 and 0.42, and PBIAS = -12.7% and +32.8% for daily calibration, and R^2 = 0.82 and 0.57, NSE = 0.80 and 0.54, PBIAS = +16.2%, +14.2% for monthly calibration, respectively. Which can be acceptable statistically.

The validation results of the model show that there are a lower values of R^2, NSE, and PBIAS values, the reason are lacking of observed data. The R^2 = 0.42 and 0.29, NSE = 0.36 and 0.22, and PBIAS = +2.1%, +16.1% for daily validation, and R^2= 0.53 and 0.55, NSE = 0.45 and 0.30, PBIAS = +33.1% and +47.9% for monthly validation period, respectively.

The results of the rainfall-runoff SWAT model illustrated the average annual rainfall for eight years (2011-2018) as equivalent to 1596 MCM and the average annual runoff as 311.77 MCM. The highest runoff occurred in September, which resulted from rainfall event in the watershed area. The lowest runoff occurred in March, which lacking the rainfall. For the land-use simulation on runoff, the result showed that the watershed with sizeable agricultural land, which decreased runoff volume in the dry season. On the other hand, it has increased runoff volume in the wet season. The result of this research confirmed that the SWAT model was statistically acceptable and can be used effectively to simulate runoff in sub-watershed of the Bang Pakong River Basin.

ACKNOWLEDGEMENTS

Many people have made invaluable contributions, both directly and indirectly, to my research. I would like to express my warmest gratitude to Prof Dr.CHEN Xiaoling, my advisor, and Assoc Prof Dr.LU Jianzhong my Co-advisor, for his and her instructive suggestions and valuable comments on the writing of this dissertation. Without their invaluable help and generous encouragement, the present dissertation would not have been accomplished.

At the same time, I am very grateful to Dr. Kitsanai Charoenjit for providing me with valuable advice and suggestions for my dissertation.

I am express one's gratitude to the Faculty of Geoinformatics, Burapha University. For rewarding me a fully funded scholarship to achieve my master's degree.

I also wish to thank my friend SCGI Batch one, who taught me a lot of knowledge and offered me a lot of help.

What's more, I gratefully thank the anonymous reviewers for their valuable suggestions for improving my papers, which made me keep moving.

I would like to thank my boyfriend, Bew Pongthep, for being so supportive while I was working on my thesis. Thanks for many constructive suggestions. Thanks for your emotional support for being so understanding and for being such a great friend.

Finally, I greatly appreciate the support and endless love of my family. Thank you to my Mom and Dad and to my sisters, Zezar. Thanks for your understanding, your never-ending encouragement, and for always being there for me. They have always been helping me out of difficulties and supporting without a word of complaint. My heart swells with gratitude to all the people who helped me.

Witchayada Prasertsri

TABLE OF CONTENTS

Page

LIST OF TABLES

Page

LIST OF FIGURES

Page

LIST OF ACRONYMS AND ABBREVIATIONS

BPRB	**:**	Bang Pakong River Basin
BPR	**:**	Bang Pakong River
EEC	**:**	Eastern Economic Corridor
SWAT	**:**	Soil and Water Assessment Tool
USGS	**:**	United States Geological Survey
GIS	**:**	Geographical Information Systems
HRUs	**:**	Hydrologic Response Units
DEM	**:**	Digital Elevation Model
DSMW	**:**	Digital Soil Map of the World
FAO	**:**	Food and Agriculture Organizations
RID	**:**	Royal Irrigation Department
DWR	**:**	Department of Water Resource
TMD	**:**	Thai Meteorological Department
%	**:**	Percent
^{o}C	**:**	Degree Celsius
hr		Hour (s)
min	**:**	Minute (s)
km	**:**	Kilometer (s)
km^2 or sq.km.	**:**	Square kilometers (s)
m^2	**:**	Square meter
m^3	**:**	Cubic meter (s)
cms or m^3/s	**:**	Cubic meter (s) per second
m	**:**	Meter
mm	**:**	Millimeter
MCM	**:**	Million cubic meter (s)
T	**:**	Ton
NSE	**:**	Nash-Sutcliffe Efficiency
R^2	**:**	Coefficient of Determination
PBIAS	**:**	Percent Bias

CHAPTER 1
INTRODUCTION

Water is a fundamental priority in resource planning and management. Water becomes an essential factor for economic growth along with boosting agriculture and industry, particularly in the aspect of a rapidly growing population and urbanization (Ghoraba, 2015).

Expansion of economically and socially proliferating, the freshwater resource was used to fulfill the demands of socioeconomic growth. Without proper management, it was putting constant pressure on a freshwater resource. Anthropogenic activities lead to degradation and fast of the desolation of water resources. Also, it affects environmental aspects such as loss of soil fertility, soil degradation, water resources deposit of sediment, invasion, and deforestation.

Increasing water demand for industrial and domestic water use in the basin increases the pressure on water resources. Abrupt and unpredictable depletion of freshwater brings the concerns of water resource management. Therefore, understanding watersheds are essential for interpreting water quality and stream health.

Nowadays, Watersheds were impacted by many multitudes of variables such as climate, hydrology, geomorphology, soils, and land cover. Watersheds are diverse and are often evaluated by looking into river characteristics, such as sediment load (Hazbavi & Sadeghi, 2017) and water quality (Kim & An, 2015), (Jabbar & Grote, 2019). Therefore, adapted hydrological models can play a vital in water resource sustainable management and decision making (K. C. Abbaspour et al., 2015).

This study was focusing on the Bang Pakong river basin, a major part of Eastern Economic Corridor (EEC). The Megaproject under the scheme of the Thailand Government, which being potentially planned to develop for substantial economies in Asia. The hydrological model was used because of the Bang Pakong river basin is gathering instant water scarcity and insufficient water management policy. Moreover, there have a few of a study with SWAT in this river basin.

The simulation of hydrological models is often used to variations in the Hydrology cycle. The Soil and Water Assessment Tool (SWAT) was applied in the Bang Pakong River Basin. SWAT is a useful model and universally used for future prediction and alternative scenario assessment. The model can simulate hydrological processes such as surface runoff, percolation, and groundwater flow (Arnold, Srinivasan, Muttiah, & Williams, 1998). The input and outputs data from the model are processed through a GIS interface. The utilizes interface in the SWAT model is amicable and accessible by the user to develop improvement using source code and model documentation (Ouessar et al., 2009), (Neitsch, Arnold, Kiniry, & Williams, 2005).

In recent decades, Various of a watershed and hydrological assessment methods have been developed to evaluate the effects of anthropogenic activities on a watershed condition (i.e., watershed assessments or analyses). SWAT model was developed for watershed assessment, such as the impact of land use changes on the watershed (Bateni, Fakheran, & Soffianian, 2013), (Deshmukh & Singh, 2016), (Peraza-Castro, Ruiz-Romera, Meaurio, Sauvage, & Sánchez-Pérez, 2018), the effect of climate change (Fan & Shibata, 2015), (Neupane & Kumar, 2015), and susceptibility to hydrologic alterations (Pyron & Neumann, 2008), (Marcarelli, Kirk, & Baxter, 2010).

This study will analyze the characteristics of geography, meteorology, and also to simulate streamflow of hydrology system in Bang Pakong river basin. As a guideline for both current and future water resources allocation planning. The study will use SWAT programs as tools in modelling the current situation of the watershed. The models are set to look for the most efficient water allocation scheme, which will be used as a guideline for support agricultural and water management in the watershed.

1.1 Problem Statement

The effect of climate change is the change in local and regional water availability since the climate system is part of the hydrologic cycle. These effects include the magnitude and runoff timing, the frequency and intensity of floods,

droughts, patterns of rainfall, extreme weather events and available water quality and quantity.

In the Bang Pakong River Basin, different kinds of floods have been occurring every year. The climate is a tropical zone which is subject to the influences of monsoons and tropical hurricanes. When a flood occurs, water in the river rises fastens, exceeding the retaining limit of the water resources, causing a sudden flood, coupled with the diversion of water from Thailand's central region and the Bangkok metropolitan area increasing flood-risks and erosion of riverbanks. Some factors are humanmade, the ill conduct of land use, the lack of appropriate land use management, and increasing deforestation of the natural water retaining resources.

Due to the climate change situation caused severe affected to the agricultural sector in the Bang Pakong river basin, especially farmers, the shorter period of rainfall means a long period of drought coupled with higher temperatures leading the droughts situation more intensive. It also affects the long-term period of the river and groundwater levels. Therefore, drought problems in the watershed are becoming more frequent severe when combined with increased water demand, resulting in normal living and destruction of ecological and environmental systems. Besides of natural phenomena is the leading cause of drought, the environmental change and imbalances of ecology system such as deforestation are also the significant factor for drought in the Bang Pakong River Basin.

The seawater intrusion is another problem that usually occurs in Bang Pakong river basin during the dry season. Seawater has been able to reach into the Bang Pakong river as far as 200 km to Sri Mahabhodi District in Prachinburi Province. It happened in seaside lands with flat topography where the flow rate in the river is low and accompanied by intensive use of upstream. Moreover, it is also caused by the lack of freshwater stock or ecosystem-fuel water to push out the seawater.

The Bang Pakong River Basin supports a large farming community, mainly involved in agroforestry, irrigated crops, livestock, fisheries, tourism, and a wide range of growing industries. Though Bang Pakong is rapidly industrializing with a high

development level, agriculture is still the most influential industry in the region. Without proper management of water resources, it will affect the economic, social, and resulting in extensive damage to properties and human lives.

The SWAT model was used to respond to the objectives in this study, By simulating the runoff in the Bang Pakong river basin. The output on sensitivity analysis, comparison between observed and predicted data in model calibration and model validation are critical factors in decreasing uncertainty output and increasing user determination in model abilities.

The goal of this thesis is to understand the relationships between hydrological processes, physical characteristics such as land use, soil and climate change which are essential for watershed management design. The results of this study can be used as a guideline to deal with the future climate and land use change to support agriculture sector and increase the capacity in planning and formulating strategies for water resources management to become the most appropriate and effective in various activities in the watershed, but more importantly, considering that they are able to produce effective models to represent historical data collected from the Bang Pakong River Basin.

1.2 Research objectives

The main objectives of the research are to simulation monthly and daily streamflow in the Bang Pakong river basin by making use of the SWAT (Soil and Water Assessment Tool) model. The specific objectives of this project are:

(1) Evaluating the performance of the SWAT model in the simulation of Streamflow in the Bang Pakong river basin.

(2) Developing the model calibrated and validated using SWAT-CUP.

(3) Integrating the SWAT model to the existing interface with the GIS application for sustainable water resources management.

1.3 Limitations

Several limitations introduced during this study. The limitations were the spatial variability associated with topography. There are extreme flattenings in the lower part of the Bang Pakong river basin, which was an effect on Watershed Delineator processed in the SWAT model. The input data as soil series data were of low quality. The lack of Meteorological data in a short period. The daily streamflow record is not continuous data and available only for a short period, which caused the calibration process very difficult. Most of the observed station cover in the upstream of the watershed, which decreases the reliable of the model in downstream. Furthermore, most of the observed station in Bang Pakong river basin is a newly installed station, which being nonrecorded available streamflow data in the period of the study.

1.4 Scope of Research Work

This research is the simulating and evaluating of rainfall-runoff by using GIS applications along with Hydrologic modelling. Figure 1 shows the location of the Bang Pakong river basin situated in the southeast of the Bangkok metropolitan and connected to the Gulf of Thailand. The coordination of Bang Pakong river basin lies between east longitude 100° 52' and 102° 33' and between north latitudes 13° 02' and 14° 32' N. With a total catchment area around 18,087 km^2. The topography condition with the high mountain range in the north part that divides from Nakorn Ratchasima province to Prachin Buri and Nakhon Nayok province. Furthermore, a high mountain range in the south part that originated a river of Bang Pakong basin.

One of the four main rivers in Thailand is the Bang Pakong River. It originated at the Nakhon Nayok and Prachin Buri rivers, which flow through Chachoengsao province, and finally ending journey in the Gulf of Thailand with river length approximately 240 kilometers (Department of Water, 2017).

The general aim of this research is to simulate the Streamflow in the Bang Pakong river basin. The data which are used to study is about ten years in the past, based on the year 2009. The SWAT model is conducted on a daily time scale to gain insights into the historical climate change in the Bang Pakong river basin. The

understanding of the total Streamflow, land use, soil, and climate with their relationship is essential to design the river management in the Bang Pakong watershed. By integrating the SWAT model with GIS application for sustainable water resources management. The results of the study can be used as a guideline to support the agriculture sector, adaptation for water resource management policy, and provide a flood prediction in future at the Bang Pakong river basin.

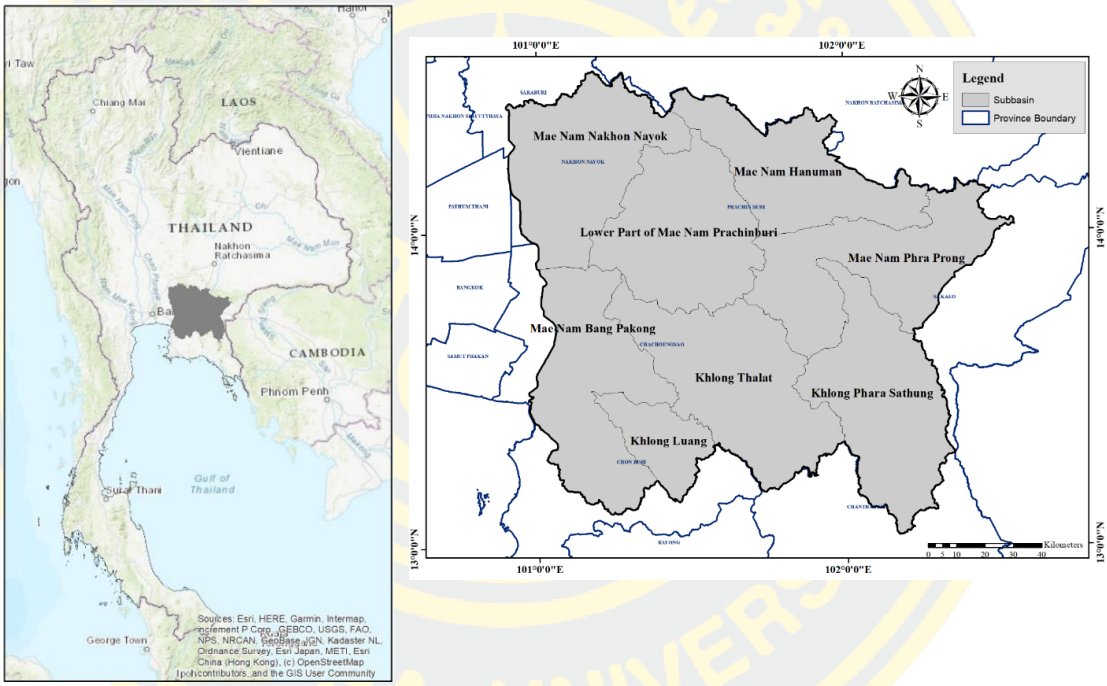

Figure 1 The boundary of the Bang Pakong River Basin

1.5 Thesis structure

This study aims to simulate the rainfall-runoff for the Bang Pakong River Basin in Thailand. This thesis is separate into five chapters. Chapter 1 presents the overview of the water resource in Thailand, the general background of the study, the problem statement, the objectives of the research, characteristics of the study area, and the limitations of the study. Chapter 2 contains a literature review in the water cycle, a

hydrological model for runoff simulation, and related to the previous research. In Chapter 3 will describe the data in use, methodology, and the process of the whole research. Chapter 4 contains the experiment result, the results of calibration and validation in the hydrologic model, and sensitivity analysis of the study area. Finally, Chapter 5 is a summary of the dissertation, including general conclusions and suggestions for future research in this regard.

CHAPTER 2
THEORIES AND LITERATURE REVIEW

The literature review in this chapter consists of five-part, i.e., Hydrologic Cycle, Hydrologic Regimes in the tropical zone, Hydrologic modelling, Physical Characteristics of a watershed, and the relevant researches for SWAT model.

2.1 The hydrologic Cycle

The hydrological cycle, as well as the water cycle. It appears and reprocesses the water cycle on Earth. Water can change the state of liquid, vapor, or ice at various places in the water cycle (Michael, 2006). The balance of water on the land is stable. Nevertheless, each type of water molecules can enter and exit through the atmosphere. Water will be confined to the reservoir and spread to others, such as the flow from rivers to oceans or evaporating from the oceans through the atmosphere by physical processes.

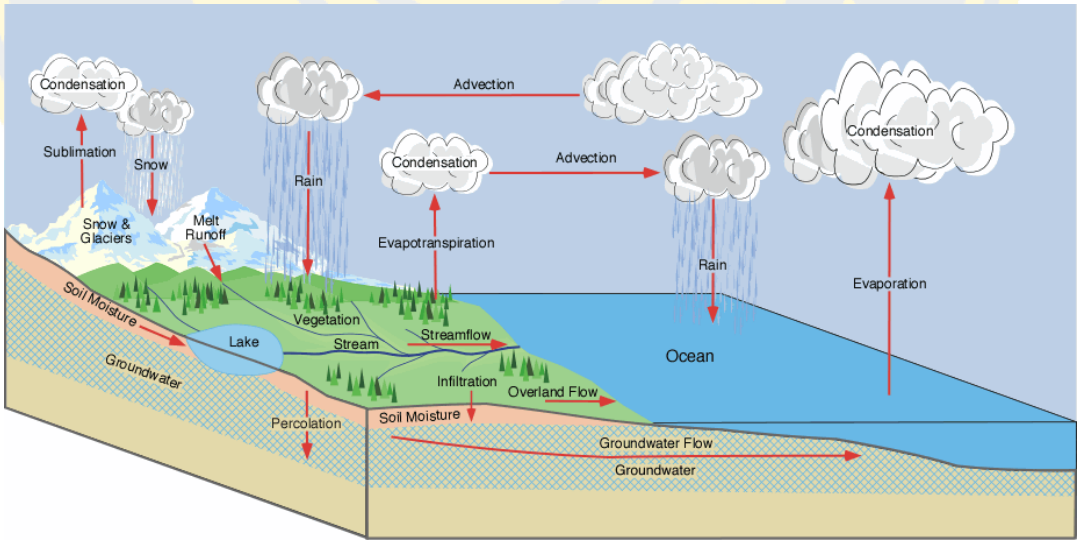

Figure 2 Concept of Hydrologic Cycle.

2.2 Hydrological regimes in tropical zones

In the tropical zones, the water obtained by sedimentation during the rainy season or seeped into groundwater and flowed out into the river in the summer season. The physicals process on water cycle includes steps of evaporation, atmospheric water retention, accelerating surface flow, and emission into the ocean. Water cycles and climate conditions form the watersheds of the hydrology system can determine seasonal and daily flow patterns (Sendzimir & Schmutz, 2018).

Rivers characterized in the tropical zone have various flow cycles linked by seasons in a particular area. Tropical regimes are similar to pluvial regimes, such as droughts in summer and abundant rainfall during the rainy season (Figure 3). The observed streamflow can perform a mixture of the hydrology system. Depend on the topical conditions and location in the catchment.

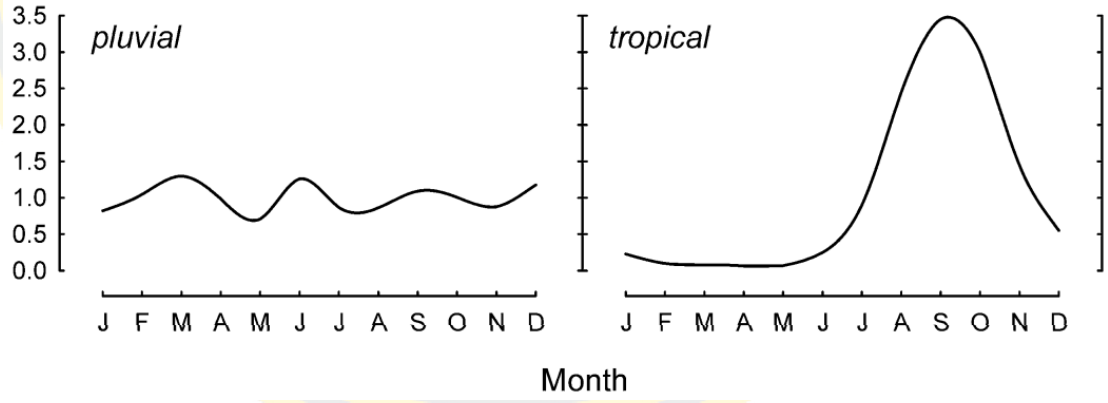

Figure 3 Simple hydrology regime (pluvial and tropical) with the monthly discharge coefficient (cm) and determined by the ratio of the average monthly discharge.

A catchment is a hydrological unit that is defined as an area of internal water collection within a drainage or basin division. Catchments lumped gathered from the tributaries into a river to become a watershed. The water balance in a given catchment

or basin is calculated from rainfall, evaporation, and runoff, including storage stages such as soil, groundwater, ice, and snow. Moreover, the release observed in the catchment is determined by meteorological and biophysical factors.

Streamflow can determine the dynamics of the river system in four dimensions (Poff & Ward, 1989). Transport of nutrients and sediment is linked with the longitudinal flow. Furthermore, floodplain depends on the connection of hydrology and flood pulses.

Streamflow vary by time, such as in hours, days, seasons, years, and longer scenarios (Poff et al., 1997). For numerous years, Streamflow from observing gauge must show the characteristics of flow volume, time, and river fluctuations. The physical geographic such as climate, geology, topography, and vegetation cover that effect on river flow by showing the regional trends based on the size of the river.

The natural flow instance is widely accepted. It consists of five components of variation: magnitude, frequency, duration, time, and rate of change. All components can be used to identify flow currents and hydrological phenomena, such as floods, which are extremely important to the integrity of the river.

2.3 Hydrological Model

Watershed models are mathematical can representations of hydrologic processes and affected socioeconomic and environmental systems (Mirchi, Madani, Watkins, & Ahmad, 2012). The purpose of a model is to simplify the actual watershed processes.

Understanding the natural processes and human activities require a relevant and reliable hydrologic process. Many mathematical models and apparent relationships have been developed in recent decades. Hydrological models are simplifications of reality by representing of the hydrologic cycle, which is primarily used for hydrologic forecasting and hydrologic process understanding. These models try to physical processes found in the real world. Usually, such as models representations of surface runoff, sub-surface flow, evaporation, evaporation, and channel flow, which being

more complicated. The purpose is to simulate the necessary hydrological variables of the rainfall-runoff as well as the interaction in water systems (Borah & Bera, 2004), (Nash & Sutcliffe, 1970), (Srinivasan, Gorelick, & Goulder, 2010). The model is supported by available documentation (Arnold et al., 2012), Multiple geographic information systems (GIS), and support as an interface tool (Di Luzio, Arnold, & Srinivasan, 2004),(Olivera et al., 2006).

2.3.1 Soil and Water Assessment Tool

The Soil and Water Assessment Tool (SWAT) is the Rainfall-Runoff (R-R model) that determines the water flow, which leaves the watershed area from precipitation. It is often applied to the problems only relating water quantities, real-time flood forecasting, and assessment of the sufficiency of natural water resources.

In the runoff process, there is a temporary dependency between rainfall and runoff, which are variables for specific hydrological systems. Temporary dependency can be explained using linear system models. The general characteristics of most R-R models are divided into catchments into many zones. Their simple structure is shown in Figure 4. The main structure is precipitation, evaporation (including interception), direct runoff, runoff in unsaturated areas (interflow), base flow and channel flow.

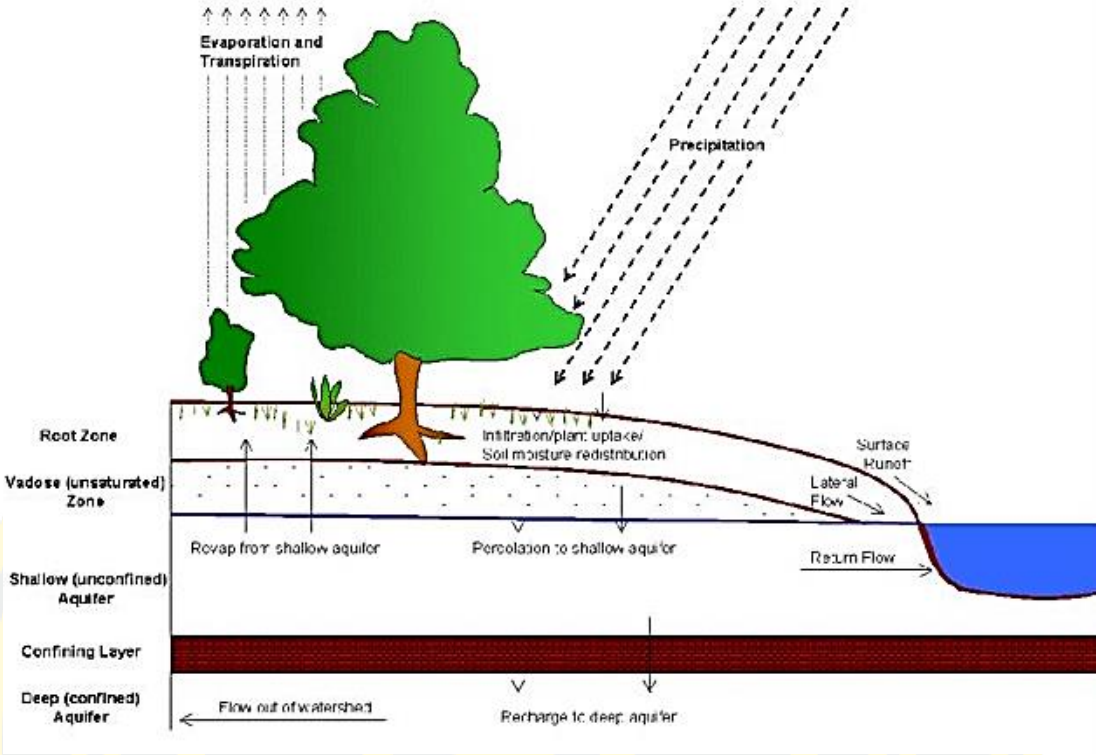

Figure 4 Schematic of the hydrologic cycle and SWAT simulation processes.

For the computation processes that operate in each of these reservoirs, the precipitation will be entered into the model in the time-series data from the meteorological station. Evaporation and interception are calculated from the time-series from the meteorological station depended on the availability of the data. The most frequently used methods are hydrographic units and various modifications. Sub-ground flow in unsaturated zones is the most crucial component of the baseflow concentration, depending on the connected model. Water control facilities are also possible for the reservoir control model in the calibration of the model (Spinosa, 2015). The values of the parameters the model are selected. Therefore, the model may simulate hydrology behavior that the true nature of water retention (Madsen, 2000).

The SWAT is a continuous-time, semi-distributed model design to a simulation of runoff, sediment yield, and agricultural chemical transport on complicated conditions (Arnold et al., 1998). The model was developed by the United States Department of Agriculture (USDA) - Agricultural Research Services (ARS)

(Neitsch et al., 2005). This model is derived from the combination of Water Resources in Rural Basin (SWRRB) (Williams, Trumbly, MacColl, Trimble, & Maley, 1985), (Arnold, 1990). The objectives of developing the SWRRB model is to predict the effect of water and sediment management decisions with plausible accuracy for ungauged rural basins throughout the United States (Arnold & Williams, 1987). Hence, SWAT is adopted to model the water resources of a watershed. The hydrologic process of SWAT model version 2012 ArcSWAT 2012.10.5 was used in this research (http://swatmodel.tamu.edu/software/arcswat).

2.4 Physical Characteristics of a watershed

2.4.1 Land use

Land use plays a vital role in creating different watershed systems for each area. The complete forest area will cause less surface flow. However, causing more rain to disappear due to increased retention and water retention around plant roots. Another in the urban area that covers the resistance area has more surface flow and fast flow rate (Heuvelmans, Garcia-Qujano, Muys, Feyen, & Coppin, 2005).

Remote sensing applications and geological information technology are used to estimate runoff using the method of Curve Service Conservation Service Curve (SCS-CN). They found that land use in urban areas increased. (1990, 1995 and 2000), while agricultural areas decreased, resulting in a bias in runoff (K. S. Tan, Chiew, Grayson, Scanlon, & Siriwardena, 2005). Moreover, increasing forest areas reduced flow and surface water (Weber, Fohrer, & Möller, 2001). However, the below increases relatively (Fohrer, Eckhardt, Haverkamp, & Frede, 2001). Increasing agricultural land-use changes have increased surface water content (Lenhart, Fohrer, & Frede, 2003). Most of the watershed areas are land use for Agriculture, and grassland areas have a small impact on surface water (Huisman, Breuer, & Frede, 2004). It is important that soil and water conservation regulations provide river basin management and to maintain water balance (Behera & Panda, 2006).

2.4.2 Geographic Information System Based Component

GIS is a computer system competent in collecting, storing, editing, analyzing, sharing, and displaying geographic references. At present, GIS is not limited to mapping. However, it involves activities such as scientific investigations, natural resource management, environmental impact assessment (EIA), and others (Peng & Tsou, 2003). GIS data sets for some catchment are considered to compare the results using the GIS method, namely Data collection, to display all geographic references in the GIS map format. Working on multiple layers. These layers can be superimposed to understand better how they work together.

In GIS, different geographic features are represented by different types of geometries, by dividing into three categories as follows: (1) Points used for geographic properties that represent positions such as village locations, (2) Lines or polylines used for linear properties such as rivers, roads, railways, and (3) Polygons Used for geography that covers specific areas of the Earth's surface, such as provinces, areas, lakes.

2.5 The relevant researches for SWAT model

SWAT was created in the 1990s, and after that SWAT has been continuously reviewed with expanding capabilities and extensive validation. The interface of the model has been developed in many interfaces such as Windows (Visual Basic), GRASS, and ArcGIS.

The global SWAT application present that it is a multipurpose model by combining a variety of environmental procedures to encourage watershed management and development more efficiently for policy decisions. SWAT is a very flexible, robust, and powerful tool to simulate various watershed problems. The applications of SWAT model trends to emerge in Europe and other countries (Arnold & Fohrer, 2005).

Used SWAT model to predict the future basin health, especially in ungauged basins. SWAT are increasingly used to predict sediment yield (Z. X. Xu, Pang, Liu, & Li, 2009), (Liu, Yang, Yu, Lung, & Gharabaghi, 2015) and nutrient loadings (Hanson,

Habicht, Daggupati, Srinivasan, & Faeth, 2017), (Malagó, Bouraoui, Vigiak, Grizzetti, & Pastori, 2017). Also, when comparing the calibration of the SWAT model with some models, SWAT will simulate the hydrological process more efficiently. For example, Studied the Polecat Creek Watershed in Virginia (Im, Brannan, Mostaghimi, & Kim, 2007), the obtain data from SWAT showed that it was highly appropriate to simulate water flow and sediment together with the Fortran (HSPF) models.

By using the SWAT model with Lake Tana basin for modelling a water balance (Setegn, Srinivasan, & Dargahi, 2008). The purpose is to examine the efficiency of the SWAT model in Streamflow predicting. SWAT is applied to the watershed to simulate daily and monthly flows. The author found that Streamflow is sensitive to HRU criteria than the subbasin discretization effect.

As shown by Jain et al. (Jain, Tyagi, & Singh, 2010), The efficiency of the SWAT model was affected by the resolution of the time series data set used in calibrating and validating the method. In general, this model works well with monthly data compared to daily data.

Successfully validated by SWAT model for streamflow and sediment yield estimating in the Lolab Basin (Gull, Ma, & Dar, 2017). The observed and simulated output are matched well, and the CN2 factor is the most sensitive parameters with four mostly sensitive parameters in the simulation of sediment yield.

Use the GIS and SWAT models for enforcement and suitability of the model to predict sediment yield in Nigeria (Daramola, Ekhwan, Mokhtar, Lam, & Adeogun, 2019). With a daily duration of 26 years using climate data, represented by three weather stations. Also, unavailability sediment data of observed, sediment samples are collected from three locations. The results show that satisfactory results can be achieved for predicting streamflow and sediments in the river basin.

Calibration and validation models are used with the SUFI-2 algorithm to predict Streamflow in the Xedone River Basin (Adeogun, Sule, & Salami, 2015). SUFI-2 provides good results for both daily and monthly simulations. For uncertainty analysis results, the 95% predictive uncertainty (95PPU) bracket is excellent with observed

runoff data. The uncertainty streamflow is captured with a bracketing value greater than 65%.

Use the SWAT model for a tropical basin in Maybar, Ethiopia (Yesuf, Melesse, Zeleke, & Alamirew, 2016). For the uncertainty analysis of predictions by calibrating and validating with monthly observed streamflow data. The goodness that compared in SWAT model is the uncertainty assessed by P-factor and R-factor using SUFI-2 and GLUE algorithms. Statistics show an acceptable between Coefficient of Determination, Nash–Sutcliffe efficiency, Percent Bias, and Root Mean Square Error-observations, Standard deviation Ratio for both calibration and validation. The period was made, the amount and extent of the similarity between predictive data and the recording of streamflow recommendations.

As shown by Zhang et al. (Zhang et al., 2017) is applied SWAT model with estimated Streamflow in the ungauged zone. By coupling the hydrological model and the hydrodynamic model. They created two hydrodynamics scenarios using the Delft3D model and calibrating output from the SWAT model with the ungauged station. The results show that there are a strong relationship and lower bias (R^2 = 0.81, PBIAS = 10.00%). This method can be used in other areas that do not have observation areas.

Conduct the SWAT model for streamflow and sediment yield modelling using the Uncertainty Program (SUFI-2) for sensitivity analysis in the Thika River (Gathagu, Mutua, Mourad, & Oduor, 2018). Data streams have been calibrated and validate with two gauging stations. Furthermore, the manual calibration of the sediment is done by limiting the MUSLE parameter by using the bathymetric survey data. Indices with p and r factors, statistical performance indicators show a matching in observed values and simulated values.

2.5.1 Hydrological modelling in Southeast Asia

Most of the SWAT models are used to study hydrology in Southeast Asia with an emphasis on application. The model's ability, land use change assessment, and climate change are the main objectives of SWAT applications that are reported for the region (M. L. Tan, Samat, Chan, Lee, & Li, 2019). Generally, model calibration and

validation are classified in a satisfactory range for excellent results based on widely-accepted performance indicators such as:

As seen in Alibuyong et al. (Alibuyog et al., 2008) have conducted SWAT model in Manupali Sub-Basin, Philippines. Aiming to estimated runoff and sediment. The analysis based on different land-use scenarios. They found that significant changes in sediment yields occurred (200% -273%) compared to runoff (3% -14%).

As shown by Tan et al. (M. L. Tan, Ibrahim, Duan, Cracknell, & Chaplot, 2015) examined how climate change may affect Streamflow, and the data is validated with long-term rainfall data with six GCMs. The best performance has been chosen as a good calibration input in the SWAT model (NSE = 0.62 for validation). The future Streamflow will decrease in the summer season and increased in the rainy season.

Sunandar, Suhendang, and Nengah (Dany Sunandar, Suhendang, & Nengah Surati Jaya, 2014) have shown SWAT models in the Asahan Basin of Indonesia to identify the greatest appropriate land use management, which will reduce the amount of sediment without affecting water yields. The development was carried out using the linear program and query methods with limited land use conditions. They found that the ideal situation could be reached by increasing forestry and arable land and reducing farmland.

According to Tarigan et al. (Tarigan, Wiegand, & Slamet, 2018) indicated that at least 30% of forestry areas need to be prevented so that watersheds can provide sustainable ecosystem services. Land use change and climate change assessment have an impact on the variability of hydrology.

As demonstrated in Xu and Chua (M. Xu & Chua, 2017) coupled the SWAT model and the hydrodynamics model called SUNTANS to simulate the transport of three-dimensional land-based pollutants in Singapore. For the result, they only report the hydrological calibration and validation experiment based on the streamflow data.

As seen in Son, Huong, and Phoung (Son, Le Huong, Phuong, & Loc, 2020), To assess the impact of land use and climate change on the hydrological processes in

Nam Rom Basin, Vietnam. The results indicated that climate change leads to a significant reduction of all hydrological components. Furthermore, surface flows are sensitive to future land use and climate change.

2.5.2 Application of SWAT model in Thailand

Thailand is located in the center of Southeast Asia (SEA). With tropical monsoon climate and topographical features that affect the distribution of rainfall. Thailand comprises several distinct geographic regions. It can be divided into two broad geographic areas: the main section with a substantial in the north and a small peninsula extension in the south. along with the hilly forest areas of the northern border, the rice fields in the central region, the vast plains in the northeast and the rugged coastline along the narrow southern peninsula. Due to the nature of drainage areas in Thailand, SWAT is widely used in all parts of the country, such as:

Ruangsang, Kanwar, and Srisuk (Reungsang, Kanwar Rameshwar, & Srisuk, 2010) have shown the study of SWAT model in Chi river basin, northeast of Thailand. For the streamflow model simulation, the results show that the statistical similitude between the measured data and model output shows a good relationship as well as other researchers in the same location (Wankrua, Kangrang, & Sriwanpheng, 2017), (Kheereemangkla, Shrestha, Shrestha, & Jourdain, 2016), (Homdee, Pongput, & Kanae, 2011), (Arunyanart, Limsiri, & Uchaipichat, 2017).

Successfully Validated in sediment processes at Lam Sonthi Basin, Central of Thailand (Phomcha, Wirojanagud, Vangpaisal, & Thaveevouthti, 2011). Calibration and validation results are reliable. Although the model is evaluated using limited data, and some algorithms are not suitable for tropical conditions. Overall, the SWAT is sufficient to predict the monthly sediment for the alluvial basin.

Integrated GIS and SWAT to assess streamflow and soil erosion and simulate the streamflow and suspended sediment (Suwanlertcharoen, 2011). The results from SWAT model are compared with the observed data, collected by weir and sampling due to ungauged stations in the basin. The results found that statistics are acceptable. Furthermore, watersheds with large tracts of forests increase the amount of streamflow

in the summer season and reduced streamflow during the rainy season while suspended sediments will be reduced in both summer and rainy season.

Applied SWAT model to examine the application for modelling sediment and water quality parameters (Yasin & Clemente, 2012). Both sediment and water quality calibration not good enough the reason for lacking the time-series information.

According to Wuttichaikitcharoen et al. (Wuttichaikitcharoen, Plangoen, & Muangthong, 2016) do a runoff simulating in river basins. Sensitivity analysis and model calibration were created from 2005-2010, and the validation of the model was continuously stimulated. The results indicate that the most sensitive variables affecting the runoff simulation are CN2, SOL_AWC, and SOL_K. Model calibration and validation give promising results in R^2, NSE, and PBIAS.

As can be seen in (Faksomboon & Thangtham, 2017), estimate the amount of suspended sediment from land utilization. The reliability of the model is calibrated using SWAT-CUP. The results indicate that land use in various situations leads to a reduction of suspended sediment in the upper Thachin River Basin. SWAT can be used for conservation for land and forest restoration, especially upstream for sustainable natural resources.

As previously mentioned, (Faksomboon, Suanmali, Chaivino, Khamcharoen, & Buasruang, 2019) applies the SWAT model to study land use changes of a head watershed on streamflow, suspended sediment, and water quality in the Khlong Lan Basin (KLW). The reliability of the SWAT model was compared with the data observed using SWAT-CUP program when compared with different situations, the water content and average BOD increased. However, Suspended sediment decreases due to increased forest and crop areas, orchards, other areas, and urban areas.

By the way, (Sangkatananon, Chotamonsak, & Dhanasin, 2018) reported on the efficiency of the model for streamflow simulation in the Wang Basin. Experiment results indicate that the SWAT model is useful in runoff simulating, especially in non-dam sub-basins and Wang river endpoints. In the wet season, the model is more effective than the dry season.

According to the topography in the Bang Pakong River Basin. This region has a flat topography in lowland areas, which is suitable for rice and other agricultural activities but causes flooding easily. The topographical features that lie on the coast are plains, some of the plains are flooded by seawater. SWAT models are not used very often in this basin because of the Digital Elevation Model (DEM), which requires more resolution, as mention in (Chaubey, Cotter, Costello, & Soerens, 2005), (Azizian & Shokoohi, 2014), (M. L. Tan, Ficklin, et al., 2015), (Buakhao & Kangrang, 2016), and this basin has an unproductive water route for studying in the model.

As mention in (Sangmanee, Wattayakorn, & Sojisuporn, 2013), the SWAT has been used for climate change predicting discharge and sediment loads in Bang Pakong Basin. The model experiment indicates that the model release forecast is considered an excellent match in the calibration and validation period. The changes in future precipitation may affect coastal areas and natural ecosystems, such as wetlands, as well as the economy of agriculture, fisheries, and other sectors, depending on water availability.

On the other hand, the challenge for this study is to understand the hydrology process in the Bang Pakong Basin for water management policies in limitation of the input data in the SWAT model.

CHAPTER 3
MATERIALS AND METHODS

3.1 Materials

The SWAT model has been chosen as a hydrological model to establish runoff at the basin scale. The model is initialized using the Hydrologic Response Units (HRU) option, which is an important option based on GIS digital elevation data, land use maps, and soil maps.

In this study, SWAT2012.10 was used to achieve the objectives. The model works in ArcGIS which require support for other software and software required for the purpose include:

1. Computer laptop
2. Microsoft Windows 10 (64-bit operating system)
3. ArcGIS 10.5.1
4. ArcGIS Spatial Analyst 10.5.1
5. ArcGIS Dot net support
6. SWAT-CUP2019 version 5.2.1.1
7. Microsoft .Net Framework 4.5
8. Adobe Acrobat Reader Version 8 or higher

3.2 General Background of Study area

Bang Pakong river basin consists of the lower Bang Pakong Basin and upper Prachinburi Basin, which has a drainage area of 8,443 km^2 and 9,651 km^2, respectively. The upper part of the Prachin Buri River is situated in a mountainous range. Beneath the mountains shows a flat landscape in a low waterlogged lowland suitable for rice and agricultural activities with a large amount of water in the rainy season and tends to be dry in the dry season. The lower part of Bang Pakong is the estuary, which has a brackish water ecosystem that reaches up to the river around 120 kilometers upstream in the summer season when the freshwater is released (Department of Water, 2006).

Bang Pakong watershed supports the livelihood of communities related to agroforestry, and fishery. Watersheds consist of mixed land use, ranging from rice in the rainy and dry season, perennials plants, rubber, wetlands, and tropical forests. The area settled in the river basin consists of villages that have gardens and mixed orchards.

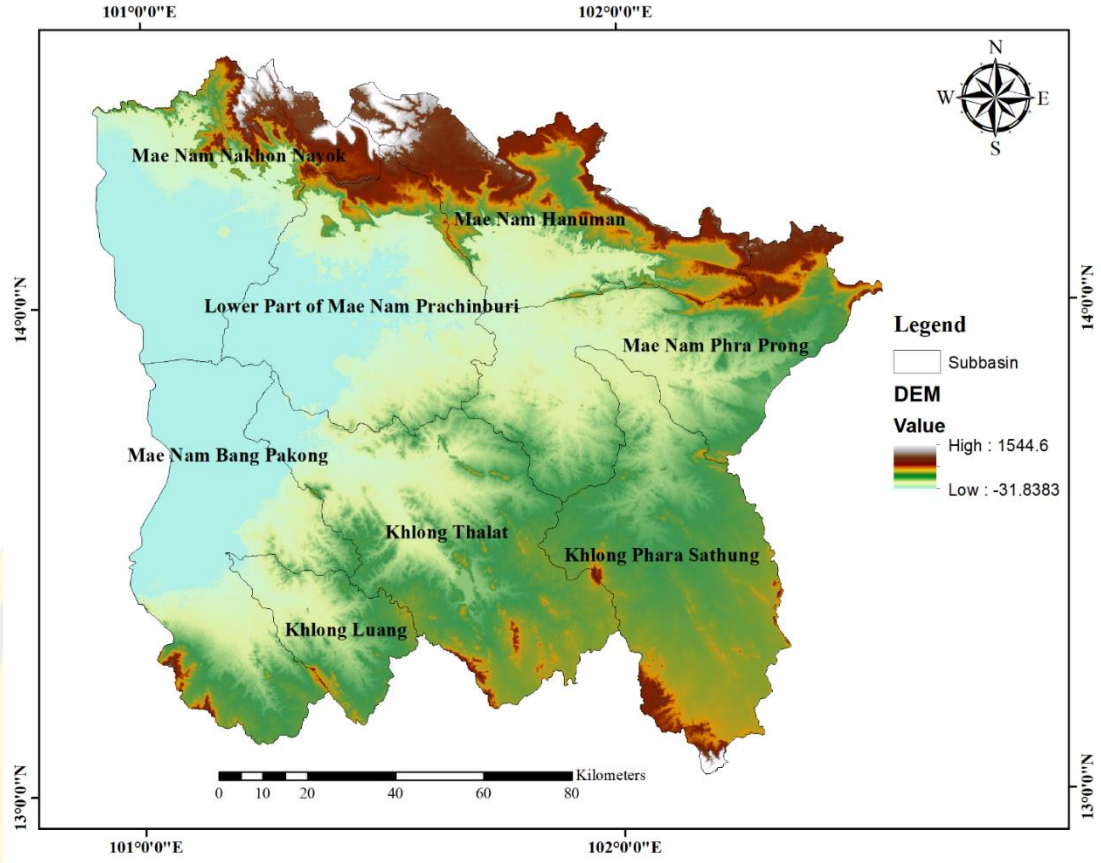

Figure 5 Subbasin in Bang Pakong watershed

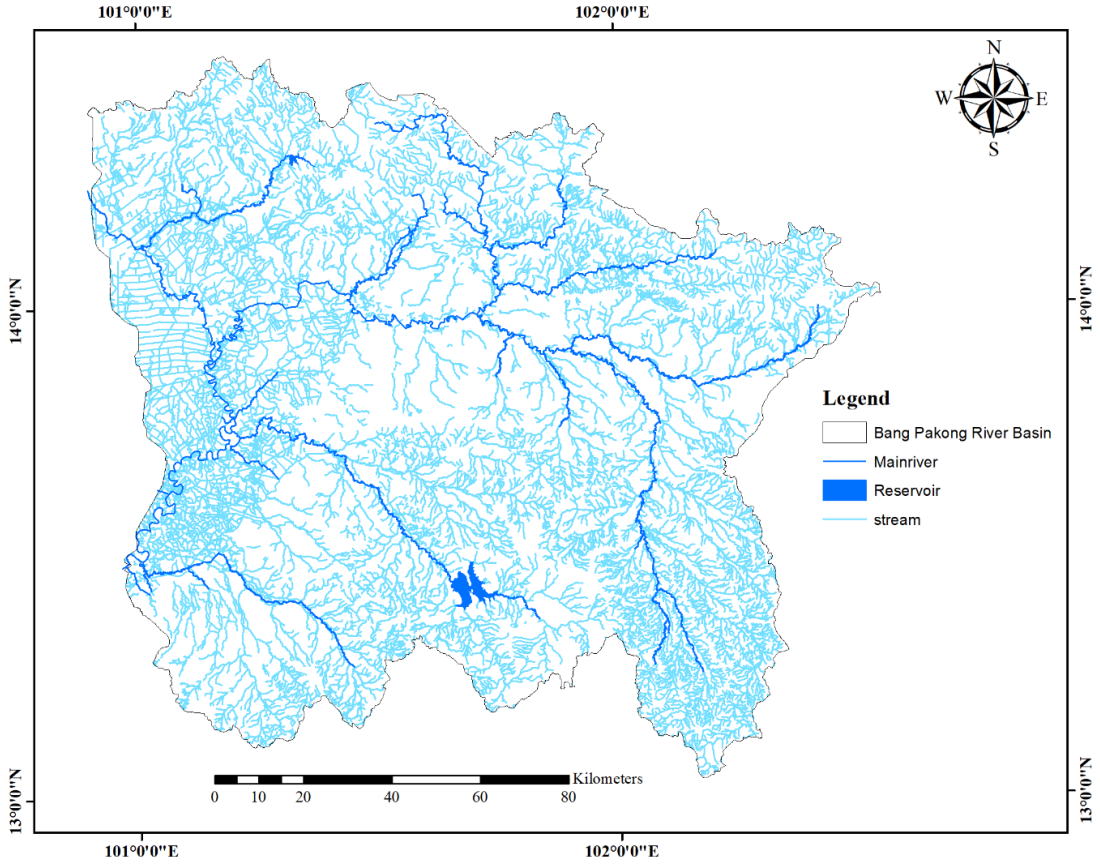

Figure 6 River network in Bang Pakong river basin

The climate in the Bang Pakong Basin is tropical monsoon with northeast monsoons during the dry season from November to April. Furthermore, the southwest monsoon in the rainy season from May to October, the watershed receives an average rainfall of 1,000-2,000 mm per year, most of which falls seasonally, with only 10% of the rainfall occurring during the dry season. According to climate data, from 2009 to 2018, the watersheds had the highest temperatures in April, with an average monthly temperature of 33.37 °C and the lowest temperature in December with a monthly average temperature of 25.35 ° C. Water shortages will be a problem during the dry season. In case there is not enough freshwater to pushing the seawater, which being freshwater unsuitable for cultivation and consumption.

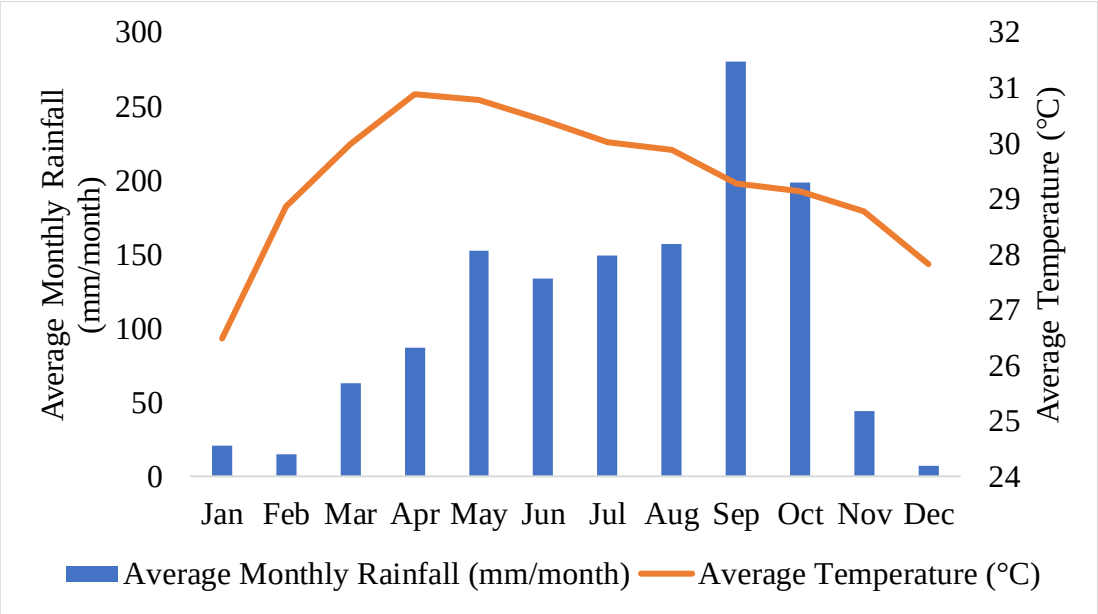

Figure 7 Average rainfall and temperature in the Bang Pakong river basin

3.3 Model Development

SWAT model was created to study watershed characterize the hydrological processes with GIS technology. The ArcGIS interface ArcSWAT used to prepare the SWAT model input data from spatial datasets. The overall methodology in this research as shown in Figure 8.

All the data required for the simulation are summarized individually. For ArcSWAT, most of the data obtained from government sources, reports, and their measurement campaigns. The model was run with ten years of weather data set from 2009-2018 for the warm-up period chosen between 2009-2010. The period data for calibration and validation processes are between 2011-2015 and 2016-2018, respectively. The agreement between observed and simulated discharge, which was expressed by Nash-Sutcliffe Coefficient (NSE), Coefficient of determination (R^2), and Percent bias (PBIAS).

3.3.1 Basic Model Overview

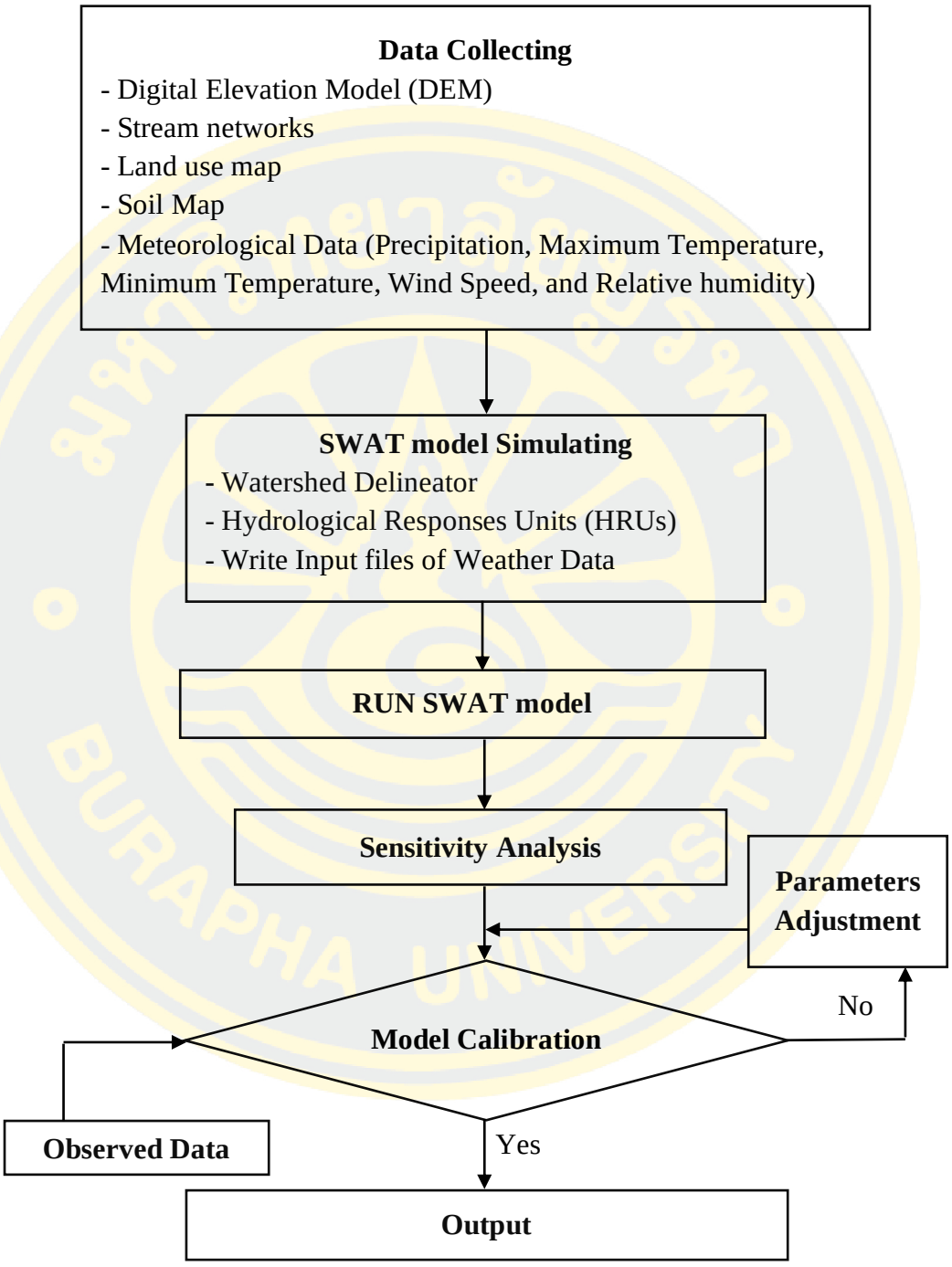

Figure 8 Overall Methodology for Hydrological Simulation

3.3.2 Data Collection

3.3.2.1 Individuals collection data

The data needed for the hydrological simulation of the Bang Pakong Basin is compiled from the Department of Water Resource (DMR) under The Ministry of Natural Resources and Environment, Thai Meteorological Department (TMD) under the Ministry of Digital Economy and Society, Royal Irrigation Department (RID) under the Ministry of Agriculture and Cooperatives, Geo-Informatics and Space Technology Development Agency (GISTDA), under the Ministry of Higher Education, Science, Research and Innovation, and Food and Agriculture Organization (FAO) under the United Nations.

3.3.2.2 Required Data, Type and Source data

The data required in the SWAT model includes DEM, land use map, soil map, and weather data. The topography data used for this study extracted from Airbus Intelligence. Water quality data as runoff data. The types and sources used to set up the models shown in Table 1.

Table 1 Data collected for this study

No	Descriptions	Data sources	Period	Data Types
I	**Spatial Data**			
1	Digital Elevation Model	Airbus Intelligence		Raster file
2	River basin and Tributaries	DWR		Vector file
3	Stream network	RID		Vector file
4	Land use	GISTDA	2017	Vector file
5	Soil types	FAO		Vector file
II	**Time series data**			
1	Maximum/Minimum Temperature	TMD	2009-2018	Excel file

No	Descriptions	Data sources	Period	Data Types
2	Relative humidity	TMD	2009-2018	Excel file
3	Wind speed	TMD	2009-2018	Excel file
4	Rainfall	TMD	2009-2018	Excel file
III	**Hydrological Data**			
1	Observe Streamflow	RID	2009-2018	Excel file

The synthesis of the rainfall-runoff in the past, as mentioned above would be performed by the SWAT model. The locations of meteorological stations were displayed in Figure 9. Furthermore, The locations of hydrological stations were displayed in Figure 10.

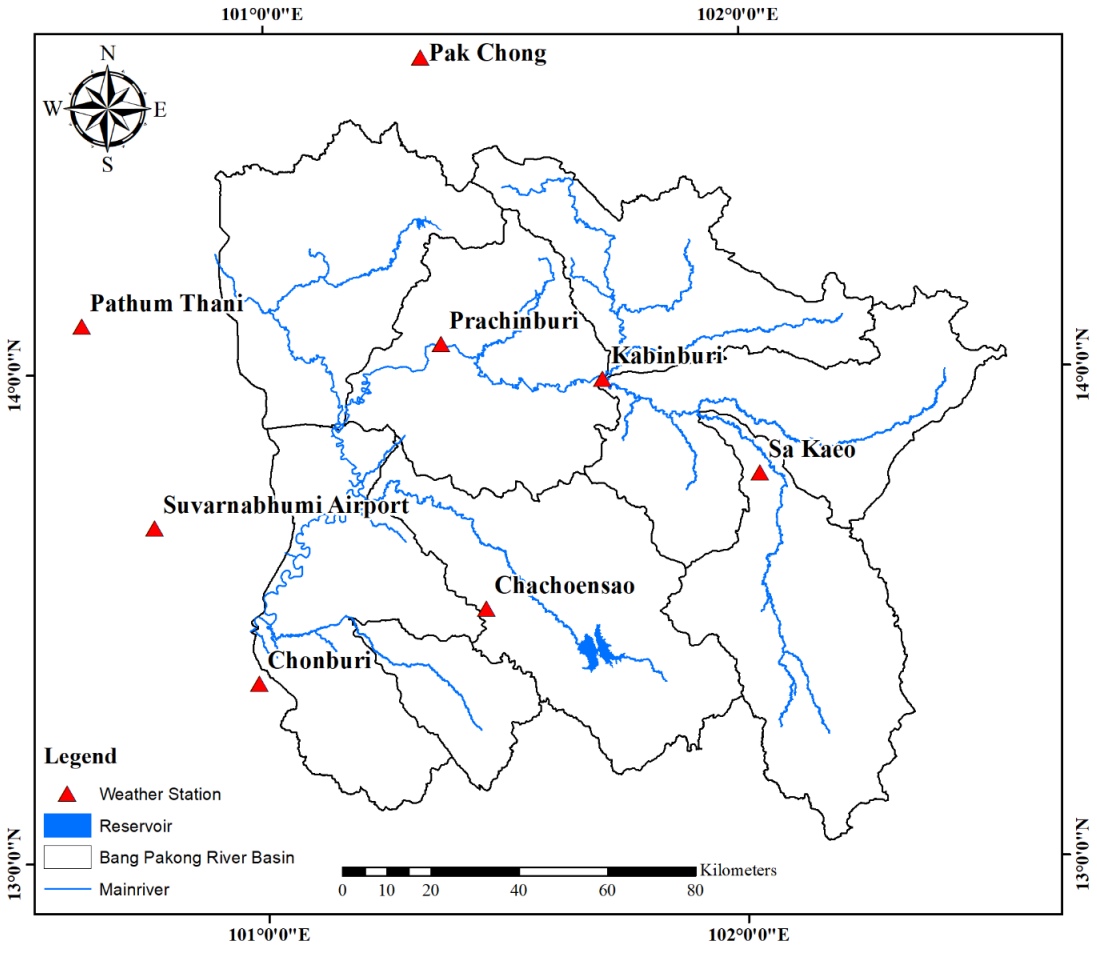

Figure 9 Picture of Meteorological station at Bang Pakong River Basin

Table 2 Detail of Meteorological station.

ST.ID	Station Name	Latitude	Longitude	Elevation (m)
419301	Pathum Thani	14.100	100.616	48.99
423301	Chachoengsao	13.515	101.458	43.76
429601	Suvarnabhumi Airport	13.686	100.767	13.75
430201	Prachinburi	14.058	101.369	186.37
430401	Kabinburi	13.983	101.707	99.64
431301	Pak Chong	14.643	101.331	274.6
440401	Sa Kaeo	13.788	102.034	138.96
459201	Chonburi	13.366	100.983	20.02

Hydrological stations, namely, KGT3 and KGT9, with daily and monthly streamflow data, were used for model calibration and validation. Because two of the observed station are matching well with the subbasin outlet, and the streamflow data are cover the period of the study.

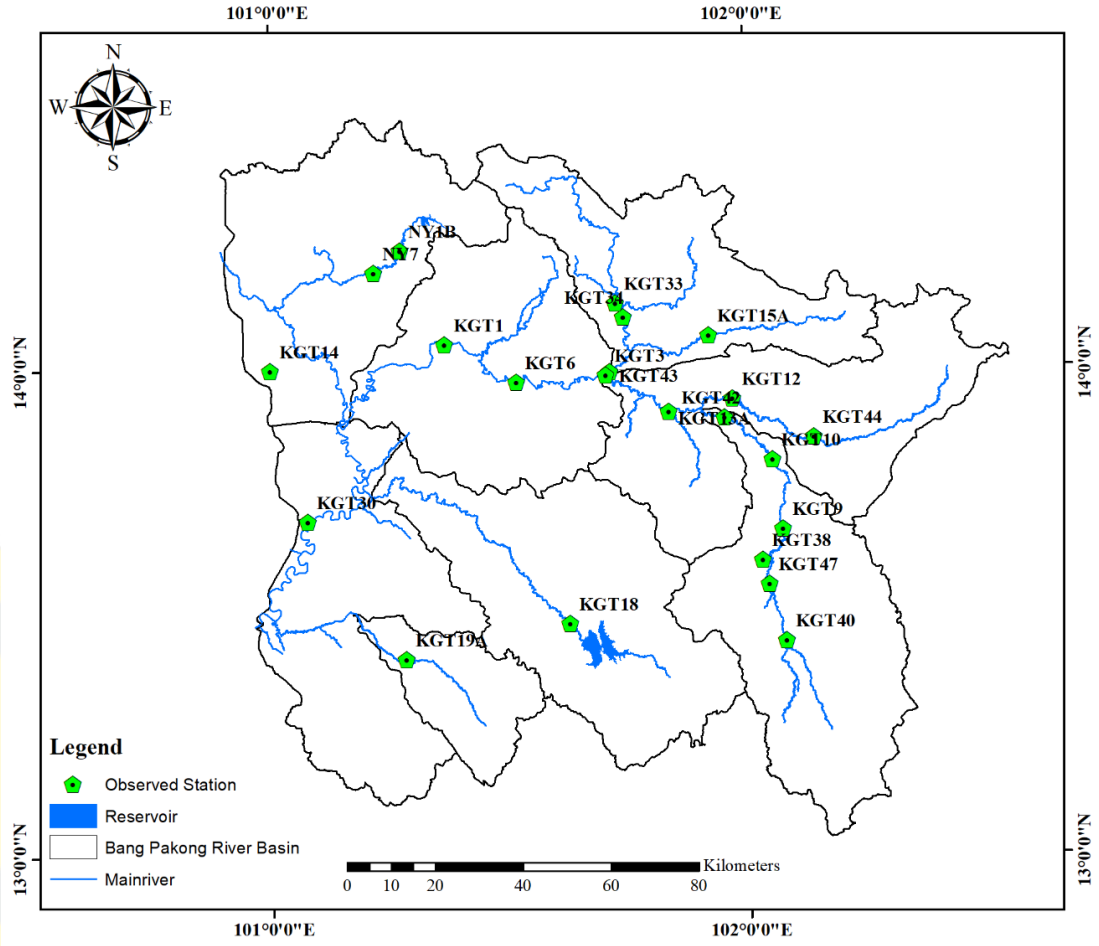

Figure 10 Picture of the hydrological station at Bang Pakong River Basin

Table 3 Detail of hydrological station

ST.ID	Name	Latitude	Longitude	Elevation (m)
1	NY1B	14.2458	101.274292	186.37
2	NY7	14.2003	101.2193	186.37
3	KGT1	14.0514	101.3674	186.37
4	KGT3*	13.9867	101.7054	99.64
5	KGT6	13.973	101.5173	99.64
6	KGT9*	13.668	102.0758	138.96
7	KGT10	13.8096	102.0543	138.96

ST.ID	Name	Latitude	Longitude	Elevation (m)
8	KGT12	13.9365	101.9723	99.64
9	KGT13A	13.91	101.8381	99.64
10	KGT15A	14.0661	101.9228	239.24
11	KGT18	13.4762	101.6259	104.29
12	KGT19A	13.4047	101.2817	50.15
13	KGT30	13.6889	101.0771	43.76
14	KGT33	14.1336	101.7277	239.24
15	KGT34	14.1045	101.7442	239.24
16	KGT38	13.6033	102.0327	138.96
17	KGT40	13.4382	102.0803	141.77
18	KGT42	13.8969	101.9549	99.64
19	KGT43	13.9934	101.7145	99.64
20	KGT44	13.856	102.1417	138.96
21	KGT47	13.5544	102.0454	138.96

* The station that has been chosen as the calibration and validation in the Bang Pakong river basin

3.4 The Soil and Water Assessment Tool (SWAT)

The SWAT model is a watershed-scale model. The model can process in a large basin without the data required for a standard calibration and validation effort (Arnold et al., 1998). These interfaces combined with GIS data sets and efficient computations for long-term processes. Continuously simulation at daily time steps, which used daily values of precipitation, maximum and minimum air temperatures, relative humidity, and wind speed with an ArcView GIS interface (ArcSWAT).

The hydrological process simulation in the SWAT can be divided into two main divisions (Arnold, Williams, & Maidment, 1995). First, the land phase or subbasin component that forces the amount of runoff suspended sediment, nutrients, and pesticide transport into the channels in each catchment. Second, the routing phase that forces the movement of water suspended sediment and nutrients, perpetually in the channels network in each catchment.

3.4.1 Land Phase or subbasin component

The simulation of SWAT is based on the water balance equation, as shown:

$$SW_t = SW_0 + \sum_{n=1}^{t} \left(R_d - Q_{surf} - E_a - W_s - Q_{gw}\right) \quad (3.1)$$

Where SW_t is the final soil water content (mm), SW_0 is the initial of soil water content on day i (mm), t is the time (days), R_d is the total of precipitation on day i (mm),Q_{surf} is the total of surface runoff on day i (mm), E_a is the total of evapotranspiration on day i (mm), W_S is the total of water entering the vadose zone from the soil profile on day i (mm), Q_{gw} is the total of return flow on day i (mm).

(1) Surface Runoff

SWAT model estimated surface runoff by detected changes in the calculation method of Soil Conservation Surveys (SCS) (United States Department of, 1989). Daily rainfall data is an essential input for the SCS curve number method. The rank of rainfall data, which is less than one day, is not enough for the SCS model, but it affects the accuracy of runoff calculations. The Modified Rational Formula was used to prognosticate the runoff rate. Moreover, surface runoff was prognosticated from daily precipitation with the equation of the SCS curve number equation as follows:

$$Q_{serf} = \frac{\left(R_{day} - Ia\right)^2}{\left(R_{day} - I_a + S\right)} \quad (3.2)$$

$$S = 254\left(\frac{100}{CN} - 1\right) \quad (3.3)$$

Where Q_{serf} is the surface runoff (mm), R_{day} is the rainfall depth for the day (mm), I_a is the initial abstraction including surface storage, interception, and infiltration before runoff (mm), which is commonly approximated as 0.2S, and S is retention parameter (mm), and CN is Curve number for the day.

The retention parameters are related to the Curve Number (CN) and vary in space due to the difference of soil, land cover, slopes, and different time according to

changes in the quantity of soil water content. The parameters related to CN are as follows:

CN value for moisture conditions I (CN_1) and III (CN_3) can be estimated using CN_2 as follow:

$$N_1 = CN_2 - \frac{20\,(100 - CN_2)}{100 - CN_2 + \exp[2.533 - 0.0036(100 - CN_2)]} \quad (3.4)$$

$$CN_3 = CN_2 \exp[0.00673\,(100 - CN_2)] \quad (3.5)$$

(2) Peak Runoff rate

SWAT estimates peak of runoff rate from a modification of the Modified Rational Formula, which can be computed using the equation:

$$qp = \frac{(p)(r)(A)}{3.6} \quad (3.6)$$

Where qp is Peak runoff rate (m^3/s), p is Runoff coefficient, r is Rainfall intensity (mm/hr) that occur during the time of concentration, and A is River basin area (km^2)

The Time Concentration (Tc) is the time when water droplets flow out from the farthest point in the river basin to the river basin outlet, which can be calculated using the equation:

$$t_{conc} = t_{ov} + t_{ch} \quad (3.7)$$

Where; t_{conc} is time of concentration in subbasin (hr), t_{ov} is the time of concentration for overland flow (hr), and t_{ch} is the time of concentration for channel flow (hr).

(3) Lateral flow

Lateral flow, as well as inter-low is the Streamflow of water which initiate below the earth-surface and above the zone when the rock is moist of water. The inter-flow in the soil layer is calculated along with the repeated distribution. The kinetic data

collection in the model was used to estimate the lateral flow in several layers of soil. This model describes the changes in conductivity, slope and water content in the soil. This SWAT is based on continuous of the balance of water mass with all the hills used as a controlled quantity (United States Department of, 1989). Lateral flow can be calculated using the kinematic data collection model as follow:

$$\frac{SW_2 - SW_1}{t_2 - t_1} = iL - \frac{q_{lat1} + q_{lat2}}{2} \quad (3.8)$$

Where SW is the drainage volume of water stored in the saturated zone (mm),t is Time (hr), q_{lat} is the water discharged from the hillslope outlet (m^3/hr), i is the water discharged in the saturated zone (m^3/hr), L is hillslope length (m), 1 starts travel time, and 2 is the end travel time

(4) Groundwater Flow

The simulation of low groundwater situations has four volume controls; Surface area, root zone, shallow aquifer, and deep aquifer, which are streamflow areas, surface runoff, flow laterally in the root zone and return flow from the shallow aquifer. Some amount of water can be returned to the deep aquifer layer, which is loose of water in the system, and there is no return back. The equation of water balance for the shallow aquifer is:

$$aq_{sh,i} = aq_{sh,i-1} + W_{rchrg} - Q_{gw} - W_{revap} - W_{deep} - W_{pump,sh} \quad (3.9)$$

Where $aq_{sh.i}$ is the amount of water stored in the shallow aquifer on day i (mm), $aq_{sh,i-1}$ is the amount of water stored in the shallow aquifer on day i-1(mm), W_{rchrg} is the amount of recharge entering the aquifer on day i (mm), W_{revap} is the amount of water moving into the soil zone in response to water deficiencies on day i (mm), Q_{gw} is the groundwater flow, or base flow, into the main channel on day i (mm), W_{deep} is the amount of water percolating from the shallow aquifer into the deep aquifer on day i (mm), $W_{pump.sh}$ is the amount of water removed from the shallow aquifer by pumping on day i (mm), and i is time (day).

The water balance for the deep aquifer is:

$$aq_{dp,i} = aq_{dp,i-1} + W_{deep} - W_{pump,dp} \quad (3.10)$$

Where; $aq_{dp,I}$ is the amount of water stored in the deep aquifer on day i (mm), $aq_{dp,i-1}$ is the amount of water stored in the deep aquifer on day i-1 (mm), W_{deep} is the amount of water percolating from the shallow aquifer into the deep aquifer on day i, and $W_{pump,dp}$ is the amount of water removed from the deep aquifer by pumping on day i.

(5) Evapotranspiration

There are three assortments for potential ET calculations.

Penman / Monteith Method (Allen, Pereira, Raes, & Smith, 1998) - requires air temperature, wind speed, relative humidity, and solar radiation to enter the model.

Priest-Taylor methods (Priestley & Taylor, 1972) - required solar radiation and temperature data to enter the model.

Hargreaves and Samani methods (Hargreaves & Allen, 2003) - require only weather temperature data to enter the model (Neitsch, Arnold, Kiniry, & Williams, 2011).

In this research, Penman/Monteith method was used to estimate the potential of ET. The equation for the evapotranspiration is:

$$ET_0 = \frac{0.408\Delta(R - G) + \gamma \frac{900}{T + 273} \bigcup_2 (e_5 - e_a)}{\Delta + \gamma(1 + 0.34u_2)} \quad (3.11)$$

Where ET_o is reference evapotranspiration [mm day^{-1}], R is net radiation at the crop surface [MJ $m^{-2}day^{-1}$], G is the soil heat flux density [MJ $m^{-2}day^{-1}$], T is the air temperature at 2 m height [°C], u_2 is the wind speed at 2 m height [m s^{-1}], e_s is the saturation of vapour pressure [kPa], e_a is the actual vapour pressure [kPa], $e_s - e_a$ is the saturation vapour pressure deficit [kPa], Δ is slope vapour pressure curve [kPa $°C^{-1}$], and γ is psychrometric constant [kPa $°C^{-1}$].

3.4.2 Routing component

SWAT model simulates water routing using hydrologic flow routing methods. Water routes were used to calculate in a daily time step, and there is no recalculation. From there, it can be modelled for a long time in a large basin by reducing the details of the cross-section area of water flow in the channel. The main channel is considered even shaped in a trapezoid and assumed that the channel slope 2:1. When the water volume exceeds the maximum amount, it can be collected by excess water channels to spread throughout flooding is considered the width of the plains. The channel input data consists of channel length, channel slope, channel depth, maximum channel width, the slope of flat area, and channel coefficient Manning's "n".

The volume of outflow in the channel can be computed as the equation:

$$O_i = SC\ (I_i + S_{i-1}) \tag{3.12}$$

Where O is the volume of outflow (m^3), I is the volume of inflow (m^3), S_{i-1} is the volume of water stored in the channel on day i-1 (m^3), i is the time (Day) on day i, SC is the storage coefficient which can compute by using this equation:

$$SC = \frac{48}{2TT+24} \tag{3.13}$$

Where TT is travel time (hr).

Manning's equation was used to estimate the flow rate and velocity in a reach segment of channel depth and 0.1 channel depth, respectively. Flow rates in channels can be calculated as the following equations:

$$qr = \frac{A}{n} R^{2/3} \sqrt{s} \tag{3.14}$$

Where qr is a rate of flow in the channel (m^3/s), n is the Manning Roughness Coefficient, A is a cross-sectional area of flow in the channel (m), R is Hydraulic radius (m), and s is Channel side slope

3.4.3 Preparation Data Input

3.4.3.1 Database

The mandatory spatial datasets and database input files for the Bang Pakong river basin. SWAT model was organized following the guidelines of the Soil and Water Assessment Tool by the user's Manual Version 2000. GIS data layers used to build the model resolution 25 m x 25 m Digital Elevation Model (DEM), the most detailed soils data from FAO, land use data from GISTDA and the stream network from the RID and weather data from TMD that shown in Figure 11 to 14. The primary data input is briefly explained below.

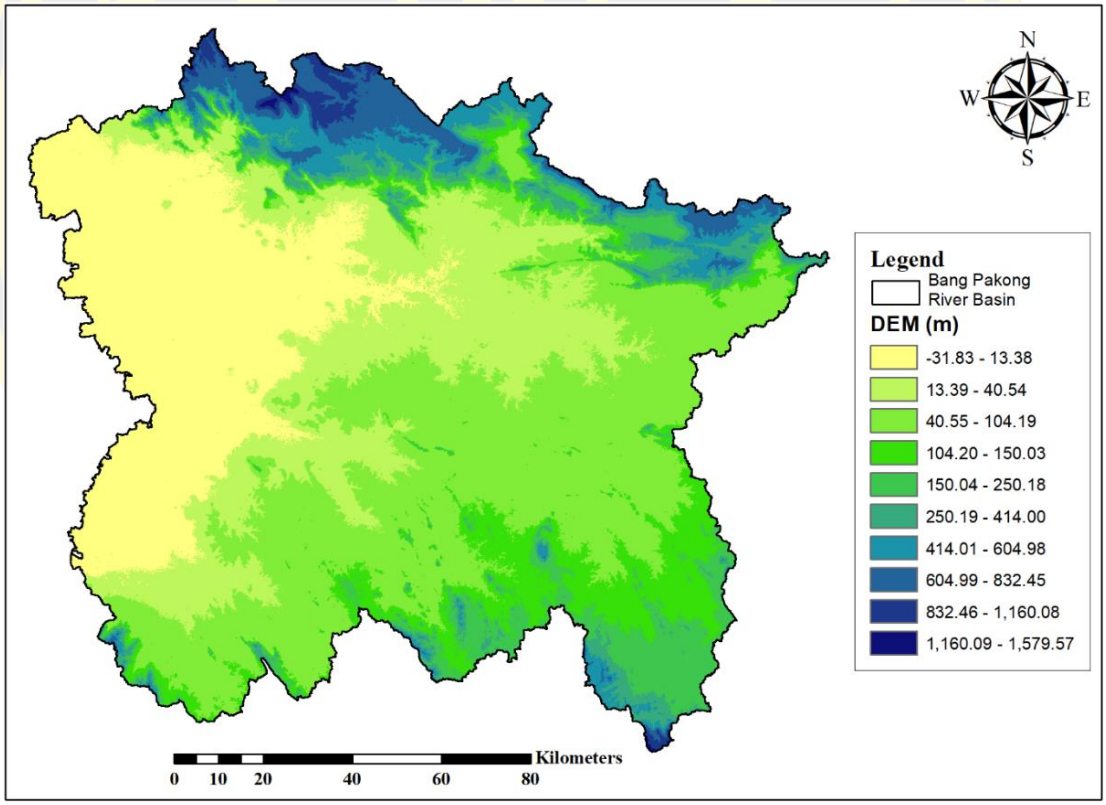

Figure 11 Data input layer to create the Bang Pakong river basin using the SWAT model (DEM)

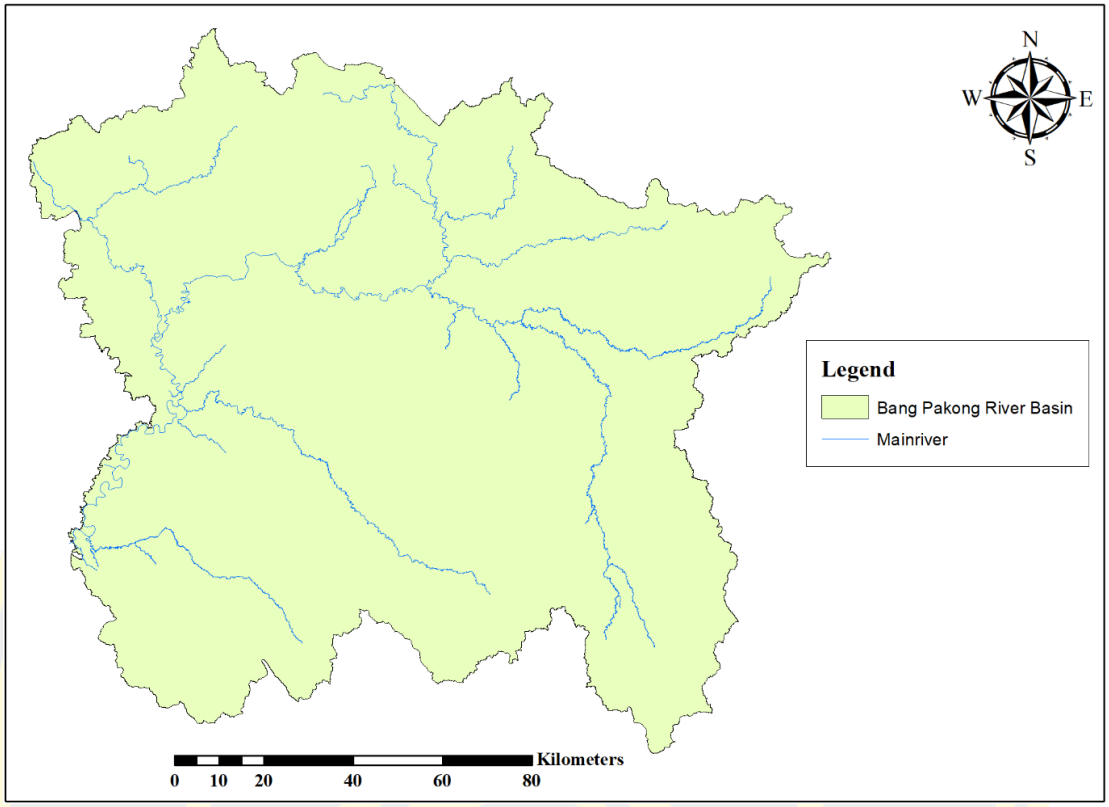

Figure 12 Data input layer to create the Bang Pakong river basin using the SWAT model (River network)

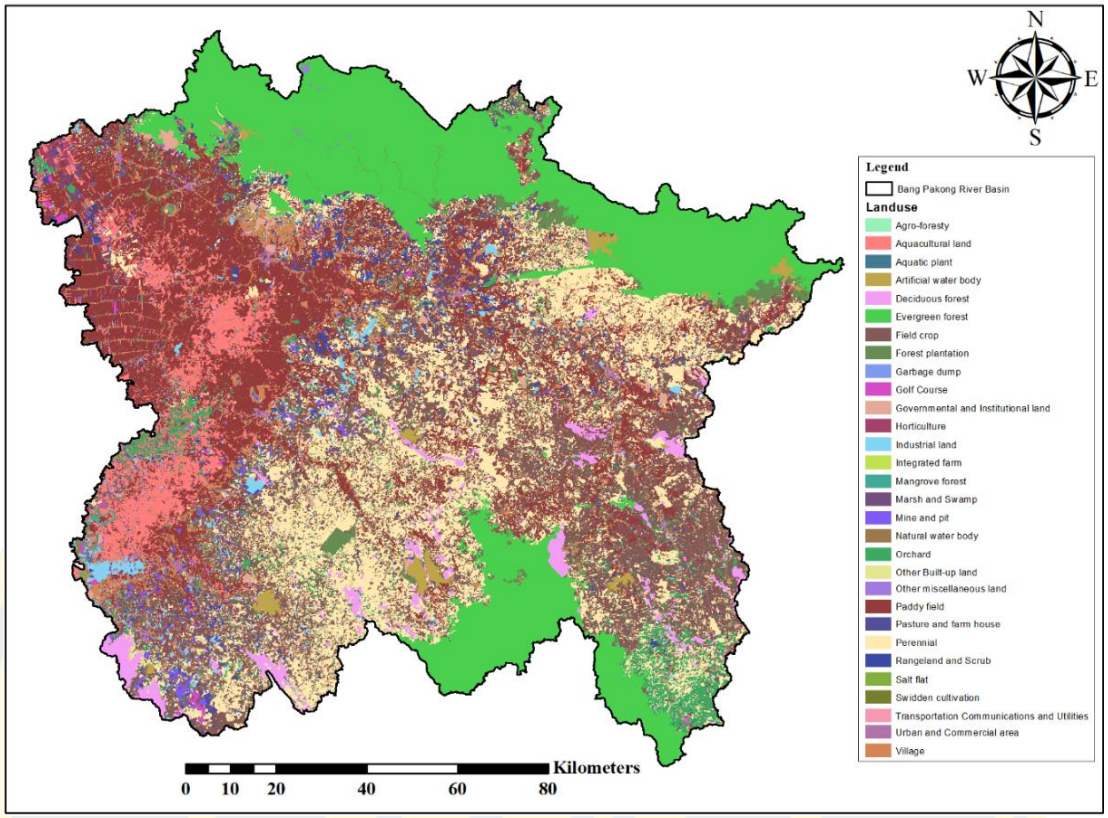

Figure 13 Data input layer to create the Bang Pakong river basin using the SWAT model (Land use)

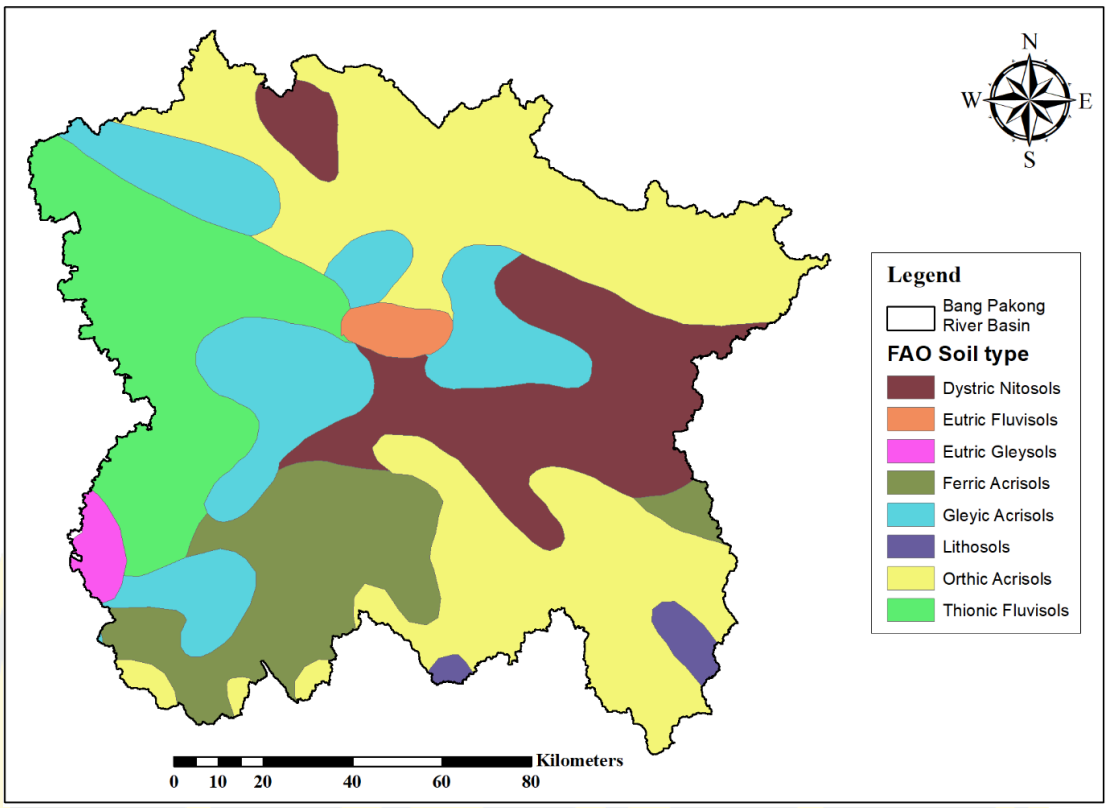

Figure 14 Data input layer to create the Bang Pakong river basin using the SWAT model (Soil)

1) Digital Elevation Model (DEM)

The DEM was derived from Airbus Intelligence, which has a spatial resolution of 25 m x 25 m. DEM was projected to WGS1984 UTM Zone47N. It was used to delineate the watershed as the drainage in final outlets and stream network.

The model input database files that were not in GIS Layers but were in the management operations such as streamflow data, point sources, and weather data. Weather data for the Bang Pakong modelling was taken from eight different gauging stations of the TMD. The selected stations are distributed all of the watersheds to effectively capture the spatial variability of the Bang Pakong river basin precipitation (shown in Table 4).

The SWAT model requires many database files, which be prepared in the form of dBase (*.dbt) files as per procedure and format specified in User's Guide of SWAT 2009 (Winchell, Srinivasan, Luzio, & Arnold, 2009).

2) Land use databases

This study covers the area of the Bang Pakong River Basin, Land Cover compiled by the Geo-Informatics and Space Technology Development Agency (GISTDA). SWAT interface requires a raster dataset to determine the spatial boundary for each class, which was a specific land use class, so the "*.dbf" file is created to convert land use into SWAT land use classes.

3) Soil databases

Soil map for Bang Pakong river basin was extracted from the Digital Soil Map of World (DSMW), produced by Food and Agriculture Organization (FAO) under the United Nations. Version number 3.6, completed in January 2003. Soil number is a sequential code, unique for each soil unit, which links the first level of soil information to the expansion data file.

4) Weather databases

The meteorological data were collected from the Thai Meteorological Department from 2009 to 2018. SWAT requires meteorological data for model simulating by using precipitation across the study area, including daily precipitation, daily maximum and minimum temperatures, daily wind speed, and daily relative humidity (Table 4).

Table 4 The interval of Meteorological data

Data	Station Name	Frequency	Elevation (m)
Precipitation, Max &Min temp, RH, Wind speed	Pathum Thani	Daily	48.99
	Chachoengsao	Daily	43.76
	Suvarnabhumi Airport	Daily	13.75
	Prachinburi	Daily	186.37
	Kabinburi	Daily	99.64
	Pak Chong	Daily	274.6
	Sa Kaeo	Daily	138.96
	Chonburi	Daily	20.02

3.4.4 Model Set-up

The first step in ArcSWAT is to divide the watershed into sub-units called subbasins, which was subbasins are divided into HRU's, by making up the basis for predicting in hydrology process. The Digital Elevation Model (DEM), with a resolution of 25 meters, obtained from Airbus Intelligence was used for delineation watershed. The mask was built with the Department of Water Resources, Thailand, by considering the criteria for dividing river basins in the upstream outlet, which considered from the location of the observation station.

DEM-based watershed delineation methods have low precision in the plain area, which Bang Pakong basin located. In this research, the "Burn-in" method collaborates with self-correction based on field surveys, which obtain from the Irrigation Department (RID), Thailand. The stream network data set is digitized from a topographic map of the scale 1:50000 of the Study area. The network stream data set is superimposed over the DEM to determine the location of the waterways. The operation of the burn-in streaming network is most important in situations where DEM does not provide sufficient details to allow the interface to predict the location of the streaming network accurately.

Apply the stream network to improve waterways and subbasin subdivision in the ordinary polder. The "burn-in" algorithm was first proposed by the Maidment of the University of Texas, US. There are effective methods to eliminate holes or depression in the stream burning algorithm. In this method, the existing network stream (polyline) data set is used to process the DEM. In essence, the height of the overlapping grids by the digital channel network decreases, when the value is increasing the slope with other surrounding grids (Saunders & Maidment, 1996). Burning the stream network to DEM can improve the hydrographic segmentation and sub-basin boundaries.

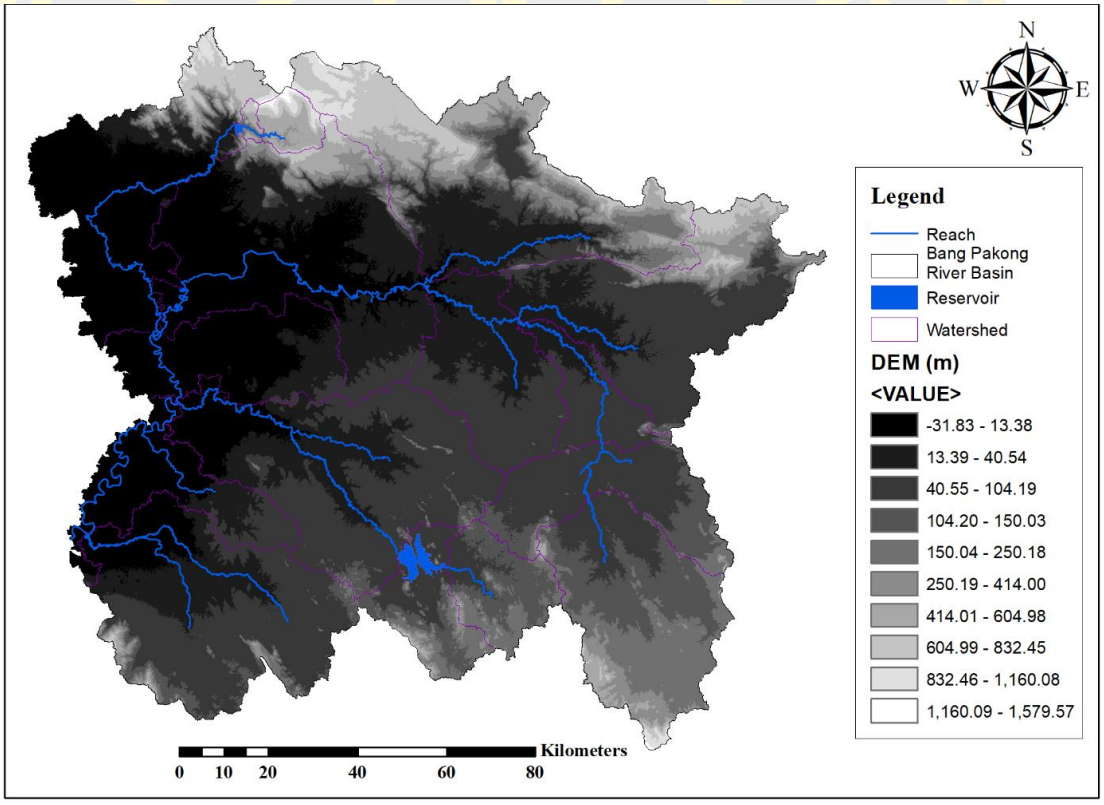

Figure 15 Subbasins from Watershed Delineator in ArcSWAT

After the watershed is divided into small subbasins, it will be divided into basic units called Hydrological Response Units (HRUs). HRUs are sub-components of

the model and grouped based on homogeneous land use, soil, geometry, and slope to represent the area within a subbasin that responds similarly to hydrology (Figure 16). SWAT allows users to define a specific HRU in many locations in the subbasin. If the HRU is repeated throughout subbasin, mean that the response to meteorological data is the same. HRUs can be classified according to modeller specifications to group certain land types. Sixteen omitting or include specific classes or have certain land types play a more important role in the model. With concern to model output, HRU yields are summed for a total yield of the subbasin (Shekhar & Xiong, 2008). Each unique HRU within a subbasin calculates independent yields for discharge, sediment, and stream quality.

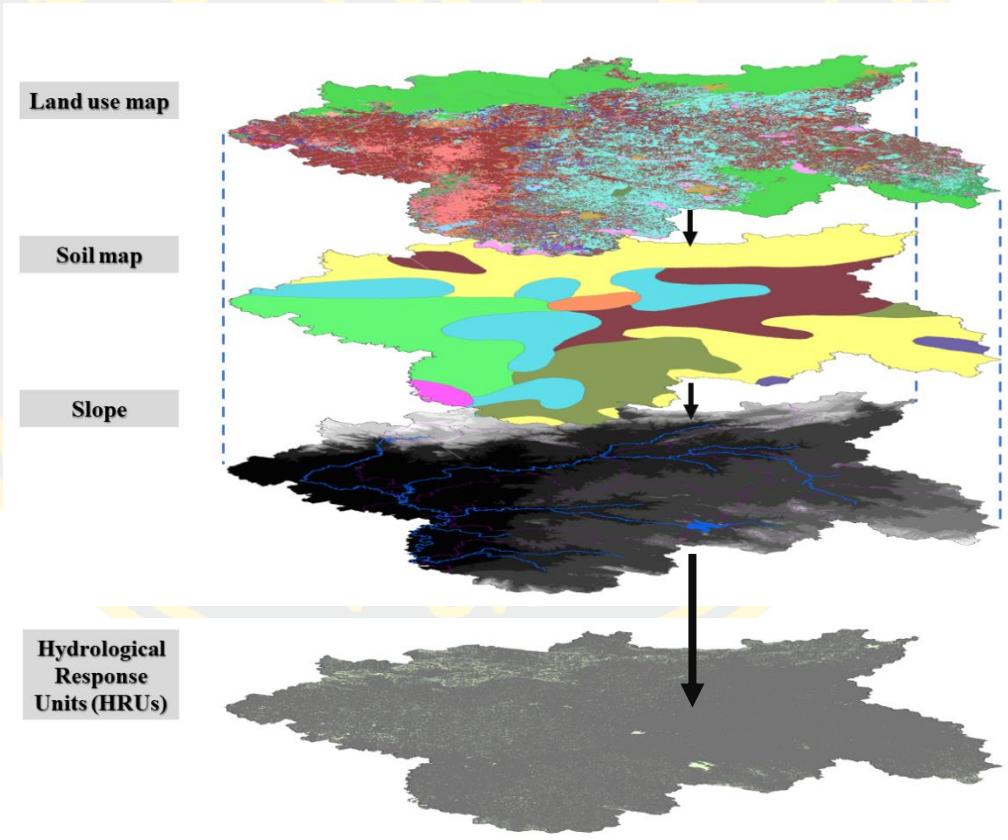

Figure 16 HRU Development

After HRUs mere obtained, the next step was to load precipitation and meteorological data files. Then, the computational methods were selected for each component, and some were left with the default SWAT selections. SCS method was selected for runoff computation. Penman/Monteith method for evapotranspiration. Muskingum method for flow routing, storage routing, and crack-flow model for percolation (Arnold et al., 1998). The schematic representation of the SWAT model set-us is shown in Figure 17.

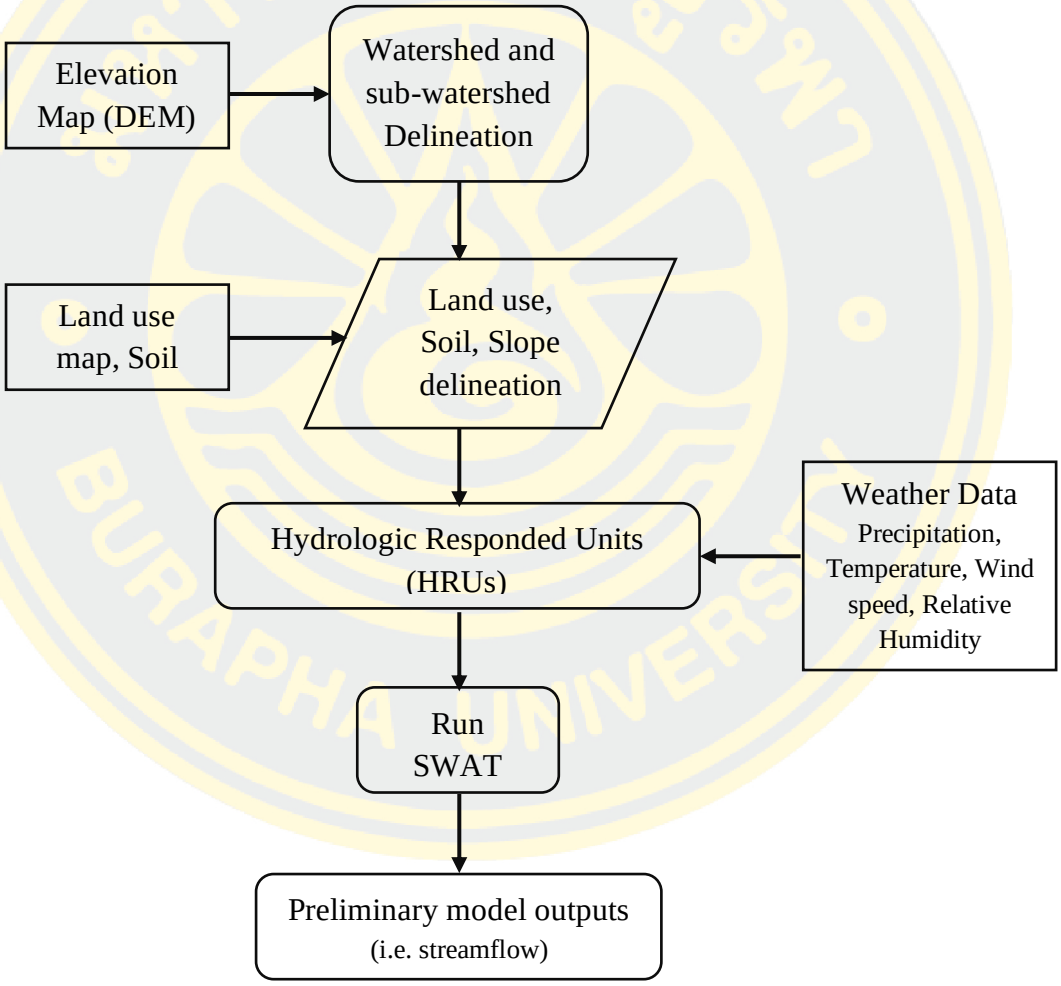

Figure 17 Schematic representation of the SWAT model set-up

3.5 Calibration and Validation Method

SWAT is a complex model that simulates a watershed process based on empirical data. Because the model is complex, calibration and validation are necessary to understand whether the model is real or inaccurate (Srinivasan et al., 2010). This is achieved by comparing the model's results with measured data. The modular sample methods for calibration and validation are used for evaluating model performance. The model was completed between 2009-2018, with 2009-2010 being a warm-up year, 2011-2015 for the calibration period, and 2016-2018 for the validation period.

The calibration process aims to obtain a setup model parameter that provides a satisfactory agreement between simulations and observations, which are optimal values for parameters specified by the user. This step can be done automatically or manually based on the defined optimization algorithm.

3.5.1 SWAT Calibration and Uncertainty Procedures (SWAT-CUP)

Abbaspour et al. (Karim C. Abbaspour et al., 2007) wrote that SWAT Calibration and Uncertainty Procedures (SWAT-CUP) is a standalone program developed for parameter sensitivity analysis, calibration, validation, and uncertainty analysis of SWAT models. Data visualization is also available in the study area, subbasins, modelled river, the outlet in each watershed, and weather stations used.

SWAT-CUP has five techniques for uncertainty analysis: Particle swarm optimization (PSO), Sequential Uncertainty Fitting algorithm (SUFI-2), Bayesian framework implemented using Markov Chain Monte Carlo (MCMC), Parameter Solution (ParaSol), and Generalized Likelihood Uncertainty Estimation (GLUE) [5]. In this study, SWAT-CUP2019 version 5.2.1.1 and SUFI-2 techniques were used for uncertainty analysis.

The uncertainty analysis of the parameters in the SUFI-2 considers all sources of uncertainty from the input variable concept model. (i.e., rainfall, temperature) and their parameters (Karim C. Abbaspour et al., 2007), (Gholami, Watson, Molla, Hasan, & Bjørn-Andersen, 2016), (Kumar, Singh, Srivastava, & Narsimlu, 2017). The

parameter uncertainty is shown in a multivariate distribution. In contrast, the output from the model is explained by 95% prediction uncertainty (95PPU) calculated at 2.5% and 97.5% levels. P-factor is the percentage of the measured data within 95PPU and varies between 0 and 1. R-factor describes the ratio of 95PPU thickness to the standard deviation of the measured variable. A P-factor of 100% and R-factor of 0 indicate that the simulated and observed variables are identical. Therefore, the balance between P-factor and R-factor should be used. R-factor is needed to be close to 1 when the P-factor is not less than 75% (Qi et al., 2016).

Initially, the range of parameters will be set to a wider range. But possible physical references to literature or from an understanding of the user in the watershed. SUFI-2 performs iterates using Latin Hypercube to draw independent parameter sets from the specified range. For each iteration, the parameter set from the previous iteration will be updated in such a way that the new parameter set has a narrower range, and the range will be centered on the best simulation (as shown in Figure 18). Repeatability in SUFI-2 will be repeated until the desired performance level is achieved.

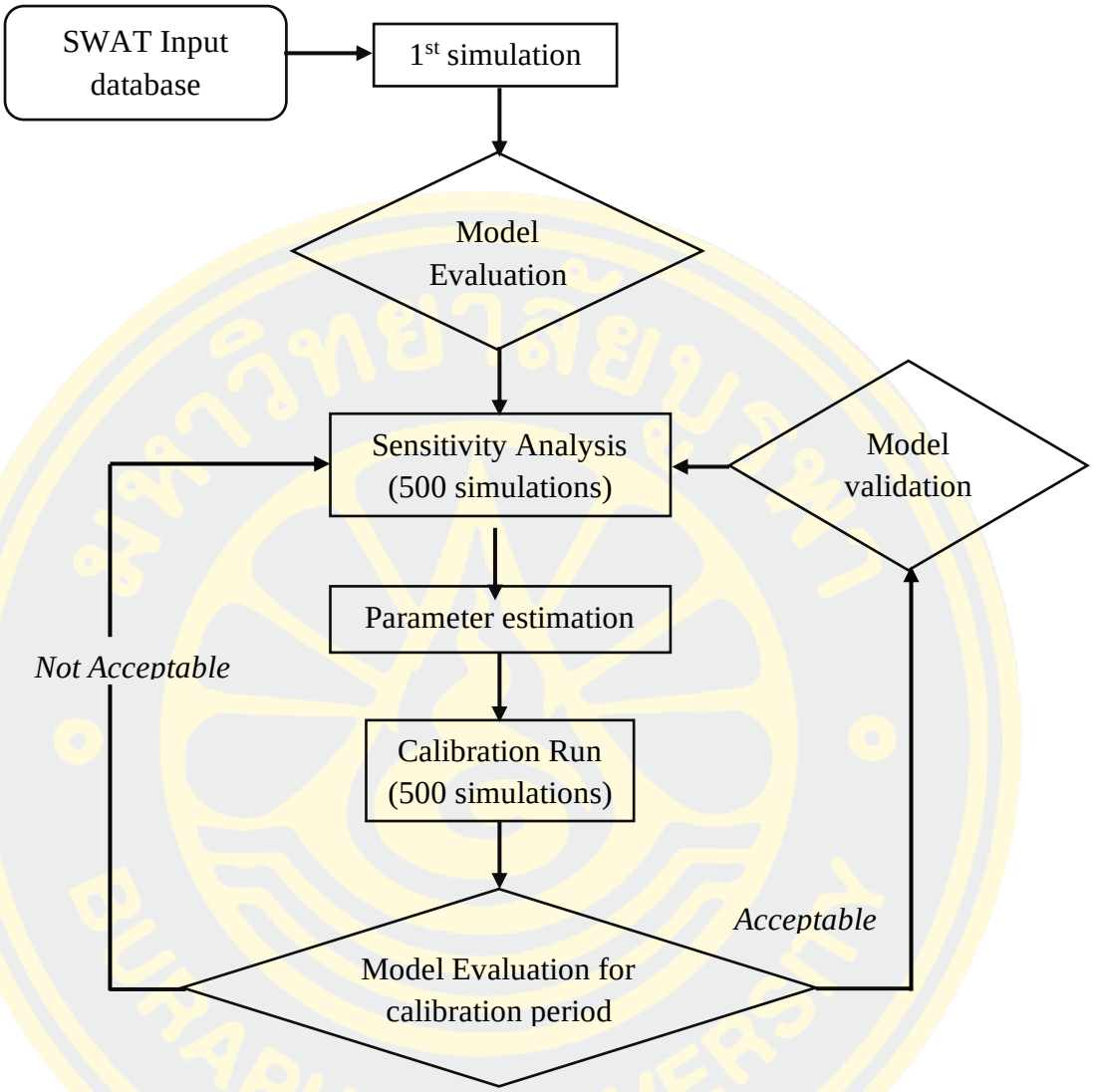

Figure 18 Schematic representation in SWAT-CUP

Abbaspour et al. (2007) developed SUFI-2 as an optimization algorithm for sensitivity analysis, calibration, and verification. Correct Summarize the following steps:

1) The objective function $g(\theta)$, and realistic parameter ranges $[\theta_{abs\ min}, \theta_{abs\ max}]$ is defined.

$$\theta_j: \theta_{abs\ min} \leq \theta_j \leq \theta_{abs\ max}, j = 1, \ldots, m \quad (3.15)$$

Where θj is the j-th parameter, and m is the number of parameters to be estimated.

2) OAT sensitivity analysis for each parameter is carried out for the ranges set in step 1 with about five simulations, as suggested by (Willmott, 1981). This step is optional but essential to reduce irrelevant parameters to the model output.

3) Latin Hypercube sampling is undertaken in the hypercube $[\theta_{min}, \theta_{max}]$ (initially set to $[\theta_{abs\ min}, \theta_{abs\ max}]$) to generate n parameter combinations. The value of n is usually set between 500 and 1000.

4) Using the corresponding objective function (g) for the n simulations, the sensitivity matrix of g(θ), denoted by J, and the parameter covariance matrix C are calculated as follows:

$$J_{ij} = \frac{\Delta g_i}{\Delta \theta_j}, i = 1, \ldots, C_2^n, j = 1, \ldots, mb_{mlt,t} \quad (3.16)$$

$$C = S_g^2 \left(J^T J\right)^{-1} \quad (3.17)$$

Where C_2^n is all possible combinations of two simulations, and S_g^2 is the variance of the objective function values resulting from the n simulations.

5) The 95% predictive interval for a parameter θj is calculated as:

$$\theta_{j,lower} = \theta_j^* - t_{v,0.025}\sqrt{C_{jj}} \quad (3.18)$$

Where θ_j^* is the parameter θ_j for the best estimates (i.e. parameters which produce the optimal objective function), v is the degrees of freedom (n-m), and C_{jj} is the diagonal element of C.

6) The 95PPU is calculated and then used to compute the P-factor and the R-factor as follows:

$$\text{R - factor} = \frac{\bar{d}_Y}{\sigma_Y} \tag{3.19}$$

Where σ_Y is the standard deviation of the measured variable Y (i.e., observed streamflow); and $\bar{d}$ is the average distance between the upper and lower boundaries of the 95PPU envelope, calculated as:

$$\bar{d}_Y = \frac{1}{k}\sum_{l=1}^{k}(Y_u - Y_L)_l \tag{3.20}$$

Where k is the number of observed data points; Y_u (97.5%) and Y_L (2.5%) represent the upper and lower boundary of the 95PPU.

$$\text{P - factor} = \frac{k}{N} \tag{3.21}$$

Where N is the total number of the measured variable Y, and k is the number of measured values enveloped by the 95PPU.

7) The goodness of the calibration and simulation uncertainty is evaluated based on how close the P-factor is to 100%, and R-factor to 1. If the two indices have satisfactory values, then the uniform distribution in the parameter $[\theta_{min}, \theta_{max}]$ is the posterior distribution. Since the parameter uncertainties are initially large, the value of

$\bar{d}$ is usually quite large as well. Thus, another iteration is required with updated [$\theta_{min,}$ θ_{max}] values, as shown below:

$$\theta'_{j,min,new} = \theta_{j,lower} - \max\left(\frac{\theta_{j,lower} - \theta'_{j,min}}{2}, \frac{\theta'_{j,max} - \theta'_{j,upper}}{2}\right) \quad (3.22)$$

$$\theta'_{j,max,new} = \theta_{j,upper} + \max\left(\frac{\theta_{j,lower} - \theta'_{j,min}}{2}, \frac{\theta'_{j,max} - \theta'_{j,upper}}{2}\right) \quad (3.23)$$

Where θ' denotes the new parameter values, $\theta_{j,lower}$ and $\theta_{j,upper}$ are calculated using parameters

3.5.2 Model Performance

The systematic and dynamic of the model can be seen by the correlation between the model predictions and the observed streamflow in the same location. By looking at the modified graph, it can be understood that the model is above prediction or lower than expected and also includes periods of higher and lower limb hydrology and decisions about model performance. However, in evaluating quantitative models, we need to use mathematical measures of model performance.

The SWAT model performance in streamflow prediction between calibration and validation periods was evaluated by using four different statistical measures. Square of Pearson's product-moment correlation coefficient (R^2) (Arnold et al., 2012), Nash-Sutcliffe efficiency (NSE) (Nash & Sutcliffe, 1970), index of agreement (*d*) (Willmott, 1981), and percent bias (PBIAS). The model performance in Bang Pakong watershed simulation using the NSE, R^2, and PBIAS only. The criteria employed herein to assess model performance are fully defined in Table 5.

The calculations of NSE, R^2, and PBIAS are calculated using equations below:

(a) Nash-Sutcliffe Coefficient

The Nash-Sutcliffe efficiency (NSE) is a standard statistic that determines the relative magnitude of the remaining variance ("noise") in comparison to the variance of the measured data ("information"). NSE indicates the plot of the observed and simulates data fits the line 1: 1 lone. As shown in the equation below:

$$NSE = 1 - \frac{\sum_{i=1}^{n}[(x_i - y_i)^2]}{\sum_{i=1}^{n}[(x_i - \bar{y})]} \quad (3.24)$$

Where x_i and y_i are observed simulated discharge dataset and $\bar{y}$ is an average of the observed dataset, respectively.

(b) Coefficient of determination

The R^2 is the percentage of variance explained by the model. It is a statistical measure of how close the data are to the fitted regression line. R^2 ranges from 0 to 1, with higher values indicating less error variance. R^2 is computed, as shown below:

$$R^2 = \frac{\sum_{i=1}^{n}.\left[(x_i - \bar{x}) \times (y_i - \bar{y})\right]^2}{\sum_{i=1}^{n}.[(x_i - \bar{x})^2] \times \sum_{i=1}^{n}.[(y_i - \bar{y})^2]} \quad (3.25)$$

Where x_i , y_i , $\bar{x}$, and $\bar{y}$ are observed and simulated data and average data of these two datasets.

(c) Percent Bias

Percent bias (PBIAS) measures the average tendency of simulated data that is larger or smaller than the observed pair (Gupta, Sorooshian, & Yapo, 1999). The optimum value of PBIAS is 0.0, with a low severity value that represents the simulation. Precise model positive values indicate model underestimation bias, and negative values indicate model overestimating bias. PBIAS is calculated with the equation, as shown below:

$$\text{PBIAS} = \left[\frac{\sum_{i=1}^{n}(y_i - \bar{y}) \times 100}{\Sigma_{1=1}^{n}(y_i)}\right] \quad (3.26)$$

Where y_i is the observation for the constituent being evaluated, $\bar{y}$ is the simulated value for the constituent being evaluated.

Table 5 Performance rating criteria for NSE, $R^{2,}$ and PBIAS in both daily and monthly calibration and validation

Performance metric	**Unsatisfactory**	**Satisfactory**	**Good**	**Very good**
NSE	< 0.5	0.50-0.65	0.65-0.75	0.75-1
R^2	< 0.5	0.5-0.6	0.6-0.7	0.7-1
PBIAS	>±25%	±15%-±25%	±10%-±15%	<±10%

CHAPTER 4
EXPERIMENTS AND RESULTS

4.1 Output from Model

4.1.1 Delineation Watershed

Delineation Watershed is a process of creating boundaries that represent a contributing area for specific control points or outlets. This model is calculated from Digital Elevation (DEM) data by calculating the flow direction combined with the flow accumulation of water network systems and the slope. The high resolution of the DEM can be determined with high accuracy and is consistent with the physical condition in the study area.

In this study, DEM data with a resolution of 25 meters × 25 meters was used to define an outlet. The calculate sub-basin parameter, by defining stream network and outlet options within the manual watershed delineator tool to creates the required layer and attributes. The sub-watershed divided depend on the outlet observe station, point sources and non-point sources to make scenarios for prediction in the future. Finally, in this study were divided into 17 sub-basins, The output from this step performance in Table 6 and Figure 19. The output from this part shows that there are three output layers: sub-basin, streams, and outlets. Each of these layers must have a set of attributes that the model setup plugin will be looking for.

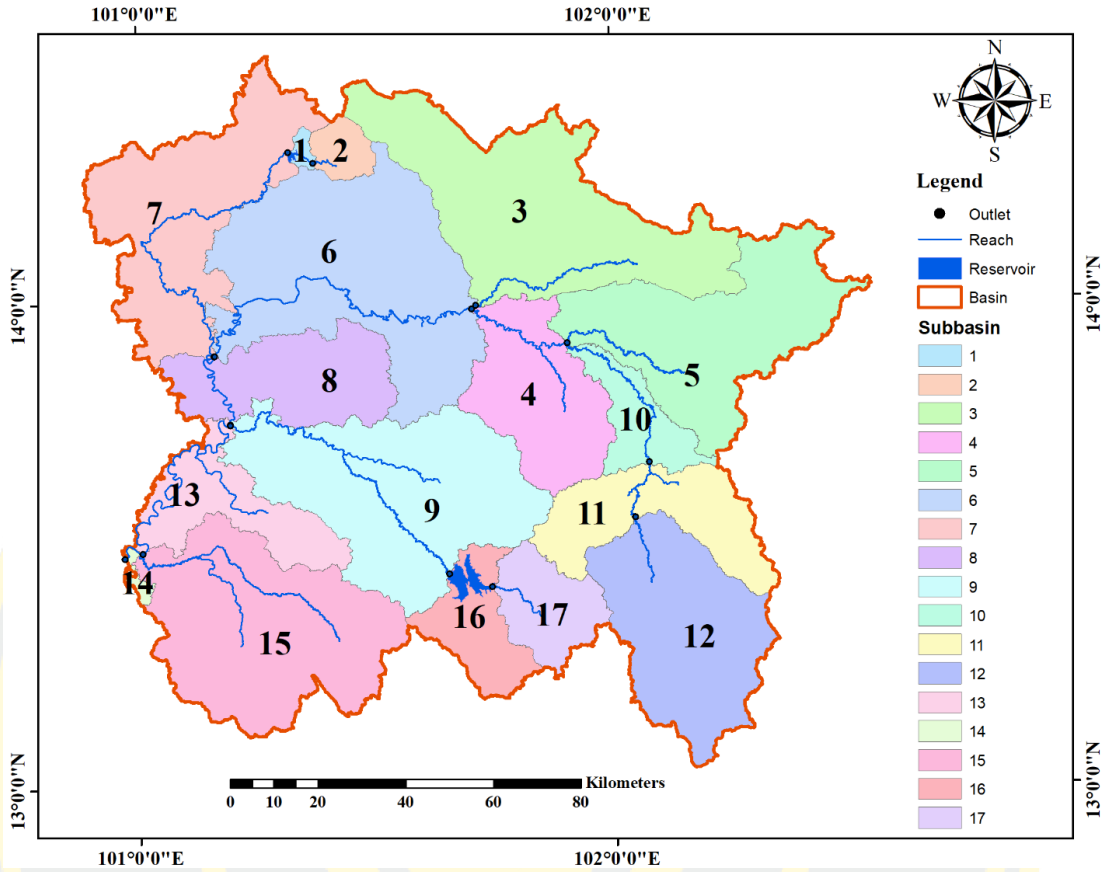

Figure 19 Sub-basin, river net, and outlet from delineation watershed

Table 6 Output from delineation watershed

Sub-basin	Area (ha)	% of Total area
1	3,755.6953	0.21
2	16,161.2485	0.89
3	213,440.6399	11.80
4	98,500.9186	5.44
5	161,875.6086	8.95
6	227,152.9421	12.55
7	165,686.0932	9.16
8	90,095.4721	4.98
9	201,558.8869	11.14
10	39,782.7061	2.20

Sub-basin	Area (ha)	% of Total area
11	84,312.8180	4.66
12	142,948.4797	7.90
13	70,498.2752	3.90
14	3,877.0144	0.21
15	192,267.8842	10.63
16	49894.2028	2.76
17	47,668.6939	2.63
Total	**1,809,477.58**	**100**

4.1.2 Specifying Contributing Area Important

In order to divide the Bang Pakong Basin into sub-basins with combinations of land use, soil, and slopes, which affect evapotranspiration, water quantity, water quality, groundwater, and other hydrological conditions. Quantitative and qualitative data are predicted separately for each HRU and routed to obtain the total quantity and quality in each watershed.

It is based on the percentage of the watershed threshold for 20% of land use and a criterion for creating homogeneous HRU. By specifying the percentage value, the total of HRUs is 99 and was created land use into 16 classes (Figure 20). The details of values after the finished generation shown in Table 7.

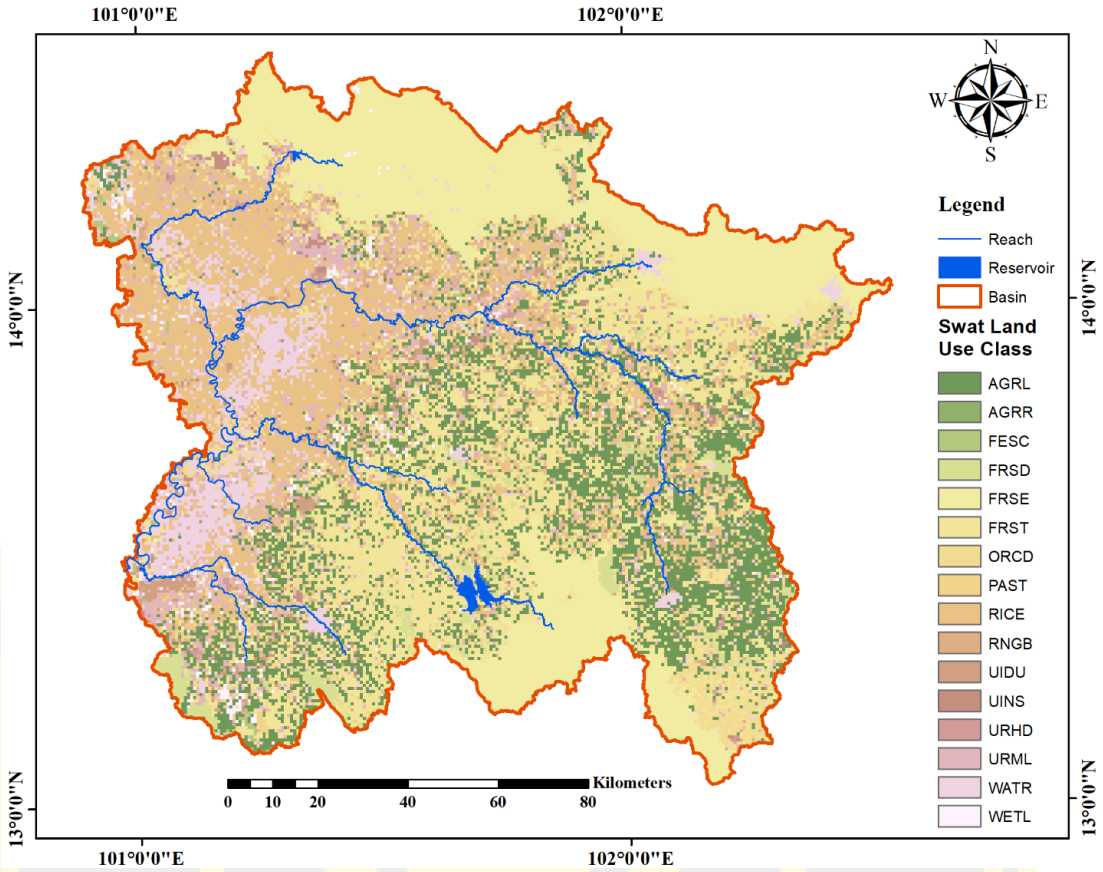

Figure 20 Land use classified by SWAT model

The result obtained that most of Land use-Land cover percentage in the Bang Pakong River basin are Forest type with Evergreen forest (20.51%), and Mixed forest (19.69%), respectively. Most of the Bang Pakong River Basin has been used for agricultural purposes, including the Paddy field or Rice field (18.17%), field crops (16.41%), and other farming activities.

Table 7 Land use class of study area after the threshold

No	Type of Land use	SWAT Code	Area (Ha)	% of Total Area
1	Agricultural land generic	AGRL	296,892.3566	16.41
2	Agricultural land row crops	AGRR	90.8273	0.01
3	Rice	RICE	328,748.8299	18.17

No	Type of Land use	SWAT Code	Area (Ha)	% of Total Area
4	Orchard	ORCD	68,138.29	3.77
5	Forest mixed	FRST	356,246.1424	19.69
6	Forest- deciduous	FRSD	36,261.2006	2.00
7	Forest- Evergreen	FRSE	371,209.5911	20.51
8	Wetlands	WETL	21,498.5506	1.19
9	Pasture	PAST	15,159.5378	0.84
10	Range-bush	RNGB	41,218.5983	2.28
11	Residential high density	URHD	5,176.7289	0.29
12	Residential med/low density	URML	100,855.6309	5.57
13	Institutional	UINS	17,692.2438	0.98
14	Industrial	UIDU	21,701.5512	1.20
15	Tall fescue	FESC	2,979.4418	0.16
16	Water	WATR	125,608.0624	6.94
	Total		**1,809,477.58**	**100**

The soil was used classified by the percentage of watershed threshold values for 10% of soil types. By specifying the percentage values, the soil types were created into nine classes (Figure 21). The details of the values after the finished generation are shown in Table 8.

Most of the soil types in the Bang Pakong river basin is Orthic Acrisols (36.94%) with a layer of clay accumulation, and this class consists only of clays with low cation exchange capacity. Thionic Fluvisols (15.61%), which was an Alluvial and floodplain soils with little profile development, and Dystric Nitosols (15.48%), which was Acid soils with a very thick layer of clay accumulation, respectively.

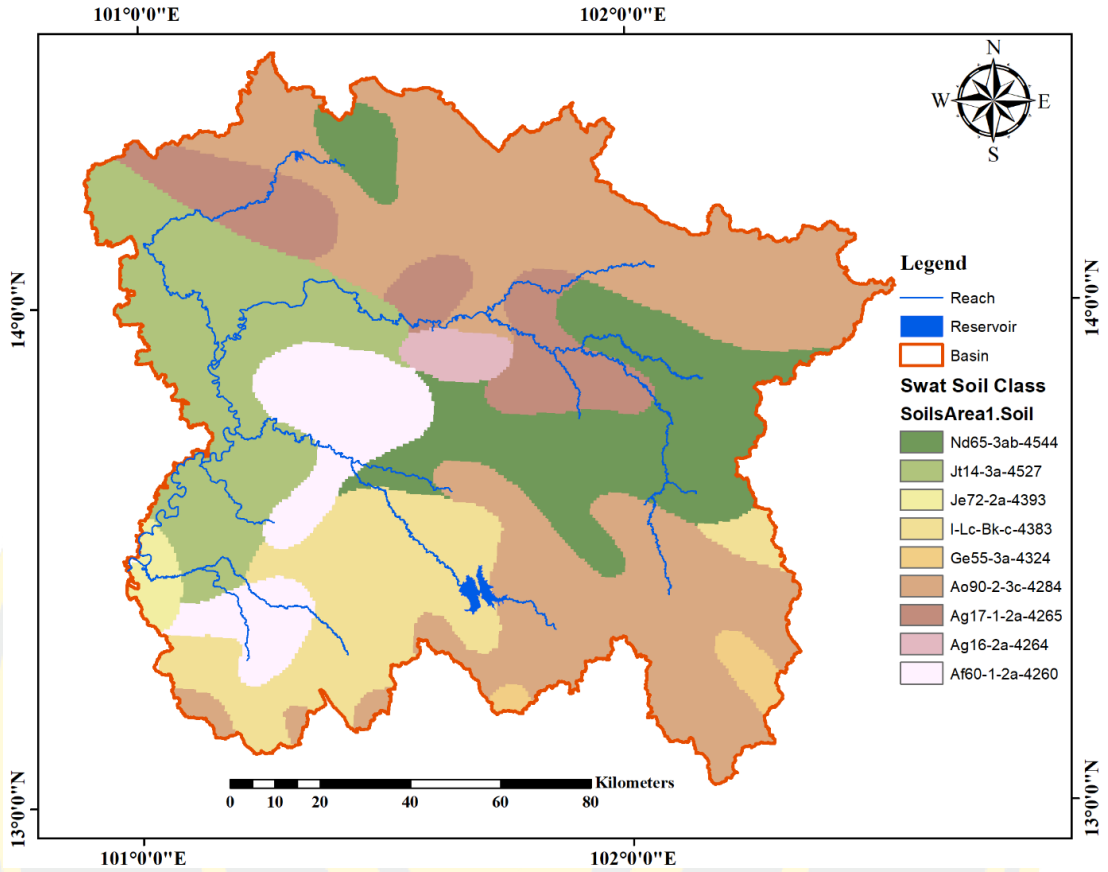

Figure 21 Soil classified by SWAT model

Table 8 Soil class of study area after the threshold

No	Soil Name	SWAT code	Area (Ha)	% of Total Area
1	Orthic Acrisols	Ao90-2-3c-4284	668,348.0072	36.94
2	Gleyic Acrisols	Ag17-1-2a-4265	151,692.6279	8.38
3	Thionic Fluvisols	Jt14-3a-4527	282,475.4620	15.61
4	Dystric Nitosols	Nd65-3ab-4544	280,101.1687	15.48
5	Gleyic Acrisols	Ag16-2a-4264	23,751.6797	1.31
6	Ferric Acrisols	Af60-1-2a-4260	139,931.8055	7.74
7	Lithosols	I-Lc-Bk-c-4383	222,988.3404	12.32
8	Eutric Fluvisols	Je72-2a-4393	20,325.0127	1.12
9	Eutric Gleysols	Ge55-3a-4324	19,863.4754	1.10
	Total		**1,809,477.58**	**100**

For the slope in this area, which has a vast difference in slope and can be accessed by assuming in the model to predict the runoff, which can be divided into five classes (Table 9). The percentage of slope in the watershed threshold value is 20%.

Most of the topography in the range of slope percentage is 0-2% and 2-5%, which cover around 31.89% and 38.43% in the downstream of a flat area in the watershed.

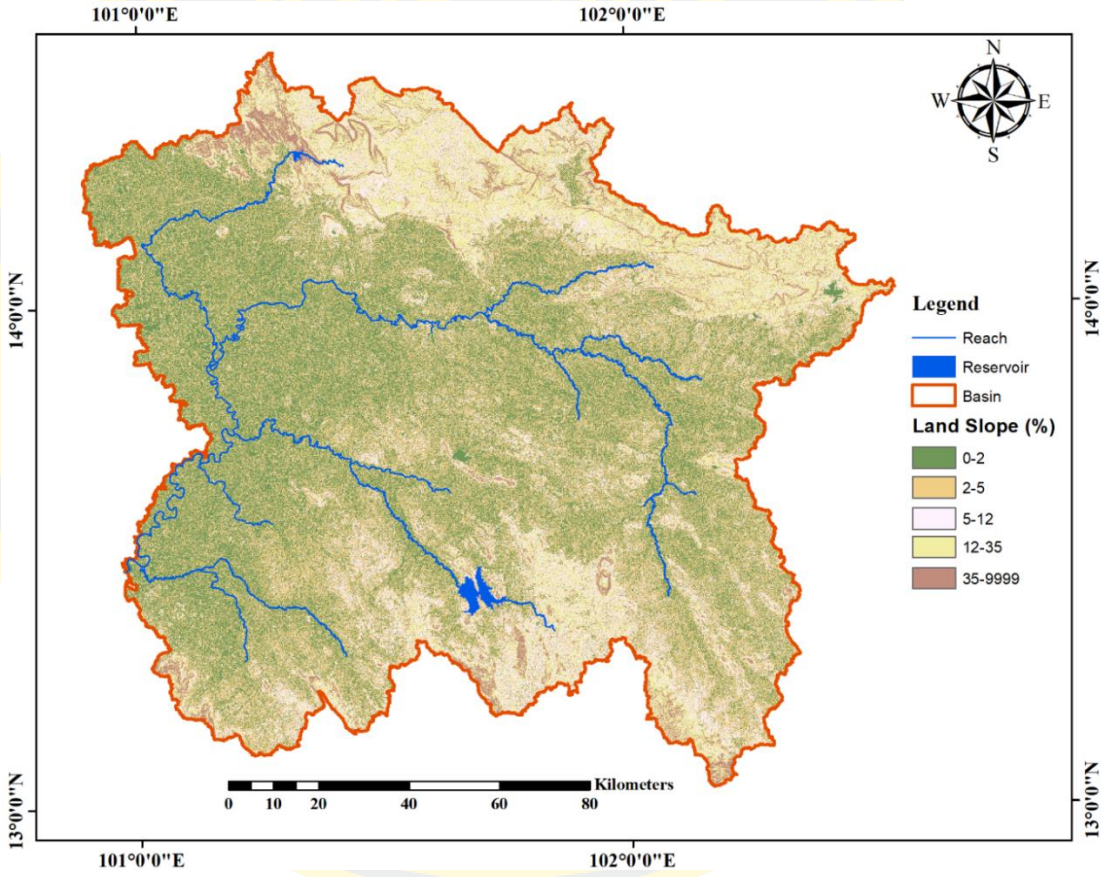

Figure 22 Slope classified by SWAT model

Table 9 Slope class of study area after the threshold

No	Lower Limit (%)	Upper Limit (%)	Area (Ha)	% of Total Area
1	0	2	577,054.5661	31.89
2	2	5	695,352.8338	38.43
3	5	12	256933.7808	14.20
4	12	35	210300.8958	11.62
5	35	9999	69835.5028	3.86
	Total		**1,809,477.58**	**100**

Modelling of Bang Pakong hydrology where water movement and related pollution are covered by the hydrology process. Also, the hydrology understanding process is necessary for the assessment of the environmental impact and economics of the Bang Pakong River Basin. This watershed is receiving the amount of water downstream with a total area of 1,809,477.58 ha. There is a three-month peak flow as of July to September and low of streamflow from November to April.

4.2 Sensitive Parameters

Sensitivity analysis was conducted before the model calibration to maintain time during the calibration. Specifying sensitive parameters allows the user to focus only on those parameters that affect most of the simulated output during the calibration because SWAT model has many parameters to handle. Some parameters do not affect the output of the model, while some parameters may have a slight effect.

4.2.1 Parameters sensitive to streamflow

Using SWAT-CUP for sensitivity analysis on the candidate parameter sets (Table 10) was use to perform the ability of the model in two observed stations at the Bang Pakong river basin, For each experiment, one iteration (i.e., 500 simulations) was run for the period 2011 to 2018, with five years calibration (2011-2015). Along with three years of validation (2016-2018).

The 17 parameters in Table 10 were used for sensitivity analysis. These parameters are used to calculate the amount of streamflow from the small-watershed. Specifying parameters is done using daily streamflow data.

Table 10 List of parameters used in the streamflow sensitivity analysis

No	Parameters	Input file	Description	Range of value
1	r_CN2	.mgt	SCS runoff curve number for moisture condition II	±25%
2	v_SURLAG	.bsn	Surface runoff lag time	0.05-24
3	v_ALPHA_BF	.gw	Baseflow alpha factor (days)	0-1
4	v_REVAPMN	.gw	Threshold depth of water in the shallow aquifer for ‘revap’ to occur (mm)	0-500
5	v_GW_DELAY	.gw	Groundwater delay (days)	0-500
6	v_RCHRG_DP	.gw	Deep aquifer percolation fraction	0-1
7	v_GWQMN	.gw	Threshold depth of water in the shallow aquifer required for return flow to occur (mm)	0-1000
8	v_EPCO	.hru	Plant uptake compensation factor	0-1
9	v_ESCO	.hru	Soil evaporation compensation factor	0-1
10	v_HRU_SLP	.hru	Average slope steepness (fraction)	0-90
11	v_SLSUBBSN	.hru	Average slope length	10-150
12	v_CH_K2	.rte	Effective hydraulic conductivity in main channel alluvium	0.01-500
13	v_CH_N2	.rte	Manning ‘n’ value for the main channel	0.01-0.3
14	v_GW_REVEP	.gw	Ground Water ‘revap’ coefficient	0.02-0.2
15	v_SOL_AWC	.sol	Available water capacity of the soil layer	0-1
16	v_SOL_K	.sol	Saturated hydraulic conductivity	0-500

No	Parameters	Input file	Description	Range of value
17	v_CANMX	.hru	Maximum canopy storage	0-50

Note: “r_” indicates that the existing parameter is added as a percentage of a given value and “v_” is the existing parameter value replaced by a given value.

4.2.1.1 Global sensitivity analysis

The global sensitivity analysis is done with the parameters shown in Table 11 From the results of the global sensitivity analysis, the most important parameters are the Initial Soil Conservation Series runoff curve number for moisture condition II (CN2), the Effective hydraulic conductivity in main channel alluvium (CH_K2), the saturated hydraulic conductivity (SOL_K), the Manning ‘n’ value for the main channel (CH_N2) and the soil evaporation compensation factor (ESCO) ranking up to the fifth position. As shown in Table 11 below, the parameters are closely linked to the watershed and hydrological characteristics of the basin. Climate situation and land use factors determine the increase and decrease of surface water flow.

In table 11, the rating for each parameter is determined by the P-value and t-stat values. The t-stat provides sensitivity measurements and, therefore, higher values of the absolute are more sensitive. On the other hand, the P-value indicates the importance of sensitivity, and the values that are closer to zero are more important. Both ranking cases (t-stat or P-value) give the same result, the parameters will have the same rank, whether they are ranked according to t-stat or P-value.

Table 11 Summary of global sensitivity analysis

Parameter Name	Parameter Description	t-Stat	P-Value	Rank
r_CN2	SCS runoff curve number for moisture condition II	-35.3	0	1
v_CH_K2	Effective hydraulic conductivity in main channel alluvium	29.885	0	2
v_SOL_K	Saturated hydraulic conductivity	-17.598	0	3
v_CH_N2	Manning ‘n’ value for the main channel	6.283	0	4
v_ESCO	Soil evaporation compensation factor	6.087	0	5
v_SLSUBBSN	Average slope length	3.144	0.002	6
v_ALPHA_BF	Baseflow alpha factor (days)	-2.313	0.021	7
v_RCHRG_DP	Deep aquifer percolation fraction	-2.199	0.028	8
v_GW_REVEP	Ground Water ‘revap’ coefficient	-0.463	0.643	9
v_SOL_AWC	Available water capacity of the soil layer	-0.386	0.698	10
v_EPCO	Plant uptake compensation factor	-0.385	0.699	11
v_SURLAG	Surface runoff lag time	-0.329	0.741	12
v_GW_DELAY	Groundwater delay (days)	-0.322	0.747	13
v_GWQMN	Threshold depth of water in the shallow aquifer required for return flow to occur (mm)	-0.24	0.810	14
v_CANMX	Maximum canopy storage	0.238	0.811	15
v_HRU_SLP	Average slope steepness (fraction)	-0.223	0.823	16

Parameter Name	Parameter Description	t-Stat	P-Value	Rank
v_REVAPMN	Threshold depth of water in the shallow aquifer for 'revap' to occur (mm)	0.152	0.879	17

Table 12 List of parameters for Model calibration, their final range, and best parameter values.

No	Parameters	Input file	Range min	Range max	Best parameter value
1	r_CN2	.mgt	-25%	25%	-0.242
2	v_SURLAG	.bsn	0.05	24	20.096
3	v_ALPHA_BF	.gw	-0.5	0.01	-0.23
4	v_REVAPMN	.gw	0	500	23.5
5	v_GW_DELAY	.gw	20	450	262.09
6	v_RCHRG_DP	.gw	0	1	0.849
7	v_GWQMN	.gw	0	500	111.5
8	v_EPCO	.hru	-0.5	0.5	0.197
9	v_ESCO	.hru	-0.5	0.5	0.021
10	v_HRU_SLP	.hru	50	150	107.099
11	v_SLSUBBSN	.hru	100	200	138.699
12	v_CH_K2	.rte	-0.5	20	13.666
13	v_CH_N2	.rte	1	2	1.939
14	v_GW_REVEP	.gw	0.02	0.2	0.175
15	v_SOL_AWC	.sol	0	1	0.335
16	v_SOL_K	.sol	0	500	69.50
17	v_CANMX	.hru	0	50	21.75

Note: "r_" indicates that the existing parameter is added as a percentage of a given value and "v_" is the existing parameter value replaced by a given value.

4.3 Model Calibration

The calibration of the SWAT model was done by using the daily observed data. At the final outlet of the subbasin for the years 2011-2015, as mentioned in chapter three, due to the limitations of the observed station. The simulated and observed daily runoff at the outlet of the subbasin were plotted for visual comparison 1:1. The model is calibrated using the value of the parameter that is specified to be highly sensitive to streamflow as described in the sensitivity analysis section. A model was run in SWAT-CUP using the default value of the parameter; there are two important problems in the balance of water in the shallow aquifer (SWAT considers only shallow aquifer water balance): a) High surface runoff, b) Low base flow (interflow or return flow). Solving these problems is a challenging task.

High surface runoff was adjusted by:

- Decreasing the curve number (CN2),
- Increasing the soil available water content (SOL_AWC), and
- Increasing the saturated hydraulic conductivity (SOL_K).

The low base flow is adjusted by:

- Decrease threshold depth of water in shallow aquifer required for the base flow to occur (GWQMN).
- Decrease groundwater revap coefficient (GW_REVAP).
- Increasing threshold depth of water in shallow aquifer for revap to occur (REVAPMN).

To calibrate and validate the available data were divided into two sets: data from the five years (2011-2015) for calibration and three years (2016-2018) for validation. The watershed characteristics, including land use, soil properties, and anthropogenic effects (e.g., agricultural management) were held constant.

For the site calibration and validation of the Bang Pakong river basin, there were selected two stations, namely, KGT3 and KGT9. These station metrics used to represent the upstream in the small watersheds in the Bang Pakong Basin.

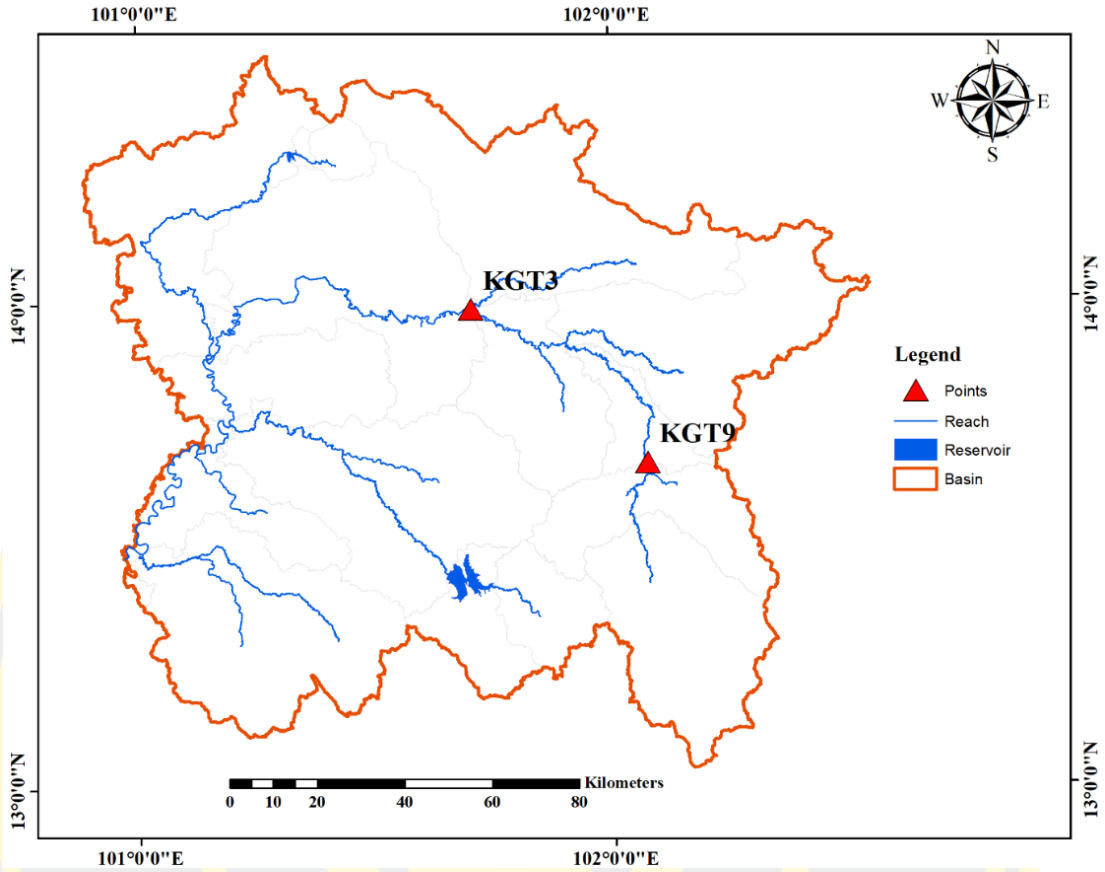

Figure 23 Station for runoff calibration in SWAT model

4.3.1 Calibrate Runoff Volume at KGT3 Station

4.3.1.1 Calibration of Daily runoff at KGT3 station

The calibration period between observed and simulated also plotted against each other in order to determine the goodness of fit (Figure 25) by using the coefficient of determination (R^2), the Nash-Sutcliffe coefficient of efficiency (NSE), and Percent bias (PBIAS). The coefficient of determination (R^2) value for daily runoff for the calibration period was 0.72, the Nash- Sutcliffe coefficient of efficiency (NSE) for the same period was found to be 0.72, and Percent Bias (PBIAS) was -12.7%, The reliable of statistic between observed and simulated indicated that the performance of the model is able to predict the daily runoff in small-watershed along with the rainfall event.

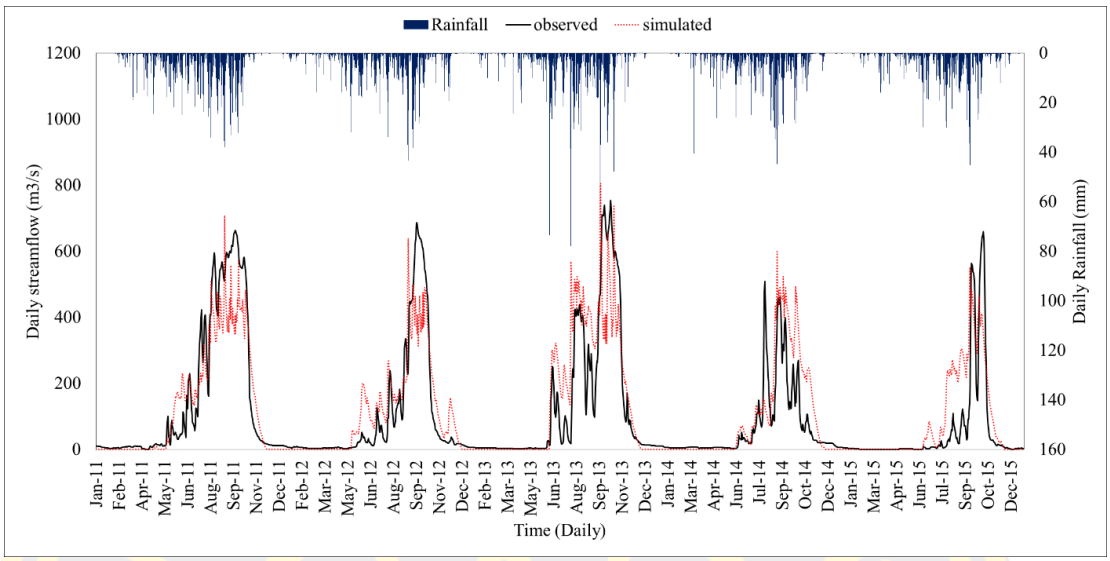

Figure 24 Comparison of observed and simulated daily runoff for the calibration period at KGT3 Station

The linear relationship between the simulated and observed streamflow shown in Figure 25 The results indicate that the streamflow for the calibration period was close to the ideal 1:1.

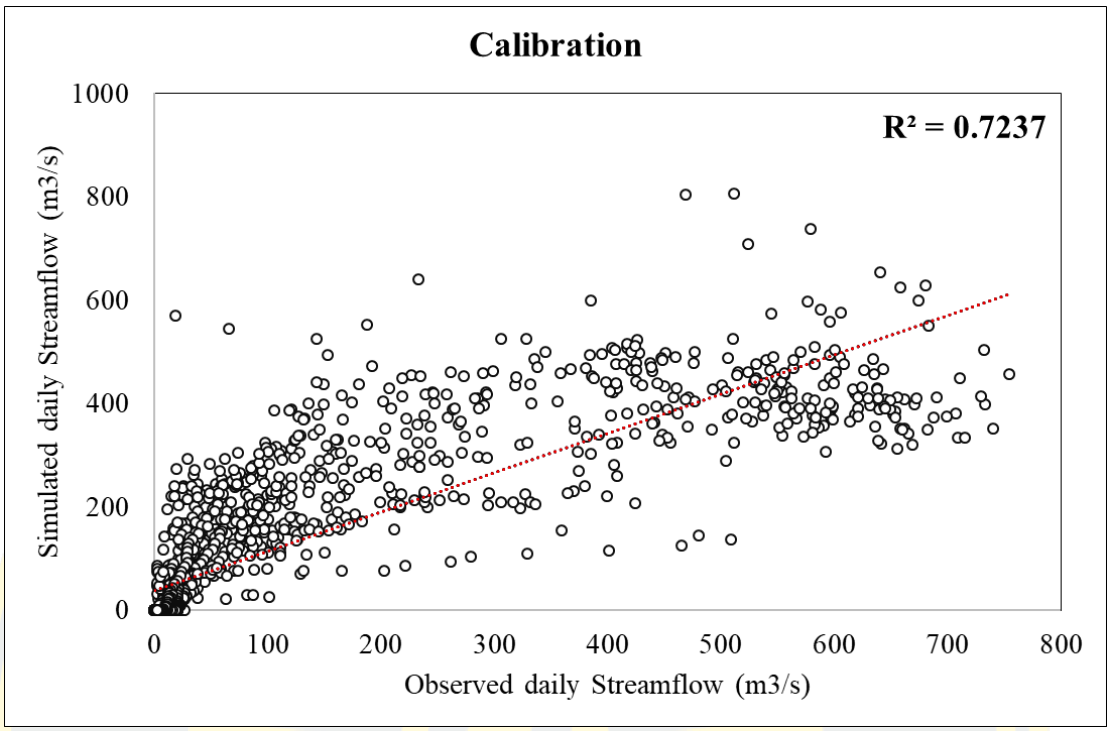

Figure 25 Goodness-of-fit for observed and simulated daily runoff for the calibration period at KGT3 Station

4.3.1.2 Calibration of Monthly runoff at KGT3 station

For the monthly calibration, the period was stated as: The coefficient of determination (R^2) value was 0.82, the Nash- Sutcliffe coefficient of efficiency (NSE) for the same period was found to be 0.80, and Percent Bias (PBIAS) was found as +16.2%

The apparent response of the calibration between the observed and simulated streamflow showed a successful simulation, as shown in Figure 26. The comparison, which was verified by the NSE, and R^2 value greater than 0.5, and PBIAS <±25%. The performance in predicting the streamflow is reasonable. These results indicated that hydrologic processes were predicted realistically by the SWAT model and could be extended to simulate other hydrologic processes, such as peak and streamflow at various watersheds.

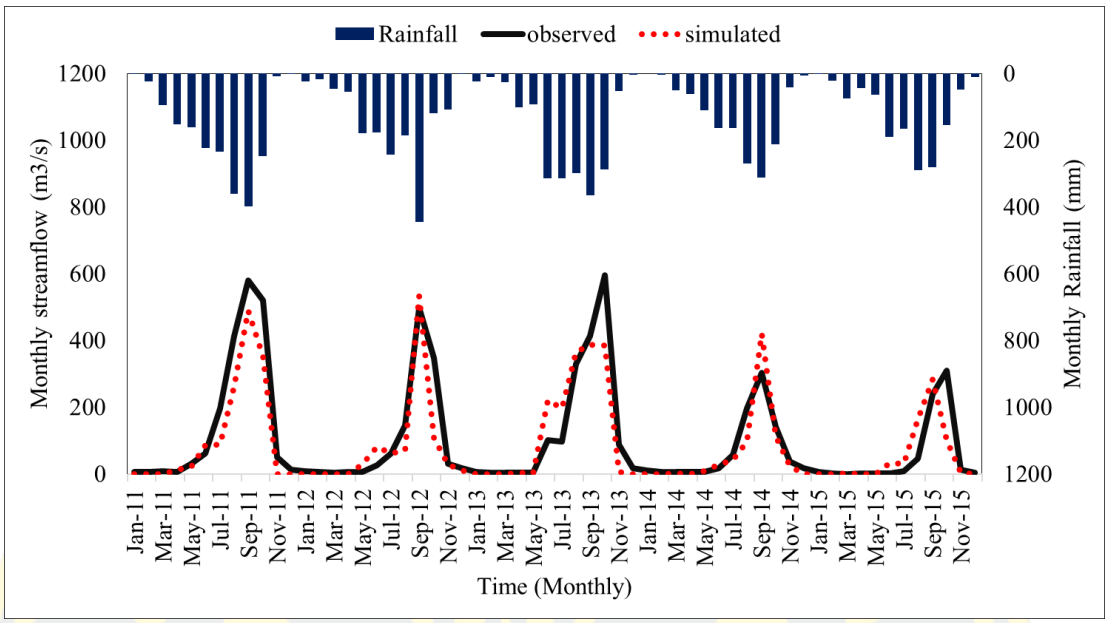

Figure 26 Comparison of observed and simulated monthly runoff for the calibration period at KGT3 Station

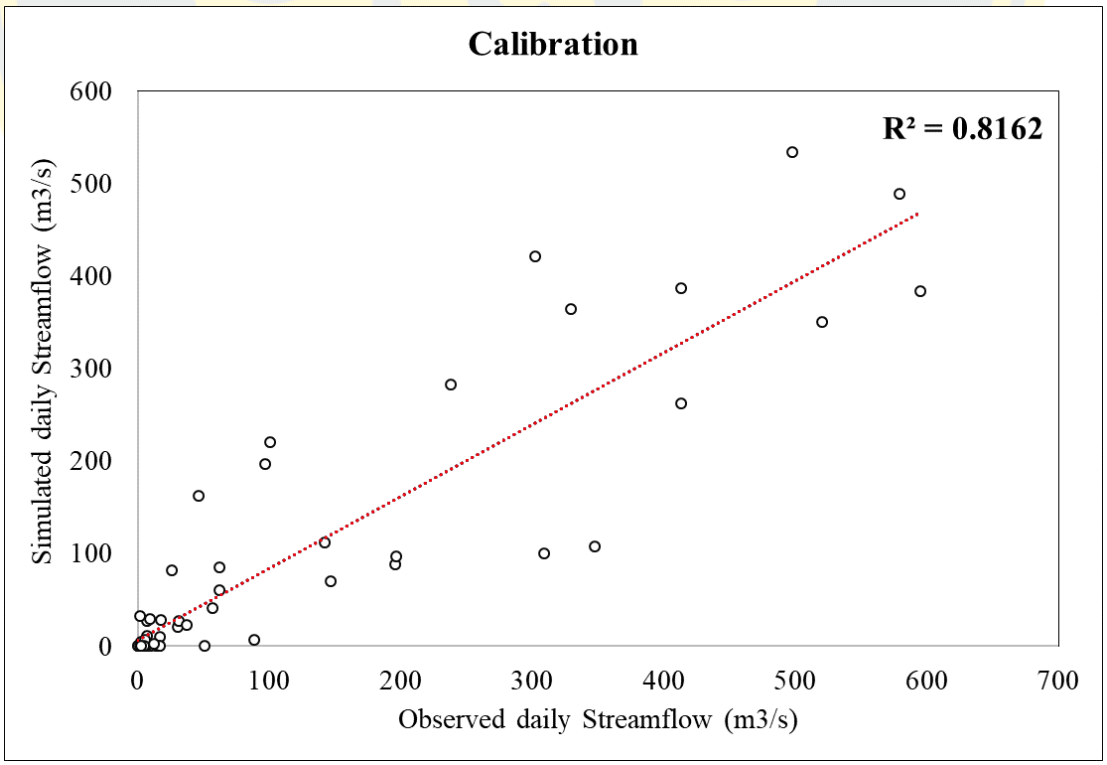

Figure 27 Goodness-of-fit for observed and simulated monthly runoff for the calibration period at KGT3 Station

4.3.2 Calibrate Runoff Volume at KGT9 Station

4.3.2.1 Calibration of Daily runoff at KGT9 station

The result shows that the coefficient of determination (R^2) value for daily runoff for the calibration period was 0.44, the Nash- Sutcliffe coefficient of efficiency (NSE) for the same period was found to be 0.42, and Percent Bias (PBIAS) was +32.8%, respectively. The linear relationship between the simulated and observed streamflows shown in Figure 29.

The graphical comparison between observed and simulated at the outlet in small-watershed by using KGT9 station (Figure 29). The SWAT model can calculate the coefficient of determination (R^2) the Nash-Sutcliffe efficiency (NSE) lower than 0.5, and Percent bias (PBIAS) higher than ±25%. The result shows that the predicted from the SWAT model was unable to simulate an extremely wet year or poorly predicted peak flows and hydrograph recession rates. Looking at Figure 28, the rainfall event is matching well with the observed data. The prediction from the model is not reliable with the rainfall event.

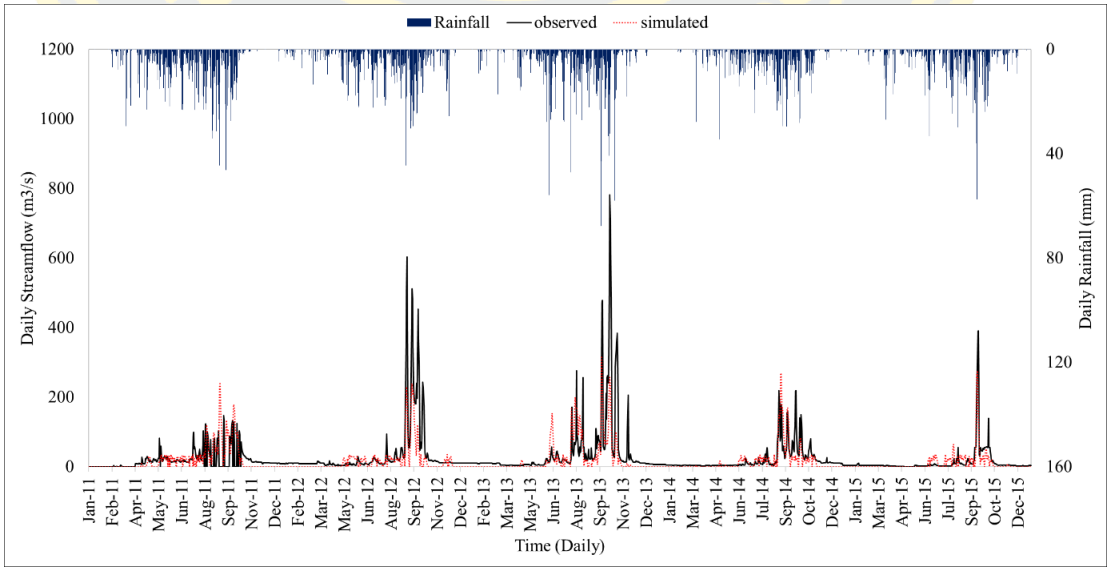

Figure 28 Comparison of observed and simulated daily runoff for the calibration period at KGT9 Station

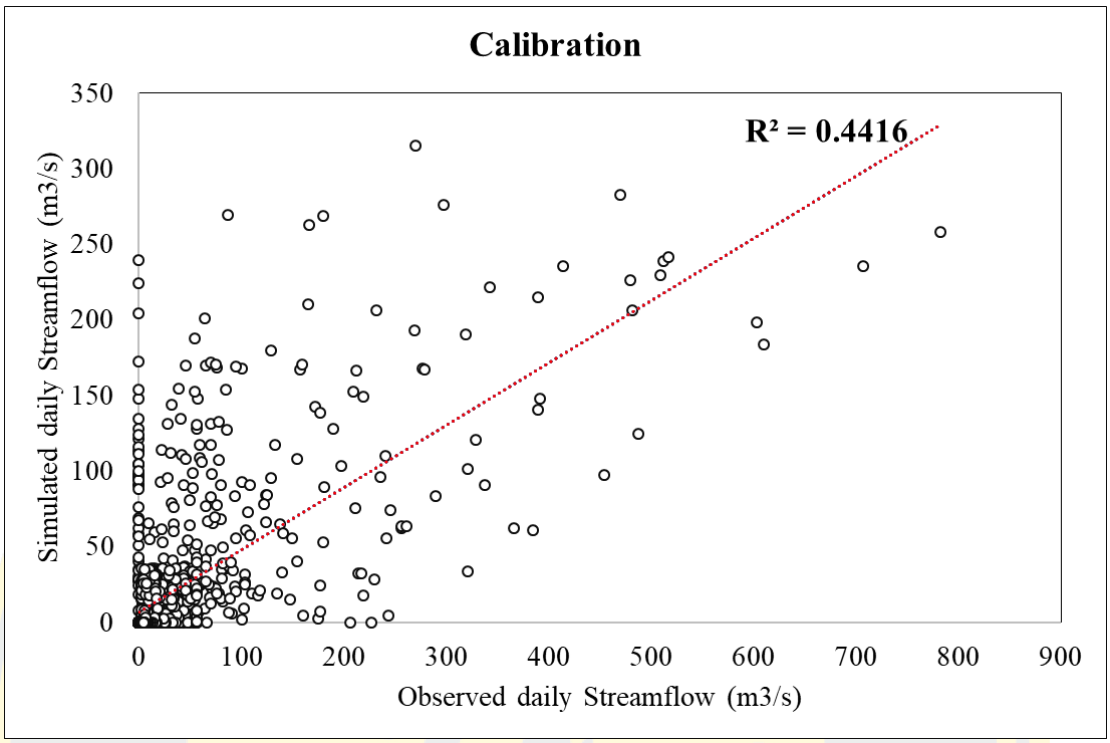

Figure 29 Goodness-of-fit for observed and simulated daily runoff for the calibration period at KGT9 Station

4.3.2.2 Calibration of Monthly runoff at KGT9 station

For the monthly calibration, the period was stated as: The coefficient of determination (R^2) value was 0.57, the Nash- Sutcliffe coefficient of efficiency (NSE) for the same period was found to be 0.54, and Percent Bias (PBIAS) is +14.2%.

The comparison, which was verified by the NSE, and R^2 values are Satisfactory (>0.5), and PBIAS <±25%. Furthermore, the goodness-of-fit is a satisfactory criterion. The performance in predicting the streamflow is reasonable. The observed and simulated as shown in Figure 30.

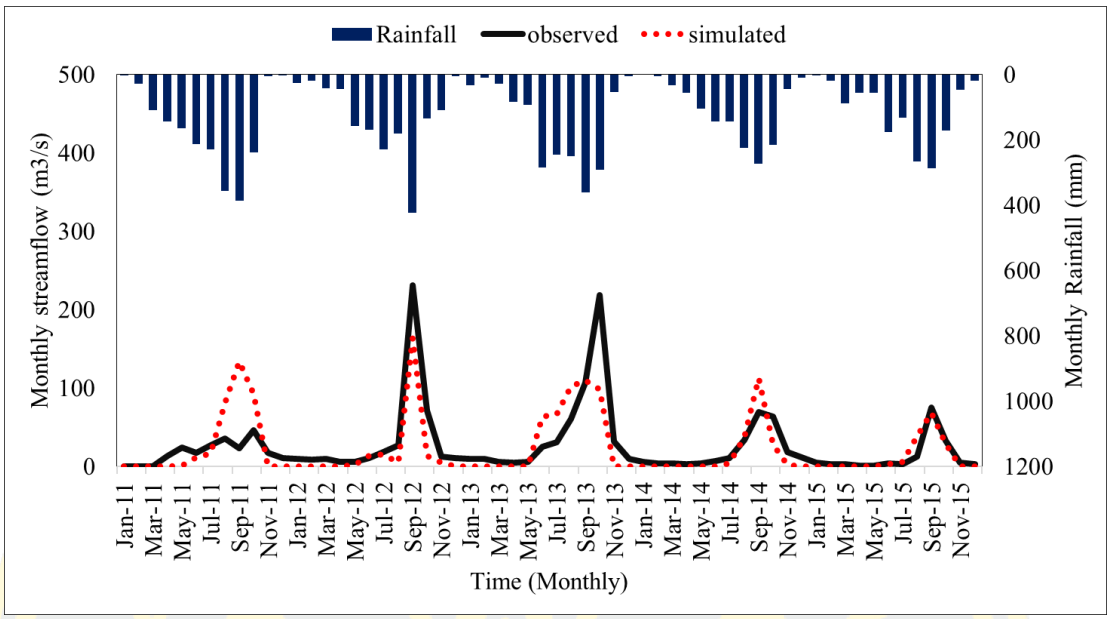

Figure 30 Comparison of observed and simulated monthly runoff for the calibration period at KGT9 Station

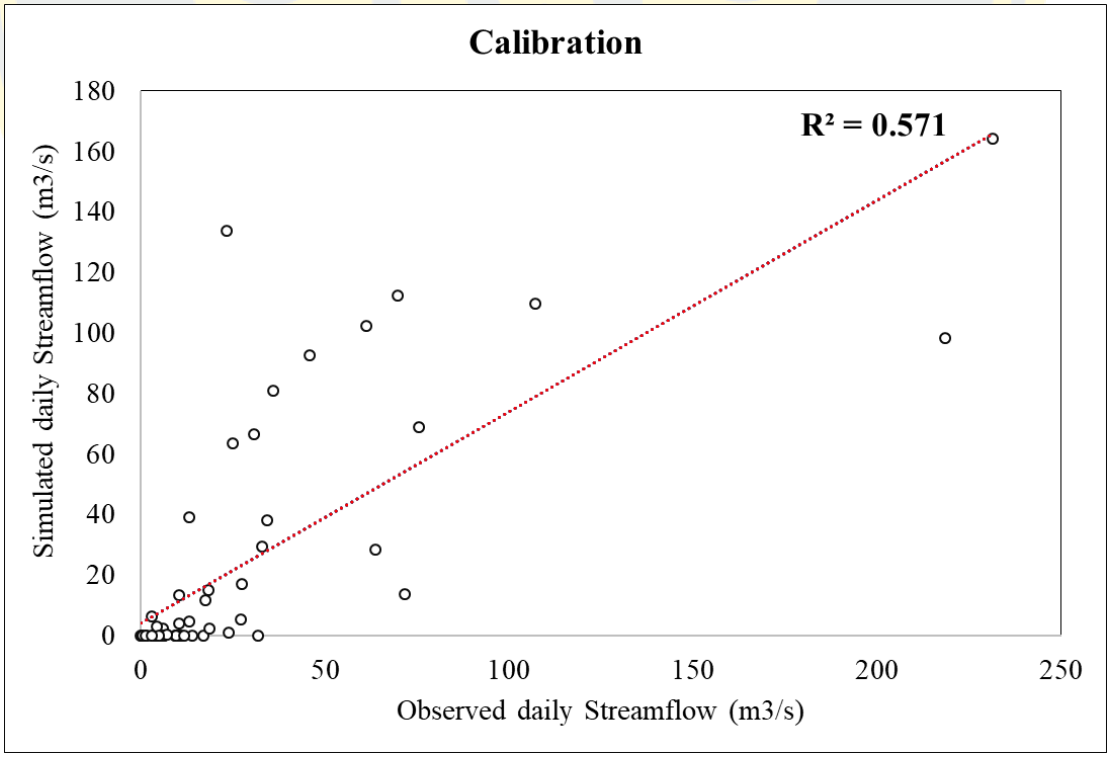

Figure 31 Goodness-of-fit for observed and simulated monthly runoff for the calibration period at KGT9 Station

4.4 Model Validation

The validation of the SWAT model was done by using the daily and monthly observed runoff data for the year 2016-2018, as mentioned in chapter three. The simulated and observed daily runoff at the outlet of the subbasin were plotted for visual comparison 1:1, by using the coefficient of determination (R^2), the Nash-Sutcliffe coefficient of efficiency (NSE), and Percent bias (PBIAS).

4.4.1 Validation of Runoff Volume at KGT3 Station

4.4.1.1 Validation of Daily runoff at KGT3 station

The statistical accuracy in the validation using the Nash-Sutcliffe efficient coefficient (NSE), the coefficient of determination (R^2), and Percent bias (PBIAS). The result in the calibration of the measure and simulated runoff at KGT3 were the R^2 was 0.42, NSE was 036, which unsatisfactory values and Percent bias (PBIAS) was +2.1%, respectively.

The linear relationship between the simulated and observed streamflow shown in Figure 33 The results indicate that the streamflow for the calibration period was not close to the ideal 1:1. The relatively low value of R^2 and NSE was due to the fact that the model overestimated some peaks. Since NSE squared the difference in observed and simulated values, the error appeared to be very high and lowers the value of NSE. In Figure 32 in August 2018, the model over predicted the runoff, which appeared to be reasonable since there was a rainfall corresponding to these peaks, which can create these events. Furthermore, relative to the discontinuous of data collecting in KGT3 Station in the validation period (2016-2018), which was no value observed data in some year.

The linear relationship between the simulated and the observed streamflow is shown in Figure 33. The results indicate that the streamflow for the calibration period is not close to the ideal 1:1. The relatively low values of R^2 and NSE are due to the fact that the model evaluates the maximum value at some point, because NSE squares difference in the observed and simulated values, so the error is very high and decreases

the value of NSE. In figure 4.14, in August 2018, the model over predicted the runoff, which seems unreliable because rainfall is consistent with these peaks. In addition, when compared to the discontinuity of data collection at the KGT3 station during the inspection period (2016-2018), where there is no observation data for some months.

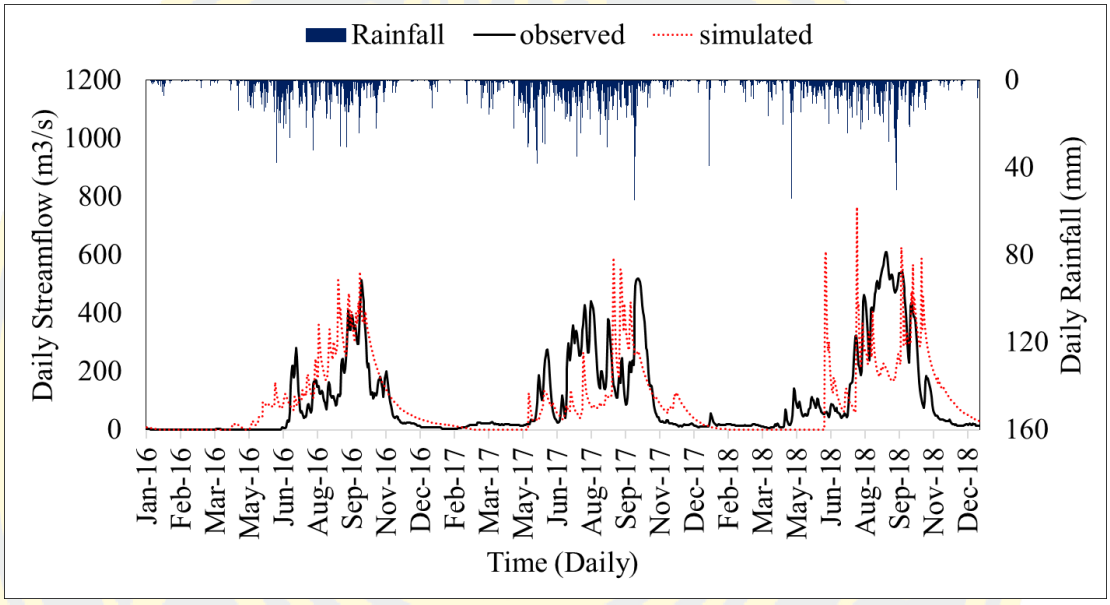

Figure 32 Comparison of observed and simulated daily runoff for the validation period at KGT3 Station

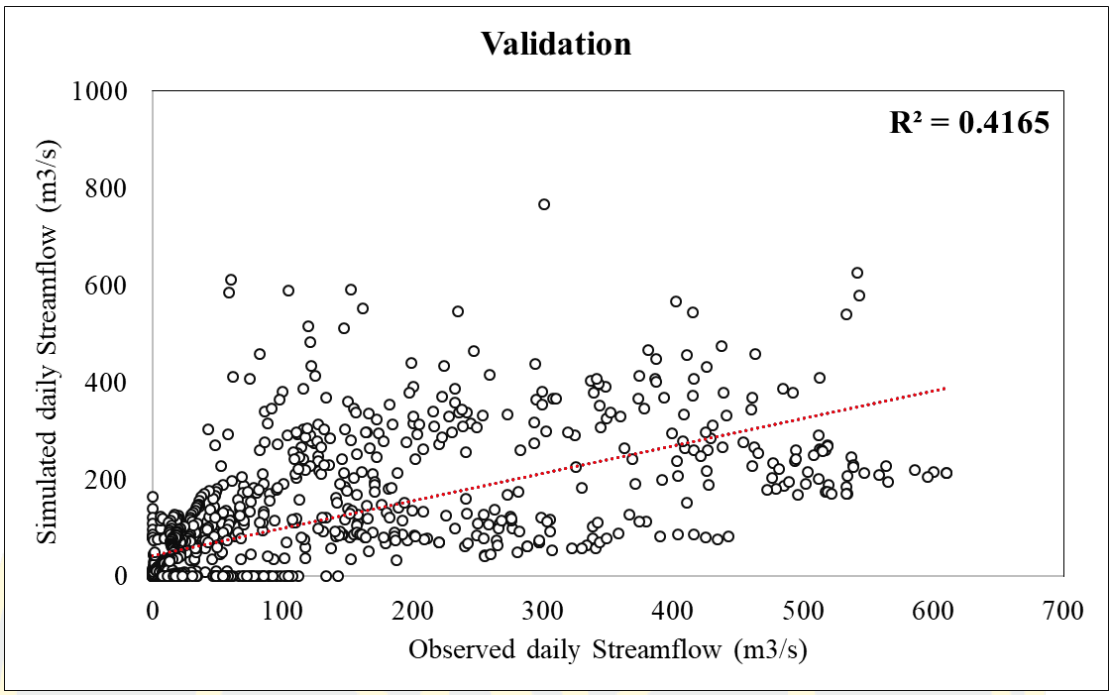

Figure 33 Goodness-of-fit for observed and simulated daily runoff for the validation period at KGT3 Station

4.4.1.2 Validation of Monthly runoff at KGT3 station

Using the same parameters as Monthly runoff calibration in SWAT-CUP, the period was stated as: The coefficient of determination (R^2) value was 0.53, the Nash-Sutcliffe coefficient of efficiency (NSE) for the same period was found to be 0.45, and Percent bias (PBIAS) are +33.2%.

The lower value for the Nash-Sutcliffe efficiency (NS) was not a surprise since there was a strange thing in the observed data. Looking at the plot of observed versus simulated runoff shown in Figure 34, one can see that in August and October every year of 2016-2018. There was a corresponding rainfall event, and the observation is responded to these events. On the contrary to this, the model not responded well to these rainfall events. Furthermore, the important reason is the discontinuous runoff data in this station, which was lacking data in some months.

The goodness-of-fit of observed and simulated monthly discharge for 2016-2018 using a scatter plot can be visualized from Figure 35 below.

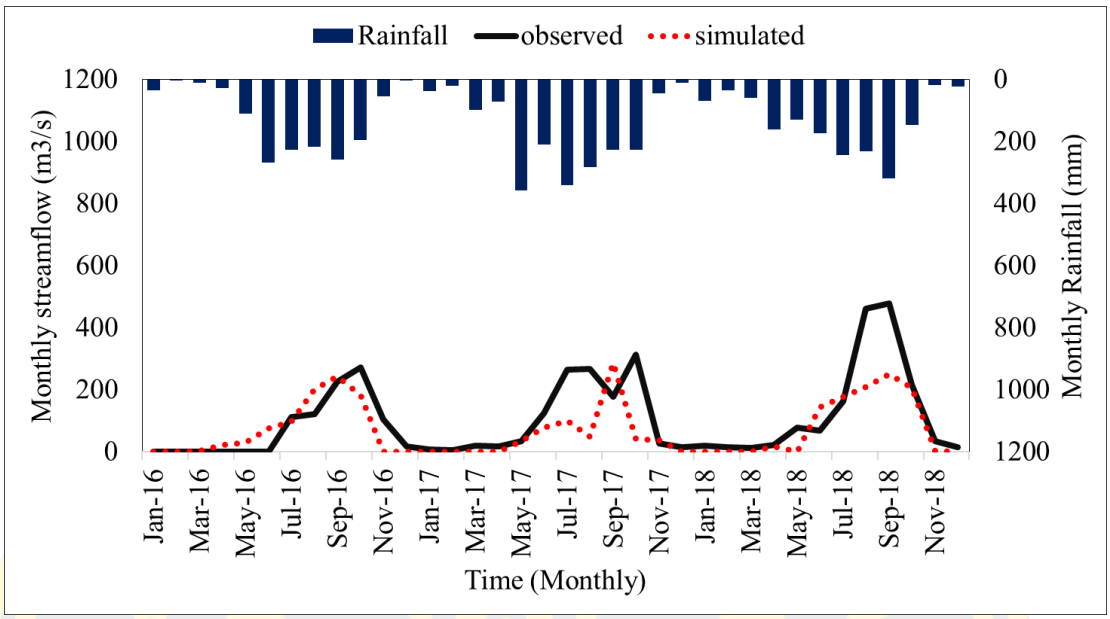

Figure 34 Comparison of observed and simulated monthly runoff for the validation period at KGT3 Station

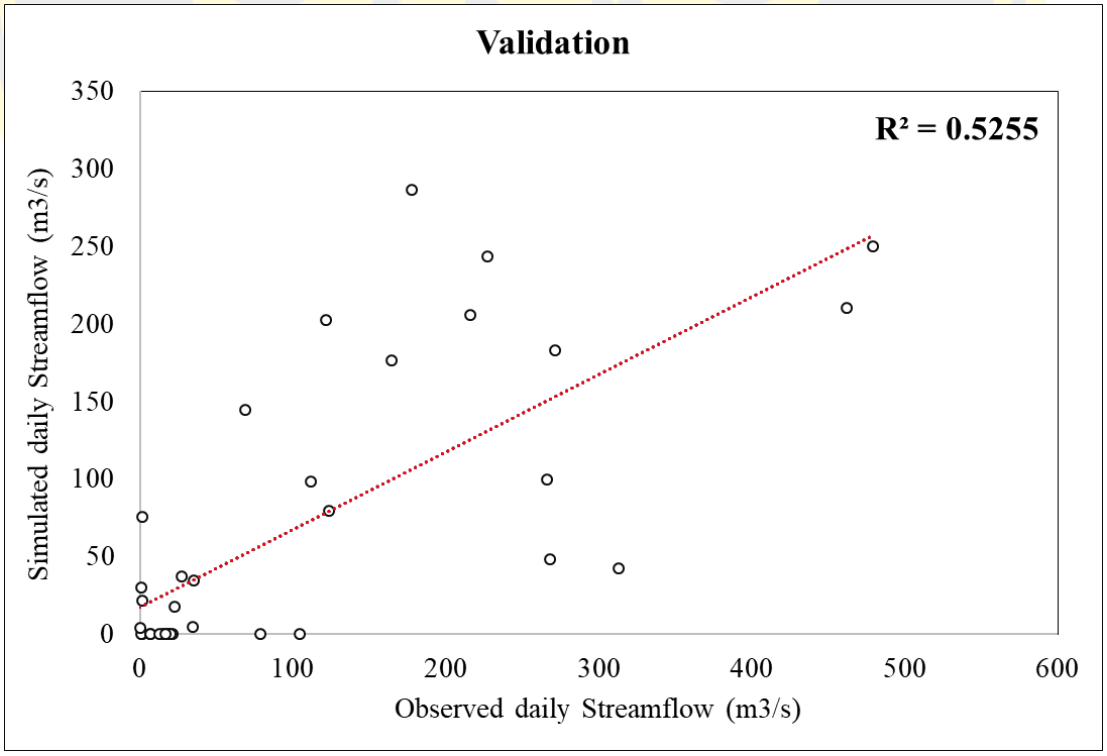

Figure 35 Goodness-of-fit for observed and simulated monthly runoff for the validation period at KGT3 Station

4.4.2 Validation of Runoff Volume at KGT9 Station

4.4.2.1 Validation of Daily runoff at KGT9 station

The statistical accuracy in the validation using the Nash-Sutcliffe efficient coefficient (NSE), the coefficient of determination (R^2), and Percent bias (PBIAS). The result in the validation of the measure and simulated daily runoff at KGT9 were the R^2 was 0.29, NSE was 0.22, which unsatisfactory values and Percent bias (PBIAS) was +16.1%, respectively.

The apparent response of the validation between the observed and simulated streamflow showed the unsatisfactory in statistic, as shown in Figure 36, The comparison which was verified by the NSE, and R^2 value lower than 0.5. For daily validation, the lower value of NSE and R^2 was not a surprise. The important reason is the discontinuous runoff data in this station, which was lacking data in some months bring the runoff values are error.

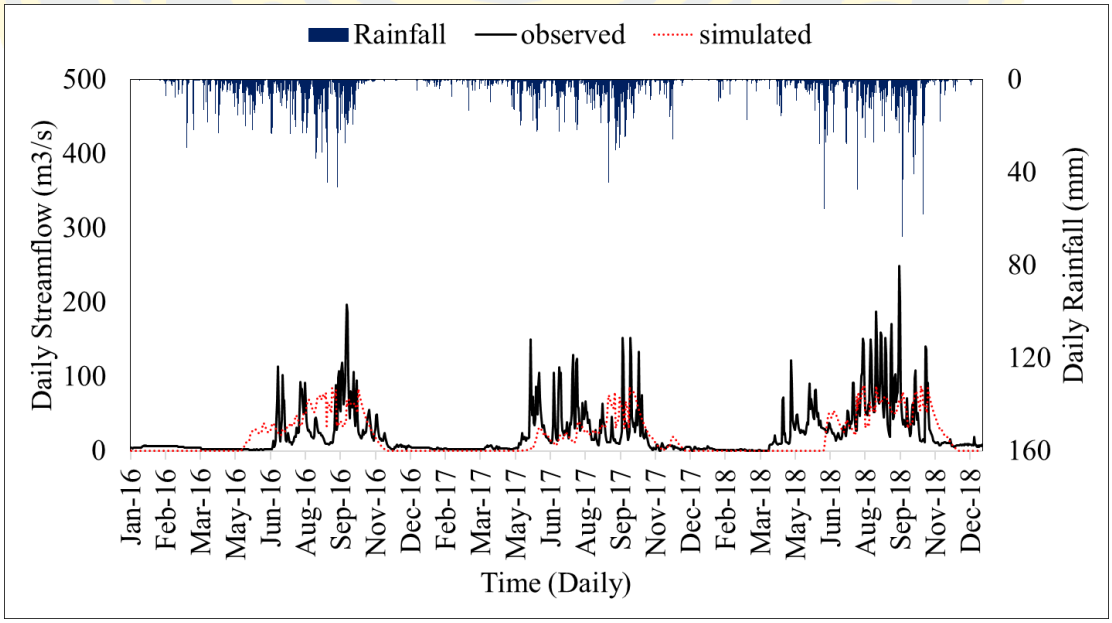

Figure 36 Comparison of observed and simulated daily runoff for the validation period at KGT9 Station.

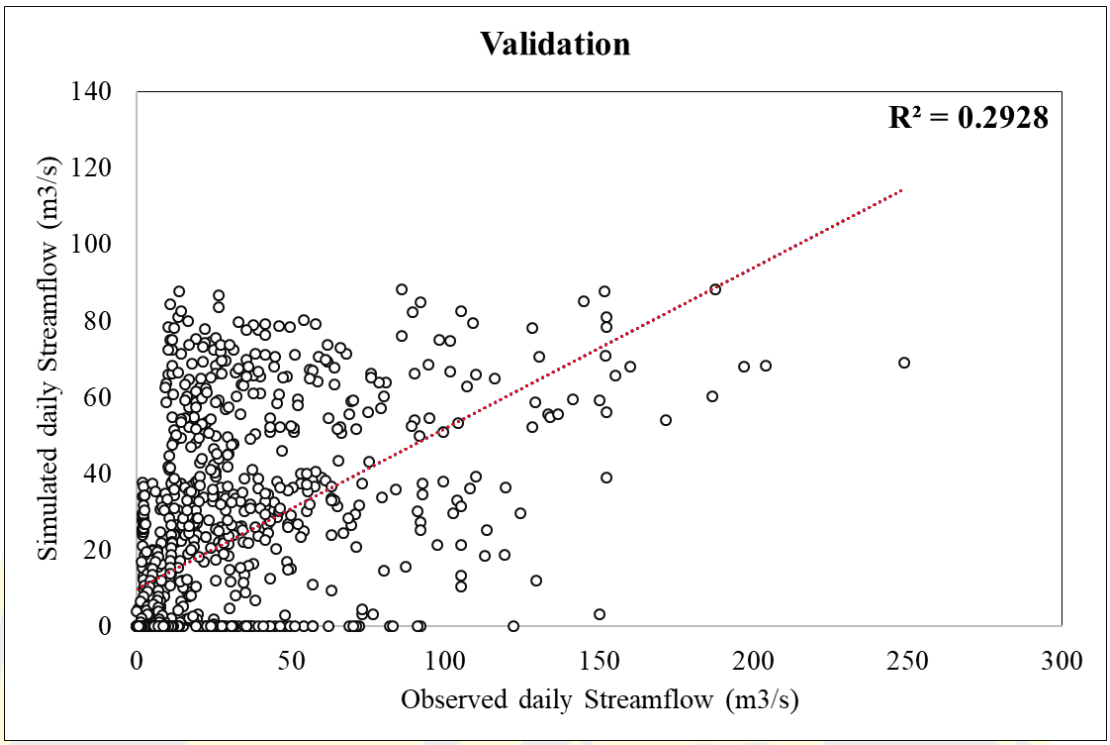

Figure 37 Goodness-of-fit for observed and simulated daily runoff for the validation period at KGT9 Station

4.4.2.1 Validation of Monthly runoff at KGT9 station

For the monthly validation, the period was stated as: The coefficient of determination (R^2) value was 0.55, the Nash- Sutcliffe coefficient of efficiency (NSE) for the same period was found to be 0.30, and Percent bias (PBIAS) was found to be +47.9%, Respectively.

The lower value for the Nash-Sutcliffe efficiency (NSE) was not a surprise, similar to the monthly validation from KGT3 station. The important reason is the discontinuous runoff data. The runoff from the observed station is corresponding with the rainfall event. On the other hand, the model not responded well to these rainfall events.

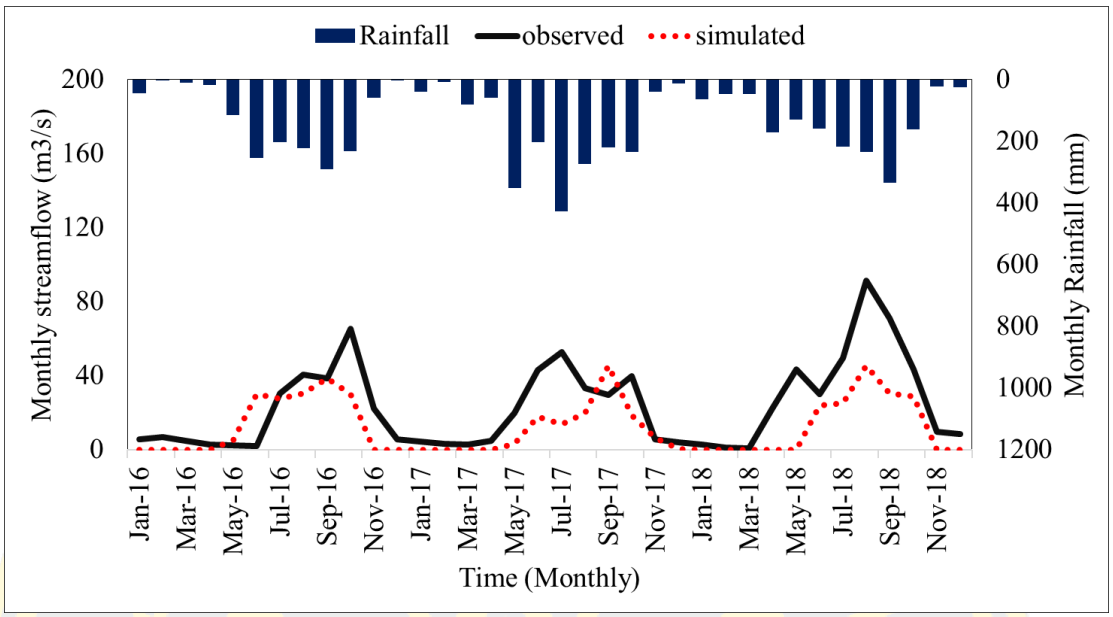

Figure 38 Comparison of observed and simulated monthly runoff for the validation period at KGT9 Station

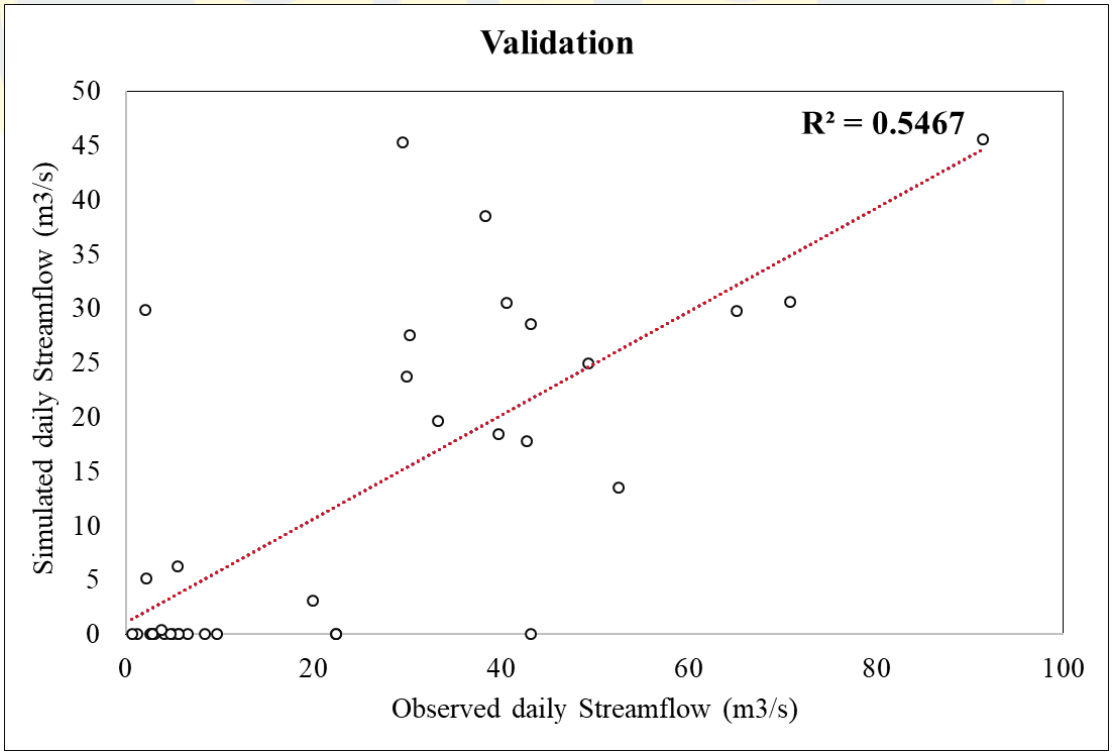

Figure 39 Goodness-of-fit for observed and simulated monthly runoff for the validation period at KGT9 Station

4.5 Summary of Model experiment

Calibration and validation of the runoff of the SWAT are performed by comparing the predicted streamflow with the corresponding streamflow measurements for eight years (2011-2018) from two gaging stations within the Bang Pakong river basin, Eastern past of Thailand.

The statistical comparison of calibration results with the observed data in KGT3 and KGT9 indicated that there is a reasonable agreement for both daily and monthly determination by using coefficient (R^2), the Nash-Sutcliffe coefficient (NSE), and Percent bias (PBIAS) with the range: R^2 = 0.72 and 0.44, NSE = 0.72 and 0.42, PBIAS = -12.7% and +32.8% for daily calibration and R^2 = 0.82 and 0.57, NSE = 0.80 and 0.54, and PBIAS = +16.2%, +14.2% for monthly calibration period, respectively.

The validation results of the model show that the lower values of R^2, NSE and PBIAS values are R^2 = 0.42 and 0.29, NSE = 0.36 and 0.22, PBIAS = +2.1%, +16.1% for daily validation, and R^2= 0.53 and 0.55, NSE = 0.45 and 0.30, PBIAS = +33.1%, +47.9% for monthly validation period, respectively.

In summary, it should be noted that the Soil and Water Assessment Model (SWAT) model evaluation can be used as a decision support tool for sustainable water resources management. SWAT is a semi-distributed model that needs distributed physical input data. Spatial and temporary information should be used to develop the SWAT project. To get good results, SWAT looks for rain gauges or precipitation stations near the center of each subbasin to create runoff. Furthermore, to get more accuracy for calibration and validation. The observed station must be used to determine the location of the station in upstream and downstream, which should cover all of the basins. In addition to improving the efficiency of the model, detailed information is needed. And the long term for further analysis.

CHAPTER 5
CONCLUSION AND FUTURE WORKS

5.1 Conclusion

There have been several water management problems in the Bang Pakong river basin. The area of study is approximately 18,087 km^2, which caused significant for the agricultural and industrial sectors. In order to provide information for water resources management, The Soil and Water Assessment Tool (SWAT) has been used to simulate the runoff in the watersheds. SWAT is a physically-based distributed model developed by the USDA - ARS to predict the impact of land management practices on water, sediment, and agricultural chemical yield in large, a complex watershed with varying soil, land use, and management condition. The principal objective of the research was to simulate streamflow in the Bang Pakong river basin and to compare the model result and field observation (measure station) in the watershed.

The SWAT model can simulate the daily water yield using Weather data, rainfall, temperature, relative humidity, and wind speed in the Bang Pakong river basin. To check the ability of the model with streamflow data from the observed station (KGT3 & KGT9) was used to compare with model simulating. The available streamflow data for calibration and validation were limited. A model was calibrated by using five years (2011 to 2015) and validated for three years (2016-2018) of daily streamflow data collected from the Royal Irrigation Department (RID). The average simulated daily and monthly runoff by SWAT were compared with the corresponding average values of the observation using graphical and statistical methods. By setup the SWAT model with watershed characteristics, including land use, soil properties, and Digital Elevation Model (DEM), combined with Geographic Information System (GIS) interface.

Model performance is adjudged base on visual comparison of the observed and simulated model as well as on statistical by using a coefficient of determination (R^2), Nash-Sutcliffe efficiency (NSE), and Percent bias (PBIAS). Additionally, ArcSWAT2012 and ArcGIS10.5, combined with Sequential Uncertainty Fitting-2

(SUFI-2) algorithms in SWAT Calibration and Uncertainty Procedures (SWAT-CUP) programs was used for sensitivity analysis.

The result from the SWAT model indicates that the Bang Pakong river basin was divided into 17 sub-basins, with 99 Hydrological response units (HRUs), sixteen types of land use, nine types of soil series, and five different range of percentage slope. For sensitivity analysis in SWAT-CUP showed that the most five parameters were sensitive to the simulation of streamflow were: the Initial Soil Conservation Series runoff curve number for moisture condition II (CN2), the Effective hydraulic conductivity in main channel alluvium (CH_K2), the saturated hydraulic conductivity (SOL_K), the Manning 'n' value for the main channel (CH_N2) and the soil evaporation compensation factor (ESCO), respectively.

The statistical accuracy in the daily runoff calibration is shown by the Nash-Sutcliffe coefficient (NSE), the coefficient of determination (R^2), and Percent bias (PBIAS). The statistic for daily runoff calibration between observed and simulated streamflow at observed station KGT3, KGT9 was stated as; the coefficient of determination (R^2 = 0.72, 0.44), the Nash-Sutcliffe efficiency coefficient (NSE = 0.72, 0.42), and Percent bias (PBIAS = -12.7%, +32.8%), respectively. The statistic for monthly runoff calibration between observed and simulated streamflow was stated as; the coefficient of determination (R^2 = 0.82, 0.57), the Nash-Sutcliffe efficiency coefficient (NSE = 0.80, 0.54), and Percent bias (PBIAS = +16.2%, +14.2%), respectively.

The validation of daily runoff for the year 2016-2018 at KGT3 and KGT9 station in sub-watershed give the low values of coefficient of determination (R^2 = 0.42, 0.29), the Nash-Sutcliffe efficiency coefficient (NSE = 0.36, 0.22), and Percent bias (PBIAS = +2.1%, +33.2%), respectively. The statistic for monthly runoff validation between observed and simulated streamflow was stated as; the coefficient of determination (R^2 = 0.53, 0.55), the Nash-Sutcliffe efficiency coefficient (NSE = 0.45, 0.30), and Percent bias (PBIAS= +33.1%, +47.9%), respectively.

In general, this model corresponded well with monthly data compared to daily data. However, in the validation period, the values are not reliable due to the discontinuity of observed data in both two stations. The model seems to have predicted runoff and under base flow predicted in some years. The reason for daily streamflow data used for validation is not reliable.

Calibration and validation of the SWAT model show that simulated daily and monthly streamflow are satisfactory agreements with measured values. The results show that the scale model of the SWAT model has the ability to simulate the runoff from the Bang Pakong River Basin.

As a result of this study, it is believed that SWAT is a reasonable option for the runoff simulation of the Bang Pakong Basin. The result of this study could have been better if spatially distributed precipitation data, long-term streamflow data, high resolution of soil data, integrated of some other climatic data such as solar radiation, good knowledge of the user in the watershed areas, and time spent.

5.2 Recommendations

1) This study applying the SWAT model to the Bang Pakong River Basin to simulate runoff is considered a preliminary work since SWAT was not applied in the same river basin before.

2) The digital elevation model (DEM) is equally important fundamental for the rainfall-runoff model for watershed delineation. High accuracy of resolution of DEM is required as essential input data.

3) Soil map was of poor quality. Therefore, this may have a big impact on water balance, and high-resolution geographic data suggest improvements to the results.

4) Concerning observed and measurement data in the SWAT model, Meteorological data and hydrological data are not systematically in this study area. The data for a study should be updated as well as available. Therefore the data should emphasize with more accuracy, which can be obtained from the extension of data.

5) Most of the measurement station is located in upstream, without stations are covering the downstream area. Moreover, measurement stations should be established for future research.

6) The process is considered a time-consuming task. Wide range of different data needs to be obtained to run the model and numerous parameters needed to be modified during the calibration which needs a lot of patience to deal with.

7) There is plenty of rooms for improvement of this work in the future.

REFERENCES

Abbaspour, K. C., Rouholahnejad, E., Vaghefi, S., Srinivasan, R., Yang, H., & Kløve, B. (2015). A continental-scale hydrology and water quality model for Europe: Calibration and uncertainty of a high-resolution large-scale SWAT model. *Journal of Hydrology, 524*, 733-752. doi:10.1016/j.jhydrol.2015.03.027

Abbaspour, K. C., Yang, J., Maximov, I., Siber, R., Bogner, K., Mieleitner, J., . . . Srinivasan, R. (2007). Modelling hydrology and water quality in the pre-alpine/alpine Thur watershed using SWAT. *Journal of Hydrology, 333*(2-4), 413-430. doi:10.1016/j.jhydrol.2006.09.014

Adeogun, A. G., Sule, B. F., & Salami, A. W. (2015). SIMULATION OF SEDIMENT YIELD AT THE UPSTREAM WATERSHED OF JEBBA LAKE IN NIGERIA USING SWAT MODEL. *Malaysian Journal of Civil Engineering, 27*(1). doi:10.11113/mjce.v27n1.356

Alibuyog, N., Ella, V. B., Reyes, M. R., Srinivasan, R., Heatwole, C. D., & Dillaha, T. A. (2008). Predicting the effects of land use on runoff and sediment yield in selected sub-watersheds of the Manupali River using the ArcSWAT model. In.

Allen, R. G., Pereira, L. S., Raes, D., & Smith, M. (1998). Crop evapotranspiration guidelines for computing crop requirements. FAO Irrig. Drain. Report modeling and application. *Journal of Hydrology, 285*, 19-40.

Arnold, J. G. (1990). *SWRRB : a basin scale simulation model for soil and water resources management*: Texas A & M University Press.

Arnold, J. G., & Fohrer, N. (2005). SWAT2000: Current capabilities and research opportunities in applied watershed modelling. *Hydrological Processes, 19*(3), 563-572. doi:10.1002/hyp.5611

Arnold, J. G., Moriasi, D. N., Gassman, P. W., Abbaspour, K. C., White, M. J., Srinivasan, R., . . . Arnold, J.-F. G. (2012). SWAT: MODEL USE,

CALIBRATION, AND VALIDATION. *Transactions of the ASABE, 55*(4), 1491-1508.

Arnold, J. G., Srinivasan, R., Muttiah, R. S., & Williams, J. R. (1998). LARGE AREA HYDROLOGIC MODELING AND ASSESSMENT PART I: MODEL DEVELOPMENT. *Journal of the American Water Resources Association, 34*(1), 73-89. doi:10.1111/j.1752-1688.1998.tb05961.x

Arnold, J. G., & Williams, J. R. (1987). Validation of SWRRB—simulator for water resources in rural basins. *Journal of Water Resources Planning and Management, 113*(2), 243-256. doi:10.1061/(ASCE)0733-9496(1987)113:2(243)

Arnold, J. G., Williams, J. R., & Maidment, D. R. (1995). Continuous-time water and sediment-routing model for large basins. *Journal of Hydraulic Engineering, 121*(2), 171-183. doi:10.1061/(ASCE)0733-9429(1995)121:2(171)

Arunyanart, N., Limsiri, C., & Uchaipichat, A. (2017). Flood hazards in the chi river basin, Thailand: Impact management of climate change. *Ecology and Environmental Research, 15*(4), 841-861. doi:10.15666/aeer/1504_841861

Azizian, A., & Shokoohi, A. (2014). DEM resolution and stream delineation threshold effects on the results of geomorphologic-based rainfall runoff models. *Turkish Journal of Engineering and Environmental Sciences, 38*(1), 64-78. doi:10.3906/muh-1401-13

Bateni, F., Fakheran, S., & Soffianian, A. (2013). Assessment of land cover changes and water quality changes in the Zayandehroud River Basin between 1997-2008. *Environmental Monitoring and Assessment, 185*(12), 10511-10519. doi:10.1007/s10661-013-3348-3

Behera, S., & Panda, R. K. (2006). Evaluation of management alternatives for an agricultural watershed in a sub-humid subtropical region using a physical process based model. *Agriculture, Ecosystems and Environment, 113*(1-4), 62-72. doi:10.1016/j.agee.2005.08.032

Borah, D. K., & Bera, M. (2004). WATERSHED-SCALE HYDROLOGIC AND NONPOINT-SOURCE POLLUTION MODELS: REVIEW OF APPLICATIONS. *Transactions of the ASAE, 47*(3), 789-803. doi:10.13031/2013.16110

Buakhao, W., & Kangrang, A. (2016). DEM Resolution Impact on the Estimation of the Physical Characteristics of Watersheds by Using SWAT. *Advances in Civil Engineering, 2016*. doi:10.1155/2016/8180158

Chaubey, I., Cotter, A. S., Costello, T. A., & Soerens, T. S. (2005). Effect of DEM data resolution on SWAT output uncertainty. *Hydrological Processes, 19*(3), 621-628. doi:10.1002/hyp.5607

Dany Sunandar, A., Suhendang, E., & Nengah Surati Jaya, I. (2014). Land Use Optimization in Asahan Watershed with Linear Programming and SWAT Model. *International Journal of Sciences: Basic and Applied Research (IJSBAR) International Journal of Sciences: Basic and Applied Research, 18*(1), 63-78.

Daramola, J., Ekhwan, T. M., Mokhtar, J., Lam, K. C., & Adeogun, G. A. (2019). Estimating sediment yield at Kaduna watershed, Nigeria using soil and water assessment tool (SWAT) model. *Heliyon, 5*(7), e02106-e02106. doi:10.1016/j.heliyon.2019.e02106

Department of Water, R. (2006). *Bang Pakong Dialogue Initiative (Final Report)*. Retrieved from https://www.scribd.com/document/262120889/THA-PDA-Bang-Pakong-Dialogue-Initiative-Final-Report

Department of Water, R. (2017). *A project to explore the design of hydrology stations for 25 major river basins in Thailand*. Retrieved from

Deshmukh, A., & Singh, R. (2016). Physio-climatic controls on vulnerability of watersheds to climate and land use change across the U. S. *Water Resources Research, 52*(11), 8775-8793. doi:10.1002/2016WR019189

Di Luzio, M., Arnold, J. G., & Srinivasan, R. (2004). Integration of SSURGO maps and soil parameters within a geographic information system and nonpoint source pollution model system. *Journal of Soil and Water Conservation, 59*(4).

Faksomboon, B., Suanmali, W., Chaivino, N., Khamcharoen, N., & Buasruang, S. (2019). Land Use Changes of Head Watershed Area on Streamflow, Suspended Sediment and Water Quality in Khlong Lan Watershed, Kamphaeng Phet Province | Faksomboon | Burapha Science Journal (วารสารวิทยาศาสตร์บูรพา). *BURAPHA SCIENCE JOURNAL, 24*(2), 532-549.

Faksomboon, B., & Thangtham, N. (2017). Application of SWAT model for studying land use changes on suspended sediment in Upper Tha Chin Watershed. *SWU Sci. J., 33*(2), 124-139.

Fan, M., & Shibata, H. (2015). Simulation of watershed hydrology and stream water quality under land use and climate change scenarios in Teshio River watershed, northern Japan. *Ecological Indicators, 50*, 79-89. doi:10.1016/j.ecolind.2014.11.003

Fohrer, N., Eckhardt, K., Haverkamp, S., & Frede, H. G. (2001). *Selected papers from the 10th International Soil Conservation Organization Meeting held May 24-29*. Retrieved from

Gathagu, J. N. a. a., Mutua, B. M., Mourad, K. A., & Oduor, B. O. (2018). Uncertainty analysis and calibration of swat model for estimating impacts of conservation methods on streamflow and sediment yield in Thika river catchment. *International Journal of Hydrology Research, 3*(1), 1-11. doi:10.18488/journal.108.2018.31.1.11

Gholami, R., Watson, R. T., Molla, A., Hasan, H., & Bjørn-Andersen, N. (2016). Information systems solutions for environmental sustainability: How can we do more? *Journal of the Association for Information Systems, 17*(8SpecialIssue), 521-536. doi:10.17705/1jais.00435

Ghoraba, S. M. (2015). Hydrological modeling of the Simly Dam watershed (Pakistan) using GIS and SWAT model. *Alexandria Engineering Journal, 54*(3), 583-594. doi:10.1016/j.aej.2015.05.018

Gull, S., Ma, A., & Dar, A. M. (2017). Prediction of Stream Flow and Sediment Yield of Lolab Watershed Using SWAT Model. *Hydrology: Current Research, 08*(01). doi:10.4172/2157-7587.1000265

Gupta, H. V., Sorooshian, S., & Yapo, P. O. (1999). Status of Automatic Calibration for Hydrologic Models: Comparison with Multilevel Expert Calibration. *Journal of Hydrologic Engineering, 4*(2), 135-143. doi:10.1061/(ASCE)1084-0699(1999)4:2(135)

Hanson, L., Habicht, S., Daggupati, P., Srinivasan, R., & Faeth, P. (2017). Modeling Changes to Streamflow, Sediment, and Nutrient Loading from Land Use Changes Due to Potential Natural Gas Development. *JAWRA Journal of the American Water Resources Association, 53*(6), 1293-1312. doi:10.1111/1752-1688.12588

Hargreaves, G. H., & Allen, R. G. (2003). History and Evaluation of Hargreaves Evapotranspiration Equation. *Journal of Irrigation and Drainage Engineering, 129*(1), 53-63. doi:10.1061/(ASCE)0733-9437(2003)129:1(53)

Hazbavi, Z., & Sadeghi, S. H. R. (2017). Watershed Health Characterization Using Reliability–Resilience–Vulnerability Conceptual Framework Based on Hydrological Responses. *Land Degradation and Development, 28*(5), 1528-1537. doi:10.1002/ldr.2680

Heuvelmans, G., Garcia-Qujano, J. F., Muys, B., Feyen, J., & Coppin, P. (2005). Modelling the water balance with SWAT as part of the land use impact evaluation in a life cycle study of CO2 emission reduction scenarios. *Hydrological Processes, 19*(3), 729-748. doi:10.1002/hyp.5620

Homdee, T., Pongput, K., & Kanae, S. (2011). Impacts of Land Cover Changes on Hydrologic Responses: A Case Study of Chi River Basin, Thailand. *Journal of*

Japan Society of Civil Engineers, Ser. B1 (Hydraulic Engineering), 67(4), I_31-I_36. doi:10.2208/jscejhe.67.i_31

Huisman, J. A., Breuer, L., & Frede, H. G. (2004). Sensitivity of simulated hydrological fluxes towards changes in soil properties in response to land use change. *Physics and Chemistry of the Earth, 29*(11-12 SPEC. ISS.), 749-758. doi:10.1016/j.pce.2004.05.012

Im, S., Brannan, K. M., Mostaghimi, S., & Kim, S. M. (2007). Comparison of HSPF and SWAT models performance for runoff and sediment yield prediction. *Journal of Environmental Science and Health - Part A Toxic/Hazardous Substances and Environmental Engineering, 42*(11), 1561-1570. doi:10.1080/10934520701513456

Jabbar, F. K., & Grote, K. (2019). Statistical assessment of nonpoint source pollution in agricultural watersheds in the Lower Grand River watershed, MO, USA. *Environmental Science and Pollution Research, 26*(2), 1487-1506. doi:10.1007/s11356-018-3682-7

Jain, S. K., Tyagi, J., & Singh, V. (2010). Simulation of Runoff and Sediment Yield for a Himalayan Watershed Using SWAT Model. *J. Water Resource and Protection, 2*, 267-281. doi:10.4236/jwarp.2010.23031

Kheereemangkla, Y., Shrestha, R. P., Shrestha, S., & Jourdain, D. (2016). Modeling hydrologic responses to land management scenarios for the Chi River Sub-basin Part II, Northeast Thailand. *Environmental Earth Sciences, 75*(9). doi:10.1007/s12665-016-5512-x

Kim, J., & An, K.-G. (2015). Integrated Ecological River Health Assessments, Based on Water Chemistry, Physical Habitat Quality and Biological Integrity. *Water, 7*(11), 6378-6403. doi:10.3390/w7116378

Kumar, N., Singh, S. K., Srivastava, P. K., & Narsimlu, B. (2017). SWAT Model calibration and uncertainty analysis for streamflow prediction of the Tons River

Basin, India, using Sequential Uncertainty Fitting (SUFI-2) algorithm. *Modeling Earth Systems and Environment, 3*(1), 1-13. doi:10.1007/s40808-017-0306-z

Lenhart, T., Fohrer, N., & Frede, H. G. (2003). Effects of land use changes on the nutrient balance in mesoscale catchments. *Physics and Chemistry of the Earth, 28*(33-36), 1301-1309. doi:10.1016/j.pce.2003.09.006

Liu, Y., Yang, W., Yu, Z., Lung, I., & Gharabaghi, B. (2015). Estimating Sediment Yield from Upland and Channel Erosion at A Watershed Scale Using SWAT. *Water Resources Management, 29*(5), 1399-1412. doi:10.1007/s11269-014-0729-5

Madsen, H. (2000). Automatic calibration of a conceptual rainfall-runoff model using multiple objectives. *Journal of Hydrology, 235*(3-4), 276-288. doi:10.1016/S0022-1694(00)00279-1

Malagó, A., Bouraoui, F., Vigiak, O., Grizzetti, B., & Pastori, M. (2017). Modelling water and nutrient fluxes in the Danube River Basin with SWAT. In (Vol. 603-604, pp. 196-218): Elsevier B.V.

Marcarelli, A. M., Kirk, R. W. V., & Baxter, C. V. (2010). Predicting effects of hydrologic alteration and climate change on ecosystem metabolism in a western U.S. river. *Ecological Applications, 20*(8), 2081-2088. doi:10.1890/09-2364.1

Michael, P. (2006). [Hydrologic Cycle].

Mirchi, A., Madani, K., Watkins, D., & Ahmad, S. (2012). Synthesis of System Dynamics Tools for Holistic Conceptualization of Water Resources Problems. *Water Resources Management, 26*(9), 2421-2442. doi:10.1007/s11269-012-0024-2

Nash, J. E., & Sutcliffe, J. V. (1970). River flow forecasting through conceptual models part I - A discussion of principles. *Journal of Hydrology, 10*(3), 282-290. doi:10.1016/0022-1694(70)90255-6

Neitsch, S. L., Arnold, J. G., Kiniry, J. R., & Williams, J. R. (2005). *SOIL AND WATER ASSESSMENT TOOL THEORETICAL DOCUMENTATION VERSION 2005*. Retrieved from

Neitsch, S. L., Arnold, J. G., Kiniry, J. R., & Williams, J. R. (2011). *Soil and Water Assessment Tool Theoretical Documentation Version 2009*. Retrieved from Texas:

Neupane, R. P., & Kumar, S. (2015). Estimating the effects of potential climate and land use changes on hydrologic processes of a large agriculture dominated watershed. *Journal of Hydrology, 529*(P1), 418-429. doi:10.1016/j.jhydrol.2015.07.050

Olivera, F., Valenzuela, M., Srinivasan, R., Choi, J., Cho, H., Koka, S., & Agrawal, A. (2006). ARCGIS-SWAT: A GEODATA MODEL AND GIS INTERFACE FOR SWAT. *Journal of the American Water Resources Association, 42*(2), 295-309. doi:10.1111/j.1752-1688.2006.tb03839.x

Ouessar, M., Bruggeman, A., Abdelli, F., Mohtar, R. H., Gabriels, D., & Cornelis, W. M. (2009). Modelling water-harvesting systems in the arid south of Tunisia using SWAT. *Hydrology and Earth System Sciences, 13*(10), 2003-2021. doi:10.5194/hess-13-2003-2009

Peng, Z.-R., & Tsou, M.-h. (2003). *Internet GIS : distributed geographic information services for the internet and wireless networks*.

Peraza-Castro, M., Ruiz-Romera, E., Meaurio, M., Sauvage, S., & Sánchez-Pérez, J. M. (2018). Modelling the impact of climate and land cover change on hydrology and water quality in a forest watershed in the Basque Country (Northern Spain). *Ecological Engineering, 122*, 315-326. doi:10.1016/j.ecoleng.2018.07.016

Phomcha, P., Wirojanagud, P., Vangpaisal, T., & Thaveevouthti, T. (2011). Predicting sediment discharge in an agricultural watershed: A case study of the Lam Sonthi watershed, Thailand. *ScienceAsia, 37*(1), 43-50. doi:10.2306/scienceasia1513-1874.2011.37.043

Poff, N. L., Allan, J. D., Bain, M. B., Karr, J. R., Prestegaard, K. L., Richter, B. D., . . . Stromberg, J. C. (1997). The Natural Flow Regime. *BioScience, 47*(11), 769-784. doi:10.2307/1313099

Poff, N. L., & Ward, J. V. (1989). Implications of Streamflow Variability and Predictability for Lotic Community Structure: A Regional Analysis of Streamflow Patterns. *Canadian Journal of Fisheries and Aquatic Sciences, 46*(10), 1805-1818. doi:10.1139/f89-228

Priestley, C. H. B., & Taylor, R. J. (1972). On the Assessment of Surface Heat Flux and Evaporation Using Large-Scale Parameters. *Monthly Weather Review, 100*(2), 81-92. doi:10.1175/1520-0493(1972)100<0081:OTAOSH>2.3.CO;2

Pyron, M., & Neumann, K. (2008). Hydrologic alterations in the Wabash River watershed, USA. *River Research and Applications, 24*(8), 1175-1184. doi:10.1002/rra.1155

Qi, J., Li, S., Li, Q., Xing, Z., Bourque, C. P. A., & Meng, F. R. (2016). Assessing an Enhanced Version of SWAT on Water Quantity and Quality Simulation in Regions with Seasonal Snow Cover. *Water Resources Management, 30*(14), 5021-5037. doi:10.1007/s11269-016-1466-8

Reungsang, P., Kanwar Rameshwar, S., & Srisuk, K. (2010). Application of SWAT Model in Simulating Stream Flow for the Chi River Subbasin II in Northeast Thailand. *Trends Research in Science and Technology, 2*(1), 23-38.

Sangkatananon, P., Chotamonsak, C., & Dhanasin, P. (2018). Performance of SWAT Hydrologic Model for Runoff Simulation in Wang River Basin. *The Journal of King Mongkut's University of Technology North Bangkok, 28*(4), 1-12. doi:10.14416/j.kmutnb.2018.09.003

Sangmanee, C., Wattayakorn, G., & Sojisuporn, P. (2013). Simulating changes in discharge and suspended sediment loads of the Bangpakong River, Thailand, driven by future climate change. *Maejo Int. J. Sci. Technol, 7*, 72-84.

Saunders, W. K., & Maidment, D. R. (1996). *A GIS ASSESSMENT OF NONPOINT SOURCE POLLUTION IN THE SAN ANTONIO-NUECES COASTAL BASIN*. Retrieved from http://www.ce.utexas.edu/centers/crwr/reports/online.html

Sendzimir, J., & Schmutz, S. (2018). Challenges in Riverine Ecosystem Management. In (pp. 1-16): Springer International Publishing.

Setegn, S. G., Srinivasan, R., & Dargahi, B. (2008). Hydrological Modelling in the Lake Tana Basin, Ethiopia Using SWAT Model. *The Open Hydrology Journal, 2*(1), 49-62. doi:10.2174/1874378100802010049

Shekhar, S., & Xiong, H. (2008). *Encyclopedia of GIS*: Springer US.

Son, N. T., Le Huong, H., Phuong, T. T., & Loc, N. D. (2020). Application of SWAT model to Assess Land Use and Climate Changes Impacts on Hydrology of Nam Rom River Basin in Vietnam. doi:10.20944/preprints202001.0362.v1

Spinosa, L. (2015). Wastewater Sludge: A Global Overview of the Current Status and Future Prospects. *Water Intelligence Online, 6*(0). doi:10.2166/9781780402154

Srinivasan, V., Gorelick, S. M., & Goulder, L. (2010). Sustainable urban water supply in south India: Desalination, efficiency improvement, or rainwater harvesting? *Water Resour. Res, 46*, 10504-10504. doi:10.1029/2009WR008698

Suwanlertcharoen, T. (2011). Application of the SWAT model to evaluate runoff and suspended sediment from a small watershed : a case study of Mae Phun subwatershed, Laplae district, Uttaradit province.

Tan, K. S., Chiew, F. H. S., Grayson, R. B., Scanlon, P. J., & Siriwardena, L. (2005). Calibration of a Daily Rainfall-Runoff Model to Estimate High Daily Flows. *International Congress on Modelling and Simulation (MODSIM05)*.

Tan, M. L., Ficklin, D. L., Dixon, B., Ibrahim, A. L., Yusop, Z., & Chaplot, V. (2015). Impacts of DEM resolution, source, and resampling technique on SWAT-simulated streamflow. *Applied Geography, 63*, 357-368. doi:10.1016/j.apgeog.2015.07.014

Tan, M. L., Ibrahim, A. L., Duan, Z., Cracknell, A. P., & Chaplot, V. (2015). Evaluation of six high-resolution satellite and ground-based precipitation products over Malaysia. *Remote Sensing, 7*(2), 1504-1528. doi:10.3390/rs70201504

Tan, M. L., Samat, N., Chan, N. W., Lee, A. J., & Li, C. (2019). Analysis of Precipitation and Temperature Extremes over the Muda River Basin, Malaysia. *Water, 11*(2), 283-283. doi:10.3390/w11020283

Tarigan, S., Wiegand, K., & Slamet, B. (2018). Minimum forest cover required for sustainable water flow regulation of a watershed: a case study in Jambi Province, Indonesia. *Hydrol. Earth Syst. Sci, 22*, 581-594. doi:10.5194/hess-22-581-2018

United States Department of, A. (1989). Runoff Curve Number Computations.

Wankrua, W., Kangrang, A., & Sriwanpheng, O. (2017). *Evaluation of Runoff in the Upper-Chi and Lumsapung Basins using Hydrologic Model and Mathematical SWAT Model*. Retrieved from

Weber, A., Fohrer, N., & Möller, D. (2001). Long-term land use changes in a mesoscale watershed due to socio-economic factors - Effects on landscape structures and functions. *Ecological Modelling, 140*(1-2), 125-140. doi:10.1016/S0304-3800(01)00261-7

Williams, R. S., Trumbly, R. J., MacColl, R., Trimble, R. B., & Maley, F. (1985). Comparative properties of amplified external and internal invertase from the yeast SUC2 gene. *The Journal of biological chemistry, 260*(24), 13334-13341.

Willmott, C. J. (1981). On the validation of models. *Physical Geography, 2*(2), 184-194. doi:10.1080/02723646.1981.10642213

Winchell, M., Srinivasan, R., Luzio, M. D., & Arnold, J. (2009). ArcSWAT 2.3.4 Interface for SWAT2005: User's Guide, Version September 2009. *Texas Agricultural Experiment Station and Agricultural Research Service- US Department of Agriculture*.

Wuttichaikitcharoen, P., Plangoen, P., & Muangthong, S. (2016). Study of Runoff Simulation in Huai Luang Watershed Using SWAT (in Thai). *CRMA Journal, 14*, 145-158.

Xu, M., & Chua, V. P. (2017). A numerical study on land-based pollutant transport in Singapore coastal waters with a coupled hydrologic-hydrodynamic model. *Journal of Hydro-Environment Research, 14*, 119-142. doi:10.1016/j.jher.2016.09.002

Xu, Z. X., Pang, J. P., Liu, C. M., & Li, J. Y. (2009). Assessment of runoff and sediment yield in the Miyun Reservoir catchment by using SWAT model. *Hydrological Processes, 23*(25), 3619-3630. doi:10.1002/hyp.7475

Yasin, H. Q., & Clemente, R. S. (2012). Application of SWAT model for hydrologic and water quality modeling in Thachin River Basin, Thailand. *Arabian Journal for Science and Engineering, 39*(3), 1671-1684. doi:10.1007/s13369-013-0770-3

Yesuf, H. M., Melesse, A. M., Zeleke, G., & Alamirew, T. (2016). Streamflow prediction uncertainty analysis and verification of SWAT model in a tropical watershed. *Environmental Earth Sciences, 75*(9), 1-16. doi:10.1007/s12665-016-5636-z

Zhang, L., Lu, J., Chen, X., Liang, D., Fu, X., Sauvage, S., & Perez, J. M. S. (2017). Stream flow simulation and verification in ungauged zones by coupling hydrological and hydrodynamic models: A case study of the Poyang Lake ungauged zone. *Hydrology and Earth System Sciences, 21*(11), 5847-5861. doi:10.5194/hess-21-5847-2017

APPENDIX

APPENDIX A

Figure Spatial Data Map

Appendix A1

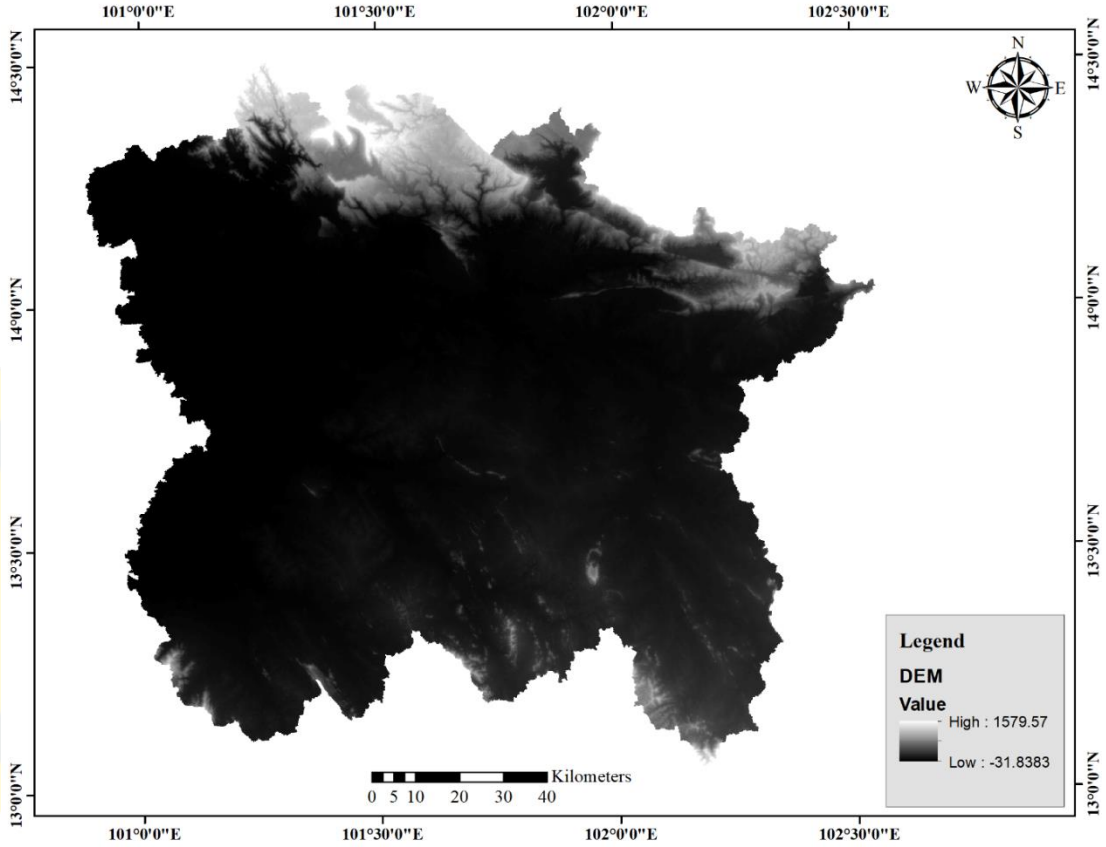

Figure 40 Digital Elevation Model (DEM) Map

Appendix A2

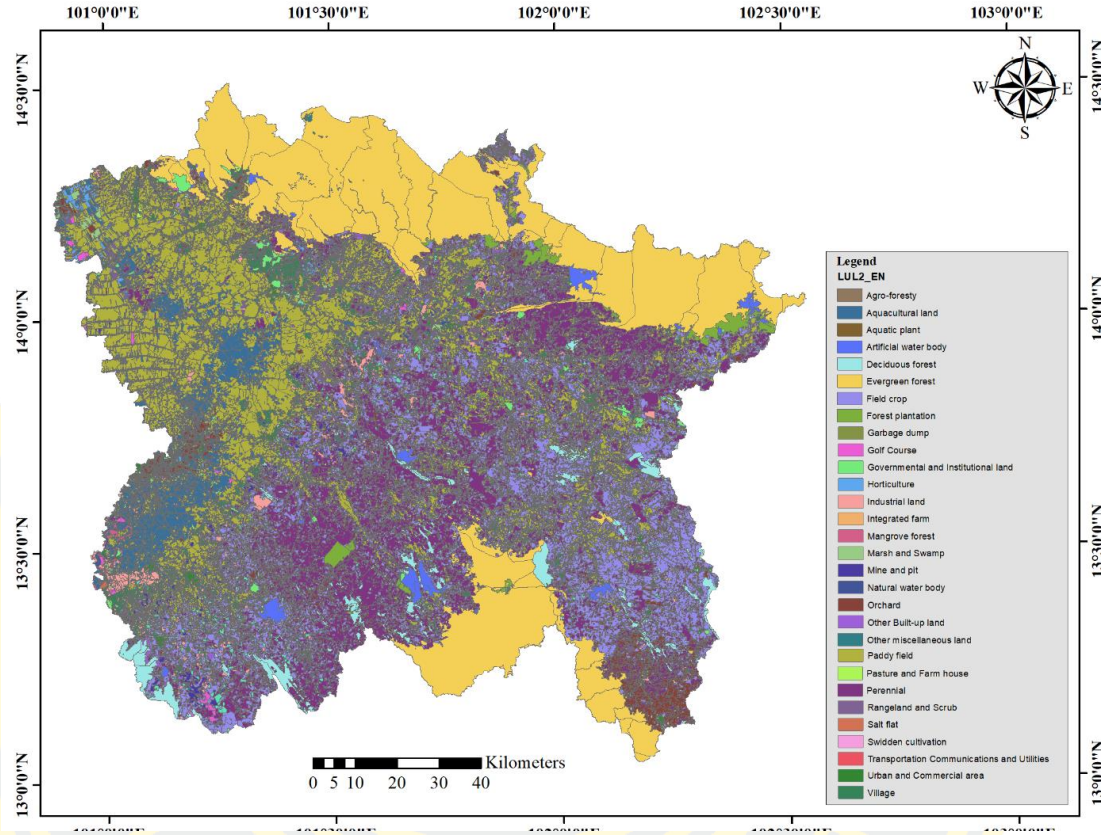

Figure 41 Land use Map

Appendix A3

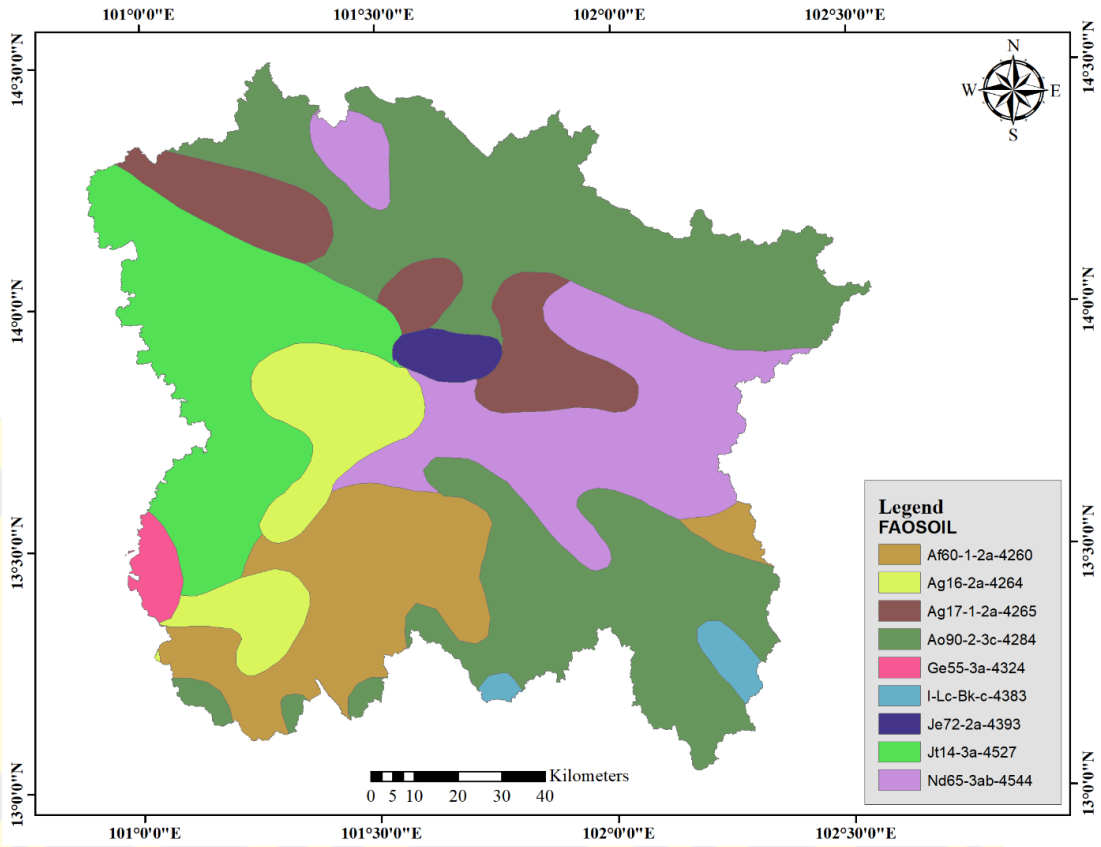

Figure 42 Soil Map

Appendix A4

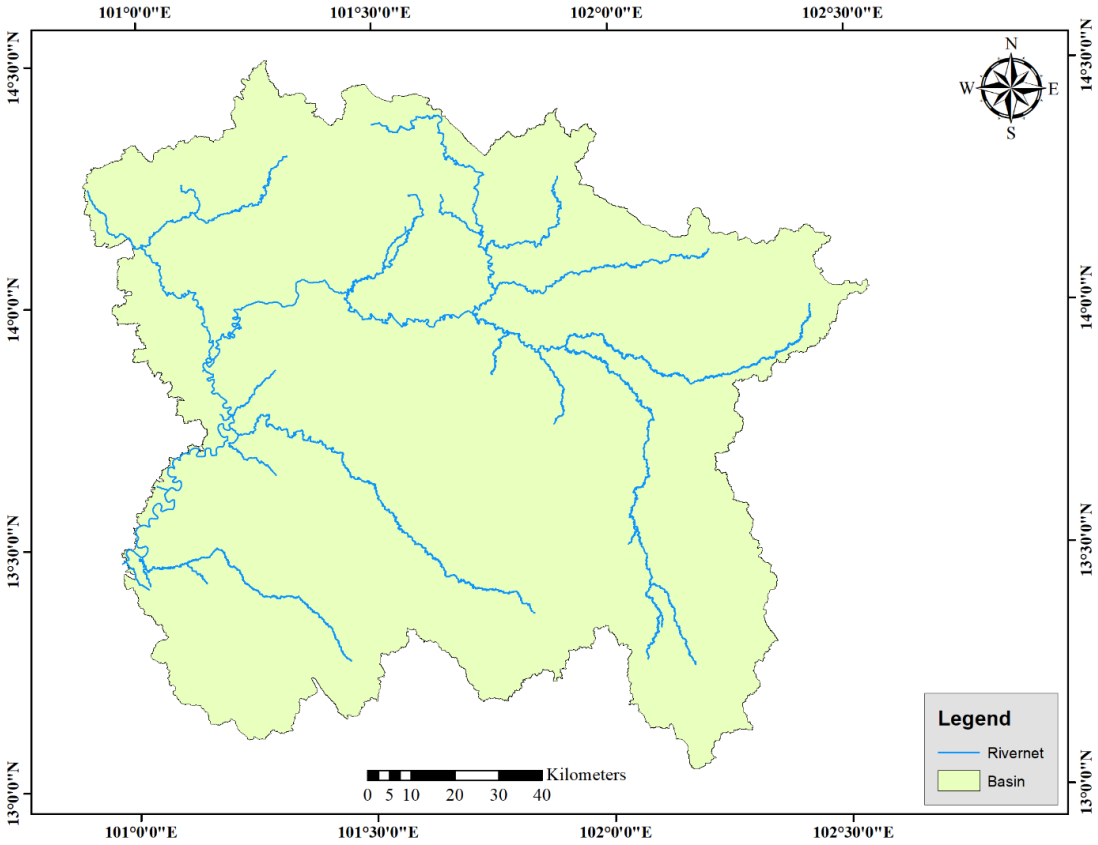

Figure 43 River net map

APPENDIX B

Data Preparation

1. Data Preparation

1.1 Digital Elevation Model (DEM)

The Digital Elevation Model (DEM) data obtained from Airbus Intelligence with 25 meters × 25 meters in grid file. DEM data was used in Watershed delineator in the SWAT model, Which cover the study area.

1.2 Land use databases

Land use data should have table data with Dbase file, which stores value and four characters in the SWAT model, as shown in Table B1. Another way to preparation can be arranged in Microsoft Excel. By specifying the column width of VALUE = 5 and LAUDUSE = 4 then Save As is .DBF4 (*.dbf).

Table 13 Land Use code database

Value	SWAT Code
1	AGRL
2	RICE
3	FRST
4	ORCD
5	PAST
6	AGRR
7	WATR
8	FRSE
9	FRSD
10	RNGB
11	WETL
12	URHD
13	URML
14	UINS
15	UIDU
16	FESC

1.3 Soil databases

Soil data must-have table data with Dbase file which stores value and four characters in the SWAT model, as shown in Table B2. Another way to preparation can be arranged in Microsoft Excel. By specifying the column width of VALUE = 5 and LAUDUSE = 4 then save as .DBF4 (*.dbf).

Table 14 Soil code database

Value	SWAT code
1	Ao90-2-3c-4284
2	Ag17-1-2a-4265
3	Jt14-3a-4527
4	Nd65-3ab-4544
5	Ag16-2a-4264
6	Af60-1-2a-4260
7	I-Lc-Bk-c-4383
8	Je72-2a-4393
9	Ge55-3a-4324

1.4 Meteorological Data

1.4.1 There are four types of meteorological data used to input to the SWAT model,

1) Daily Rainfall (mm)

2) Daily Minimum and Maximum temperature (°C)

3) Daily Wind speed (m/s)

4) Daily Relative humidity (%)

The meteorological database must be prepared for each type of data in two forms, which are location file (*.dbf) and data file (* .dbf). The format of the location

file is a data table. The integrity of the XY coordinate data file is given in Table B3. The data format file is a data table, which contains the data at the measurement station. The data is arranged into two columns. Column one is the date, and column two is the numeric value

For example, the daily rainfall data table: Column one is DATE is equal to 8, and column two is PCP (rainfall data, mm) is equal to 19. Set 5 decimal point. And for file database naming. Should match with the measuring station. As shown in table B4.

Table 15 Meteorological Station Database

ID	NAME	LAT	LONG	ELEVATION
1	pcp_419301	14.100	100.616	48.99
2	pcp_423301	13.515	101.458	43.76
3	pcp_429601	13.686	100.767	13.75
4	pcp_430201	14.058	101.369	186.37
5	pcp_430401	13.983	101.707	99.64
6	pcp_431301	14.643	101.331	274.6
7	pcp_440401	13.788	102.034	138.96
8	pcp_459201	13.366	100.983	20.02

Table 16 Rainfall Database for SWAT model

DATE	PCP
1/1/2009	6.53
1/2/2009	12.65
1/3/2009	16.5
1/4/2009	5.03
1/5/2009	9.09

The database of daily minimum and maximum temperatures contain with: Column one: DATE is equal to 8, column two: MAX (Maximum temperatures, °C) is equal to 20, and column three: MN (Minimum temperatures, °C) is equal to 20. Set 5 decimal point. And for file database naming. Should match with the measuring station. As shown in table B5.

Table 17 Maximum and Minimum temperatures Database for the SWAT model

DATE	MAX	MIN
1/1/2009	26.34	18.22
1/2/2009	27.4	17.53
1/3/2009	28.59	16.5
1/4/2009	30.24	17.06
1/5/2009	31.18	17.82

The database of Wind speed contains with: Column one: DATE is equal to 8, column two: WND (m/s) is equal to 20. Set 5 decimal point. And for file database naming. Should match with the measuring station. As shown in table B6.

Table 18 Wind speed Database for the SWAT model

DATE	WND
1/1/2009	4.72
1/2/2009	4.56
1/3/2009	3.75
1/4/2009	3.1
1/5/2009	2.8

The database of Relative Humidity contains with: Column one: DATE is equal to 8, column two: HMD (Relative Humidity, %) data is equal to 20. Set 5 decimal

point. And for file database naming. Should match with the measuring station. As shown in table B7.

Table 19 Relative Humidity Database for the SWAT model

DATE	HMD
1/1/2009	69.28
1/2/2009	66.52
1/3/2009	68.47
1/4/2009	69.45
1/5/2009	67.23

APPENDIX C

Hydrological Data

Appendix C1 Discharge at KGT3 Station

Table 20 Daily Discharge (m3/s) at KGT3 station in 2011

Day	Jan	Feb	Mar	Apr	May	Jun	Jul	Aug	Sep	Oct	Nov	Dec
1	10.6	4.2	8.6	2.6	15.2	58.2	210.8	322.4	527	662.1	138	17.8
2	10.4	4.2	7.8	2.2	15.4	47.1	209.6	384.8	543.3	662.1	120.6	17.6
3	10.2	4.4	7.8	2.4	14.4	44.1	217.4	405	548.8	655.5	109.8	17
4	10	4.8	8.6	2	13.6	46.5	229.4	407.7	555.4	653.3	99.4	16.2
5	9.8	4.6	9.6	1.8	13.8	48.9	216.8	380	568.6	648.9	91	16.2
6	9.8	5	10	2	12.8	51.9	176.6	327.2	566.4	634.6	80.2	15.6
7	9.6	4.2	9.4	1.6	13.6	46.8	156	251.6	551	624.7	77.8	15
8	9.4	5	9.2	1.4	15.8	44.1	123	199.4	537	606	66.6	14.4
9	9.2	4.4	9	1.4	16	39.9	103.4	168.2	519	582.9	61.8	14.2
10	8.8	4.4	8.6	1.4	16.4	32.7	83	161.6	510	564.2	56.7	14
11	8.4	4.4	8.4	1.2	12.2	30.9	76.6	237.8	524	557.6	53.1	13.8
12	7.6	4.8	8.4	1.4	11.4	31.2	72.6	370.4	544.4	554.3	49.5	13.2
13	7	5.8	8.2	1.4	10.6	36	65	407.7	569.7	551	46.5	13
14	6.6	5	8.2	1.4	10.2	40.5	57	403.2	590.6	549.9	43.8	12.6
15	6.4	4.6	8.4	3.4	12	47.1	76.2	416.7	597.2	547.7	39.3	12.6

Table 20 Daily Discharge (m3/s) at KGT3 station in 2011 (Cons.)

Day	Jan	Feb	Mar	Apr	May	Jun	Jul	Aug	Sep	Oct	Nov	Dec
16	6.2	4.2	9.8	5.2	12.8	46.2	125	476	590.6	555.4	39	12.6
17	6	4.2	11.2	9.4	11.4	44.4	124	515	582.9	562	37.5	12.6
18	5.6	4.4	10.6	11.4	13.8	46.8	118.2	529	580.7	578.5	33	12.4
19	5.4	5.4	10.4	8.8	21.3	50.1	110.6	549.9	586.2	582.9	30.9	12.4
20	5	6.6	10.2	7.4	81.4	55.5	100.2	576.3	596.1	573	29.4	12.4
21	4.6	6.8	10	6.6	86.6	114.2	151.5	596.1	601.6	556.5	27.9	12.2
22	4.6	6.8	10	7.4	101.4	106.2	241.1	584	598.3	540	27	12.2
23	4.4	7.4	10.2	10.6	63	87.4	294.3	554.3	596.1	524	26.1	12.2
24	4.4	8	9.8	11.2	38.1	71	322.4	511	604.9	501	24.9	12.4
25	4.4	7.4	9.2	13	30.9	59.8	369.6	455	618.1	471	21.6	12.2
26	4.2	7.4	9	15.6	17.6	50.7	399.6	423.9	618.1	431.1	20.8	12.2
27	4.2	8.2	9	16.8	13.2	36	423.9	416.7	615.9	370.4	20.2	12.2
28	4.2	8.8	8.8	17	25.5	164.6	364.8	406.8	631.3	288.7	19.4	12.2
29	4.2		8.8	17.2	69.8	153.5	295	404.1	652.2	231.8	18.8	12.2
30	4.2		8.6	16.2	87.4	123.5	263.5	453	657.7	157.5	18.2	12
31	4.2		8.2		73.8		285.2	506		145.5		12
Total	6.76	5.55	9.16	6.71	30.69	61.86	195.56	412.93	579.44	520.13	50.96	13.54

Table 21 Daily Discharge (m3/s) at KGT3 station in 2012

Day	Jan	Feb	Mar	Apr	May	Jun	Jul	Aug	Sep	Oct	Nov	Dec
1	12	8.4	3.8	5.4	3.4	23.7	18.3	238.1	336.2	636	57.9	35.4
2	12	8.2	3.6	5.2	2.8	23.7	21	238.1	316.2	630	53.4	33.9
3	11.8	7.8	3.6	5	2.2	24	33.6	217	273.1	621	51	27
4	11.6	7.6	3.6	4.8	2.2	28.2	43.5	162	238.1	614	46.8	23.1
5	11.6	7	3.6	4.8	2.2	28.8	43.2	129.5	226.6	608.6	42.9	16.8
6	11.4	6.6	3.4	4.6	2.6	39.9	76.4	114	233.2	598.7	40.2	14.7
7	11.4	6.4	3.4	4.6	2.6	52.2	126.4	93.2	328.2	582.5	35.4	15
8	11.4	6.2	3.4	4.4	2.6	44.4	104	76.4	427.4	563.6	32.7	15
9	11.2	6.2	3.2	4.4	2.8	45	94.4	67.8	449.8	545.6	30.9	14.4
10	10	6.2	3.2	4.6	3.2	34.8	78	68.4	442.6	531.2	30.6	18
11	8.8	5.8	3.2	4.6	4	37.8	61.5	78.4	441	514.1	29.7	17.7
12	7.6	5.4	3	4.6	4.8	33.6	51.9	84.8	448.2	493	28.2	17.7
13	7.2	5.2	3.4	5.4	5	27.6	58.8	109.2	452.2	477	27.6	18.6
14	6.8	5	3.4	5.6	4.8	23.4	72	123.2	450.6	461.8	27	18.3
15	6.4	4.8	3.6	5.8	4.8	22.2	73.6	126.4	477	439.4	27	17.7

Table 21 Daily Discharge (m3/s) at KGT3 station in 2012 (Cons.)

Day	Jan	Feb	Mar	Apr	May	Jun	Jul	Aug	Sep	Oct	Nov	Dec
16	6	4.8	4.2	6	4.8	21.3	69.9	132	506	392.2	26.7	17.7
17	5.8	4.6	4.2	5.8	5.6	21.3	53.4	142.5	531.2	329	26.4	17.7
18	5.8	4.4	4.2	5.4	6	21	48	140	561.8	271	26.4	17.4
19	5.6	4.4	4.2	6.4	6.2	28.8	34.5	168.4	596.9	227.2	24	15.9
20	5.6	4.4	4	7.2	6.2	33.3	32.7	182.8	626	195.4	22.5	15.3
21	5.6	4.2	4	7.2	7	26.1	29.1	160.5	638	157	21.9	14.4
22	5.6	4.2	4.4	7.2	8.4	22.5	23.4	136.5	671	136.5	21	14.1
23	6	4	4.4	6	7.8	21.3	24	114.4	687.3	116	19.8	13.8
24	7.4	4	4.4	5.6	7.6	20.7	21.9	96.4	682	104	19.5	13.5
25	8.4	4	4.6	5.6	7.4	15	21.9	89.6	672	92.8	21.3	12.3
26	8.6	3.8	4.4	5	7.6	14.1	27.6	93.2	655	88	23.1	11.8
27	8.4	3.8	4.4	4.8	9.2	12.3	52.5	118.8	645	82	25.2	11.4
28	8.4	4	4.4	4.6	11.2	12.3	94	163.6	643	78	26.1	10.4
29	8.4	3.8	4.6	4.4	22.2	12.9	94.8	238.8	638	63.9	28.5	9.8
30	8.6		4.4	3.6	22.5	12	133.5	306	639	59.7	37.5	8.8
31	9		4.2		21		206.8	331.4		57.3		8.4
Total	8.53	5.35	3.88	5.29	6.8	26.14	62.08	146.5	497.75	347.31	31.04	16.65

Table 22 Daily Discharge (m3/s) at KGT3 station in 2013

Day	Jan	Feb	Mar	Apr	May	Jun	Jul	Aug	Sep	Oct	Nov	Dec
1	8.2	4.6	4.2	2.7	3.9	3.3	67.6	424.86	290.38	649.2	233.6	28.4
2	7.4	4.6	4	2.55	4.35	3.45	50.9	403.54	258.4	641.1	195.1	26
3	7.2	4.6	4	2.55	4.65	3.45	42.8	407.64	203.5	633.9	166.6	24.4
4	6.8	4.6	3.8	2.4	4.5	3.45	24	425.68	159.4	640.2	135.4	22.8
5	6.8	4.6	3.8	2.25	4.65	4.5	16.8	420.76	123.5	658.2	115.5	21.4
6	6.6	4.4	3.8	2.25	4.5	7	17.4	414.2	107.5	674.4	101.2	20.4
7	6.4	4.4	3.6	2.25	4.05	23.2	19.8	406	102.5	683.4	92.4	17.4
8	6.2	4.4	3.4	2.25	3.75	25.8	26	424.04	98.8	732	83.6	16.8
9	6.2	4.4	3.4	2.25	3.45	26	53.9	437.16	128.2	754.5	86.4	16.2
10	6.2	4.4	3.4	2.1	2.85	16.4	76.8	439.62	190	729.3	119.5	15.4
11	6	4.8	3.2	2.25	2.85	12.8	96.8	424.86	243.64	698.7	171.4	15.2
12	6	4.8	3.2	2.25	2.7	14.8	102.5	401.9	268.24	665.4	145	15.2
13	5.8	4.8	3.2	2.25	4.8	73.2	91.2	385.5	263.32	643.8	96.8	14.8
14	5.8	4.8	3.2	2.25	5.1	152.8	90	402.72	293.66	620.4	82.8	14.4
15	5.8	4.8	3	2.25	4.95	180.4	82.8	406.82	387.96	596.1	75.6	14.2

Table 22 Daily Discharge (m3/s) at KGT3 station in 2013 (Cons.)

Day	Jan	Feb	Mar	Apr	May	Jun	Jul	Aug	Sep	Oct	Nov	Dec
16	5.4	4.8	3	2.25	3.75	219.6	63.6	394.52	430.6	579	90	14
17	5	4.8	3	2.25	3.15	251.84	47.9	367.46	457.66	588	86.4	14
18	5	5	3	2.4	2.85	246.92	35.9	331.38	468.32	600.6	68	14
19	5	5	3	2.4	2.85	216.8	28.1	285.46	468.32	599.7	60.2	13.8
20	5	5	3	2.25	3	186.4	24	209.1	510.96	592.5	56.9	13.8
21	5	4.8	3	2.25	3	147.4	21.2	143.8	576.3	580.8	50.3	13.8
22	4.8	4.8	3	2.55	2.7	111.5	19	105.5	680.7	569.18	44.9	13.6
23	4.8	4.6	3	2.85	2.85	97.6	18.4	126.5	710.4	558.52	40.7	13.4
24	4.8	4.4	3	3	2.85	121	65.6	173.8	706.8	552.78	39.2	13.2
25	4.8	4.4	3	3.3	2.85	159.4	149.2	218.9	708.6	547.04	34.4	13.2
26	4.8	4.4	3	3.15	3.15	173.8	221.7	282.18	732.9	537.2	34.1	13
27	4.6	4.2	3.4	3.15	3.3	166.6	243.64	318.26	740.1	521.62	37.7	13
28	4.6	4.2	3.6	3	3.15	145.6	232.2	292.02	714.9	492.1	37.7	12.8
29	4.6		3.6	3.45	3	120.5	218.9	245.28	689.7	445.36	34.1	12.8
30	4.6		3.6	4.5	2.85	103	345.32	239.2	669	373.2	31.4	12.6
31	4.6		3.6		2.85		416.66	257.58		293.66		12.6
Total	5.64	4.62	3.35	2.59	3.52	100.62	97.12	329.56	412.81	595.22	88.23	16.02

Table 23 Daily Discharge (m3/s) at KGT3 station in 2014

Day	Jan	Feb	Mar	Apr	May	Jun	Jul	Aug	Sep	Oct	Nov	Dec
1	12.4	5.85	5.1	4	6	4.8	32.8	74.38	334.75	176	107	22
2	12.2	5.7	5.1	4	6	4.4	24.83	68.25	384.9	202.6	80.33	21
3	11.8	5.7	5.1	4.4	6	4	24.55	72.68	447.05	233.3	73.53	20.75
4	11.8	5.7	5.1	4.4	6	4.2	26.48	95	461	258.9	62.25	20.25
5	11.6	5.55	5.1	4.4	6	3.8	26.2	125.05	448	233.3	55.15	20.25
6	11.4	5.55	5.4	5.2	5.8	3.6	25.65	211.7	438.5	165.8	47.9	20.25
7	11.2	5.55	6.2	5	6	3.6	25.1	358.8	443.25	131.65	55.5	20
8	11.2	5.4	6.6	5	6.2	3.2	18.5	480	460	152.6	53.1	20
9	11.2	5.4	6.8	4.8	6.2	3	19.75	509	420.9	143.2	46.28	19.75
10	11	5.4	7	4.8	6.2	3.2	19.25	465	357.9	191.4	41.9	19.75
11	11	5.25	7	4.6	6.2	3	20.5	401.1	289.3	234.9	35.9	19.5
12	11	5.25	7	4.6	6	3	18.75	328.8	261.3	246.1	30.88	19.5
13	10.8	5.25	7.4	4.6	6	3	17.5	278.9	319.45	264.5	28.95	19.5
14	10.8	5.25	7.4	4.6	6	3.2	20.75	261.3	305.85	270.1	28.4	19.25
15	10.6	5.25	7.4	4.8	5.8	4.6	37.7	221.5	298.2	222.2	28.13	19.25

Table 23 Daily Discharge (m3/s) at KGT3 station in 2014 (Cons.)

Day	Jan	Feb	Mar	Apr	May	Jun	Jul	Aug	Sep	Oct	Nov	Dec
16	10.6	5.25	7.2	4.8	5.8	6.4	58.65	202.6	332.2	152	28.13	19
17	10.4	5.25	7.2	4.8	5.8	11	64.13	165.2	380.4	111	27.85	19
18	10.4	5.25	7.2	4.8	5.6	17.25	49.53	128.35	398.4	87.25	27.3	19
19	10.4	5.25	7.2	4.6	5.8	43.7	51.15	131.65	384	75.23	26.48	18.75
20	10.2	5.25	7.2	4.6	5.8	33.63	54.8	99	338.15	59.7	23	18.75
21	10	5.25	7.2	4.6	5.6	31.7	69.85	78.2	272.5	58.65	21.25	18.5
22	9	5.25	7.2	4.6	5.6	33.08	69.45	71.45	206.8	76.5	20.75	18.25
23	7.8	5.25	7.2	4.8	5.6	28.68	85	77.35	165.2	70.65	20.75	15.5
24	6.8	5.25	7.2	5.2	5.4	52.13	107.5	89.05	136.05	58.3	20.5	13.5
25	6.6	5.1	7.2	5.4	5.4	44.33	111	105	121	58.3	20.25	11.5
26	6.4	5.1	7.2	5.4	5.4	30.88	110.5	95.5	132.2	52.78	20.25	10.25
27	6.2	5.1	7.2	5.4	5	33.63	111	87.25	145.4	58.3	20.25	9
28	6	5.1	7.2	5.4	5.4	36.5	150.35	139.9	128.9	80.33	21	8
29	6		7.2	5.8	5.4	35.9	133.85	180.2	124	83.3	22.5	7.4
30	5.85		7	6	5.2	32.25	100.5	201.2	126.7	85.9	22.25	7.2
31	5.85		7		5		83.73	286.1		107		7
Total	9.63	5.35	6.73	4.85	5.75	17.52	57.07	196.43	302.08	141.99	37.26	16.83

Table 24 Daily Discharge (m3/s) at KGT3 station in 2015

Day	Jan	Feb	Mar	Apr	May	Jun	Jul	Aug	Sep	Oct	Nov	Dec
1	6.8	2.8	0	0.5	1.6	0.9	6.4	10.8	110.2	153.2	26.2	4
2	6.8	2.8	0	0.5	1.6	0.7	7.4	15.2	123	149	23.8	2.9
3	6.6	2.8	0	0.5	1.7	0.6	7.8	25	113	247	22.4	2.3
4	6.6	2.6	0	0.5	1.8	0.5	7.6	26.6	101.4	424.95	20.2	1.9
5	6.4	2.6	0	0.5	1.9	0.3	7.6	29.4	85	504.6	17.6	1.7
6	6.4	2.6	0	0.5	1.9	0.2	7.6	32.6	71.5	539.8	15.4	1.6
7	6	2.2	0	0.5	1.9	0.2	7.4	24.6	72.4	583	14.2	1.2
8	6	2.2	0	0.4	1.9	0	7.4	24.6	56.2	595.8	12.4	1
9	5.8	2	0	0.6	1.9	0	6.8	38	37.8	621.1	12	0.9
10	5.4	1.6	0	0.6	2	0	6	46	29	638.1	13	0.4
11	5.2	1.4	0	0.6	2	0	5.8	60.4	35.4	644.9	15.8	0.3
12	5	1.2	0	0.6	2	0	4.8	57.1	70.3	653.4	15.2	1.1
13	5	1	0	0.6	2	0	4	86.2	91.8	660.2	13.4	1.5
14	4.8	1	0	0.5	2.1	0	4	110.2	92.6	638.1	13	2.6
15	4.8	0.9	0	0.5	2.2	0	9.6	85	119	592.6	11.6	2.9

Table 24 Daily Discharge (m3/s) at KGT3 station in 2015 (Cons.)

Day	Jan	Feb	Mar	Apr	May	Jun	Jul	Aug	Sep	Oct	Nov	Dec
16	4.6	0.7	0	0.5	2.2	1.2	11.8	72.1	143	504.6	11.8	2.6
17	4.6	0.6	0	0.5	2.2	10.2	12	68.5	187	374.19	13.2	2.6
18	4.4	0.5	0	0.5	2.2	6	12.2	60.4	356	259	12.2	3.4
19	4.4	0.4	0	0.5	2.2	6	12.4	49	530.2	171.8	11	3.6
20	4.2	0.4	0	0.4	2	6	8.6	39.8	563.8	120.6	10.8	2.7
21	4.2	0.4	0	0.4	1.9	4.6	22.8	33	555.8	90.2	10	4.8
22	4	0.4	0	0.4	1.9	2.8	27	36.8	538.2	76.3	9.4	4
23	3.8	0.3	0	0.4	1.7	2.4	19.6	29.2	535	61.6	7.8	3.8
24	3.8	0.3	0	0.4	1.8	2.5	12.8	21	530.2	46.6	6.6	3.6
25	3.6	0.2	0	0.6	1.9	2.4	7.2	17.4	509.4	39.2	5	3.6
26	3.6	0.1	0	1	1.7	2.4	5	17.4	470.35	33.4	4.8	5.4
27	3.4	0	0	1	1.5	2.4	4.4	34.6	381.05	30.2	4.4	5.4
28	3.4	0	0	1.3	1.4	2.5	5.4	49	274	29	5.8	3.4
29	3.2		0.3	1.3	1.3	2.6	7.6	61.9	199.6	28.6	5.6	3.2
30	3.2		0.5	1.5	1.1	3.6	7.4	73.3	164.6	28.4	5.6	3
31	3		0.5		1.2		8.8	100.6		29.4		2.7
Total	4.81	1.21	0.04	0.62	1.83	2.03	9.2	46.31	238.23	308.67	12.34	2.71

Table 25 Daily Discharge (m3/s) at KGT3 station in 2016

Day	Jan	Feb	Mar	Apr	May	Jun	Jul	Aug	Sep	Oct	Nov	Dec
1	2.6	1.3	0.1	3.2	0.4	1.2	6	89.95	111.1	359.5	170.6	25.9
2	2.6	1.3	0.1	3.2	0.2	1	7.4	75.1	116.05	336.3	170.6	23.5
3	2.5	1.2	0.1	3	0.2	1	21.34	67.1	116.05	307.25	181.6	21.34
4	2.2	1.1	0.1	3	0.2	0.8	31.9	58.8	103.9	294.5	170.6	22.96
5	2	1.1	0.1	2.8	0.6	0.8	28	68.7	96.25	293.75	156.8	23.8
6	1.8	1	0	2.4	0.4	1	31.3	109.75	82.3	342.7	141.25	22.42
7	1.7	1	0	2	0.4	1.2	63.1	158	85.9	414.85	112.45	21.34
8	1.7	0.9	0	1.8	0.4	1.4	151.7	165.2	111.1	463.3	141.8	24.1
9	1.7	0.9	0	1.6	0.4	1.6	195.9	161	119.8	512.7	176	24.4
10	1.7	0.8	0	1.6	0.4	1.6	219.7	172.4	120.9	492	188.75	25.3
11	1.7	0.8	0	1.2	0.2	1.4	219.7	168.8	115.6	460.75	199.8	23.8
12	1.7	0.8	0	1.2	0.2	1.4	179	147.85	124.75	438.65	179.65	25.9
13	1.7	0.7	0	1.2	0.2	1	192	149.5	222.5	414.85	158	23.5
14	1.6	0.7	0	1	0.6	0.4	249.5	150.05	241.25	373.2	133	22.15
15	1.5	0.7	0	1	0.4	0.4	276.5	126.95	244.25	341.1	110.2	21.34

TTable 25 Daily Discharge (m3/s) at KGT3 station in 2016 (Cons.)

Day	Jan	Feb	Mar	Apr	May	Jun	Jul	Aug	Sep	Oct	Nov	Dec
16	1.5	0.6	0	1	0.6	0.2	281.75	124.2	203.05	299	93.55	21.34
17	1.5	0.6	0	0.8	0.8	0.2	248.75	126.95	195.25	232.3	83.2	22.15
18	1.5	0.5	0	0.8	1	0.2	192	135.2	207.8	215.5	69.9	21.61
19	1.4	0.5	0	0.8	1.2	0	130.8	128.05	240.5	227.4	52.85	20.53
20	1.5	0.5	0	0.8	1.2	0	107.95	110.65	282.5	200.45	47.25	19.18
21	1.6	0.5	0	1.2	1	0	68.7	100.3	348.3	147.85	44.1	17.02
22	1.5	0.4	0	1.6	1	0	58.1	94.9	410.6	120.9	40.25	14.59
23	1.5	0.4	0	1.6	1.2	0	64.3	80.05	380.85	126.4	43.75	14.86
24	1.6	0.3	0	1.6	1.2	0	56.7	69.1	341.9	129.15	47.25	13.78
25	1.6	0.3	0	1.4	1.2	0.6	49.7	95.8	343.5	107.95	45.15	13.24
26	1.5	0.3	0	1.4	1.2	3.6	41.65	146.75	385.95	112.9	43.05	11.08
27	1.5	0.2	0	1.2	1.2	9.4	46.55	164.6	392.75	126.95	39.2	9.2
28	1.5	0.2	0	1	1	8.8	43.75	154.45	377.45	121.45	34.3	9
29	1.4	0.1	0	0.8	1	6.4	49.35	131.9	349.1	117.05	32.5	9.4
30	1.4		0	0.8	1	6	70.3	122	344.3	129.15	28	8.4
31	1.3		0		1.2		85	114.25		154.45		8
Total	1.69	0.68	0.02	1.57	0.72	1.72	111.88	121.56	227.18	271.43	104.51	18.88

Table 26 Daily Discharge (m3/s) at KGT3 station in 2017

Day	Jan	Feb	Mar	Apr	May	Jun	Jul	Aug	Sep	Oct	Nov	Dec
1	8.4	3.6	15.67	20.8	17.4	165.8	101.5	366.6	341.8	238.2	53	12.4
2	8.4	3.6	15.67	20.6	17	137	75.4	305	303.4	222.1	45.8	14.6
3	8.4	3.4	15.94	20.8	16.6	117	53.4	266.2	268.3	293.5	43	14.2
4	8.4	3.4	16.75	20.2	16.4	103	40.2	265.5	225.6	426.6	42.2	13
5	8.4	3.4	16.48	20	16	116.5	67.8	305	182	494.5	32.4	12.6
6	8.2	3.2	15.4	19.4	14.8	156.8	141.2	403.4	152	512.5	29.1	13.4
7	8.4	3.2	15.4	18.4	14.6	208.1	210.9	442.6	147.2	517	28.2	15.6
8	8.4	3.2	16.21	18.2	14.4	241.7	264.1	433.8	133.5	518.8	27.3	18.2
9	8.4	3.2	17.29	17.8	14.4	254.3	297	425	117.5	518.8	28.8	17.6
10	8.2	3.2	17.83	17.6	15	274.6	264.8	415.4	109	514.3	26.4	17
11	8.2	3.2	23.5	17.8	15.4	275.3	239.6	389.8	110	508	25.2	16.6
12	8.2	3.2	24.1	18	16	258.5	262.7	349	144.2	493.6	23.7	16.8
13	8.2	7.2	24.1	18	16.6	231.9	298.6	297	183.2	461	25.5	16.2
14	8.2	6.4	23.5	17.6	18	185.6	337.8	254.3	171.8	425.8	32.7	16.8
15	8.2	5.8	23.5	17.6	18	146	357.8	208.8	161.6	403.4	33.4	18.4

Table 26 Daily Discharge (m3/s) at KGT3 station in 2017 (Cons.)

Day	Jan	Feb	Mar	Apr	May	Jun	Jul	Aug	Sep	Oct	Nov	Dec
16	8.2	5.4	21.88	18	19.2	114	337.8	177.8	234.7	391.4	32.4	18.4
17	8.2	5.4	22.96	18.2	20	84.6	297	154.4	246.6	370.6	28.8	21
18	8.2	7.4	22.42	18.6	20.4	65.4	333.8	145.4	200.6	329.8	24.9	21
19	8.2	7.6	22.42	18.8	27.9	53	340.2	143.6	156.2	280.9	22.8	18.2
20	8.2	8.6	23.23	18.8	36.2	43	329.8	168.8	121.5	272.5	22.8	16
21	8.2	8.4	22.42	18.8	32.4	37.8	306.6	201.2	100	241	20.8	15
22	8.2	8.2	22.42	18.4	30.9	34.6	280.2	201.8	86	193.4	21.6	14.2
23	7	8.6	22.69	17.6	32.1	28.8	255	185.6	88.5	164.6	21.3	13
24	4	9.2	23.23	16.8	30	23.7	255	162.8	110.5	150.2	20.2	12.6
25	4	11.35	23.23	16.6	28.8	24.3	259.9	143	152.6	153.2	20	11.2
26	3.8	12.43	22.15	16.6	31.8	26.1	287.9	140	220	151.4	19	9.6
27	3.8	14.05	23.23	17.4	45.4	33.8	343.4	147.8	231.9	130.5	18	9.4
28	3.6	14.86	23.8	17.6	67.8	51.8	362.6	182	198.8	107.5	16.8	11.4
29	3.6		24.4	17.8	93	88.5	402.6	275.3	197.6	84.6	16	11.6
30	3.6		26.8	17.6	152	117.5	427.4	379.4	235.4	70.2	14	11.6
31	3.6		25.9		187.4		410.6	373.8		60.2		11.6
Total	7.06	6.45	21.11	18.35	35.35	123.3	265.89	268.07	177.73	312.91	27.2	14.81

Table 27 Daily Discharge (m3/s) at KGT3 station in 2018

Day	Jan	Feb	Mar	Apr	May	Jun	Jul	Aug	Sep	Oct	Nov	Dec
1	11.8	19.8	14.4	7.6	142.5	107.5	54.4	462	595.4	319.2	60.7	17.5
2	11.2	19.6	14.4	7.8	133.5	104	47.2	454	564.6	425	54.1	15.2
3	11.2	19.8	14.6	7.6	105	85	40.6	438	532.7	437	49.3	14.2
4	11	19.6	15	7.6	90.2	77.8	43	409	517.3	426	49	14
5	10.4	19.2	14.4	9	80.2	72.2	49.6	368.6	518.4	402	48.1	14
6	10.2	18.4	15	13.8	76.2	61.6	49.6	325.4	533.8	387	46.3	14
7	11.4	18	16.6	18.7	89	59.8	57.1	272.8	532.7	387	43.6	14.4
8	12.4	17.4	20	14.8	98	57.7	54.4	237.8	521.7	374	39.7	14.4
9	11.4	16.8	20.4	18.1	84.6	55.3	47.5	302.4	496	338.9	37	14.4
10	15.6	17.2	19	22	66.1	54.4	43.9	407	479	299.2	35.8	15.2
11	33.8	16.2	18	17.5	55.9	58.3	48.1	416	472	253.2	35.8	16
12	57.4	15.4	17	12	47.8	60.1	82.2	421	476	204.6	35.8	17.5
13	49	15.2	15.8	8.6	46.3	61.6	127.5	416	481	163.5	35.2	19.3
14	40.2	15.2	15.4	7.8	49.3	58	156.5	408	494	136	34.3	20.5
15	29.7	15	15.4	7.6	48.1	48.1	159	429	515.1	119	33.7	18.4

Table 27 Daily Discharge (m3/s) at KGT3 station in 2018 (Cons.)

Day	Jan	Feb	Mar	Apr	May	Jun	Jul	Aug	Sep	Oct	Nov	Dec
16	8.2	5.4	21.88	18	19.2	114	337.8	177.8	234.7	391.4	32.4	18.4
17	8.2	5.4	22.96	18.2	20	84.6	297	154.4	246.6	370.6	28.8	21
18	8.2	7.4	22.42	18.6	20.4	65.4	333.8	145.4	200.6	329.8	24.9	21
19	8.2	7.6	22.42	18.8	27.9	53	340.2	143.6	156.2	280.9	22.8	18.2
20	8.2	8.6	23.23	18.8	36.2	43	329.8	168.8	121.5	272.5	22.8	16
21	8.2	8.4	22.42	18.8	32.4	37.8	306.6	201.2	100	241	20.8	15
22	8.2	8.2	22.42	18.4	30.9	34.6	280.2	201.8	86	193.4	21.6	14.2
23	7	8.6	22.69	17.6	32.1	28.8	255	185.6	88.5	164.6	21.3	13
24	4	9.2	23.23	16.8	30	23.7	255	162.8	110.5	150.2	20.2	12.6
25	4	11.35	23.23	16.6	28.8	24.3	259.9	143	152.6	153.2	20	11.2
26	3.8	12.43	22.15	16.6	31.8	26.1	287.9	140	220	151.4	19	9.6
27	3.8	14.05	23.23	17.4	45.4	33.8	343.4	147.8	231.9	130.5	18	9.4
28	3.6	14.86	23.8	17.6	67.8	51.8	362.6	182	198.8	107.5	16.8	11.4
29	3.6		24.4	17.8	93	88.5	402.6	275.3	197.6	84.6	16	11.6
30	3.6		26.8	17.6	152	117.5	427.4	379.4	235.4	70.2	14	11.6
31	3.6		25.9		187.4		410.6	373.8		60.2		11.6
Total	7.06	6.45	21.11	18.35	35.35	123.3	265.89	268.07	177.73	312.91	27.2	14.81

Appendix C1 Discharge at KGT9 Station

Table 28 Daily Discharge (m3/s) at KGT9 station in 2011

Day	Jan	Feb	Mar	Apr	May	Jun	Jul	Aug	Sep	Oct	Nov	Dec
1	0	0	0	9	17.4	26.6	18.6	18	80.3	88	27.3	12.5
2	0	0	0	9.5	14.5	28.7	18	30.1	0	82.1	24.5	11
3	0	0	5.4	9.5	13	20.4	18	49.8	0	66.8	23.8	9
4	0	0	3.6	9	12.5	24.5	16.2	35	0	106	23.1	9
5	0	0	2.4	9	18.6	21	16.2	22.4	0	124	23.1	11.5
6	0	0	0.6	7.5	22.4	19.2	18.6	20.4	82.1	132.4	19.8	11.5
7	0	0	0	8.5	23.8	16.2	16.2	19.2	81.2	0	21.7	12
8	0	0	0	10	19.2	14	16.2	29.4	65	0	21.7	12
9	0	0	0	9.5	18.6	15.6	13.5	34.3	104	128.8	21.7	11.5
10	0	0	0	9.5	21.7	13.5	13.5	64.2	0	0	23.1	12
11	0	0	0	9.5	17.4	13.5	13.5	103	0	0	21	11.5
12	0	0	0	8	15	14.5	12.5	0	0	0	17.4	11.5
13	0	0	0	7	14.5	15.6	12.5	0	0	0	14	11.5
14	0	0	0	28	18.6	14	12	94	0	0	12.5	11.5
15	0	0	0	9	22.4	16.2	21	124	0	125.2	13	11.5

Table 28 Daily Discharge (m3/s) at KGT9 station in 2011 (Cons.)

Day	Jan	Feb	Mar	Apr	May	Jun	Jul	Aug	Sep	Oct	Nov	Dec
16	0	0	0	8.5	24.5	18.6	22.4	0	0	0	12.5	12
17	0	0	0	9	25.2	16.2	22.4	0	0	0	13.5	11.5
18	0	4.2	0	8.5	82.1	13.5	21	0	0	0	15	11
19	0	0.6	0	9	0	14.5	20.4	100	147.2	103	14	11
20	0	0	0	10.5	59.4	19.2	22.4	72.2	134.8	91	14.5	11
21	0	0	0	23.1	39.2	20.4	34.3	48.3	0	0	15.6	11
22	0	0	0	22.4	28	19.2	85	42	0	0	13	11
23	0	1.2	0	29.4	20.4	18.6	100	34.3	0	72.2	14	10.5
24	0	0.6	0	28.7	15.6	18	51.4	27.3	0	54.6	13	10.5
25	0	0	0	24.5	19.8	16.2	57.8	77.6	0	46.2	14	10.5
26	0	0	0	23.1	24.5	14.5	43.4	0	0	42	13.5	10
27	0	0	0	18.6	30.8	14	28.7	0	0	36.4	13	10
28	0	0	0	15	29.4	13.5	25.2	0	0	33.6	13	10.5
29	0		0	14.5	28.7	14.5	27.3	0	0	31.5	12.5	10
30	0		0	19.2	23.8	16.8	31.5	0	0	30.8	13	10
31	0		0		21.7		19.2	71.3		29.4		10.5
Total	0	0.24	0.39	13.88	23.96	17.37	27.38	36.03	23.15	45.94	17.06	10.98

Table 29 Daily Discharge (m3/s) at KGT9 station in 2012

Day	Jan	Feb	Mar	Apr	May	Jun	Jul	Aug	Sep	Oct	Nov	Dec
1	9	11	8.5	5.82	4.27	4.27	13.01	43.68	30.76	366	17.8	12.61
2	10	11	8.5	5.82	4.27	4.52	15.01	22	25.5	229.67	17.8	11.81
3	10	11	8.5	4.27	4.27	9.81	15.01	19	27.36	47.76	17.4	11.81
4	10.5	10.5	8.5	4.27	4.27	16.21	18.2	22.5	32.12	71	15.81	11.01
5	10	10.5	8.5	4.27	4.27	28.72	22	17	154.2	65.5	15.81	11.01
6	9	10.5	8.5	5.82	4.27	22	26	15.81	209	52.52	15.41	11.01
7	8.5	10.5	8.5	5.82	4.27	16.21	25	14.21	509	66.6	13.81	11.01
8	9	10	8.5	4.52	4.27	15.01	24.5	16.21	603.2	174.9	13.81	11.01
9	8.5	10	8.5	6.62	4.27	15.41	19.4	13.41	389	243	13.41	11.01
10	8.5	10	8.5	6.22	4.27	11.81	16.61	13.01	108.6	227	11.81	11.01
11	9	10	8.5	16.61	5.82	11.01	15.41	16.21	53.88	176.8	11.81	11.01
12	9	8.5	8.5	11.81	9.41	7.82	21	13.81	79.8	75.4	11.81	11.01
13	8.5	8.5	8.5	7.82	9.81	7.82	19.4	13.81	54.56	40.96	11.81	11.01
14	8.5	8.5	8.5	5.82	7.82	7.82	16.21	16.61	61.1	28.72	11.81	11.01
15	8.5	8.5	8.5	5.82	5.82	5.82	11.41	26.68	154.2	24.5	11.81	11.01

Table 29 Daily Discharge (m3/s) at KGT9 station in 2012 (Cons.)

Day	Jan	Feb	Mar	Apr	May	Jun	Jul	Aug	Sep	Oct	Nov	Dec
16	8	8.5	8.5	4.52	4.27	5.82	9.81	42.32	269.32	24.5	11.81	11.01
17	9.5	8.5	8.5	9.41	4.27	5.42	9.01	36.2	414	28.72	11.81	11.01
18	10.5	8.5	8.5	9.81	5.82	7.82	8.22	53.2	511.8	39.6	11.81	9.81
19	10.5	8.5	16.2	7.82	6.22	10.61	10.21	43	481	24.5	11.81	9.81
20	9.5	8.5	16.2	5.82	13.01	10.21	11.01	25.5	342.2	19	11.81	9.81
21	9.5	8.5	13.5	5.82	7.82	9.81	9.41	24	232	17.8	11.81	9.81
22	11	8.5	13.5	4.27	6.22	7.82	7.82	18.6	212	17.8	12.61	9.81
23	10.5	8.5	13.5	4.27	7.42	7.82	7.82	17.8	189.3	17.8	11.81	9.81
24	10	8.5	11	4.27	4.52	7.02	7.82	18.2	180.4	17.8	11.81	9.81
25	10.5	8.5	11	4.27	7.42	5.82	7.82	22	180	19.4	11.81	9.81
26	10	8.5	11	4.27	4.77	5.82	7.82	23	214	17.8	11.81	9.81
27	10.5	8.5	11	5.82	9.41	7.82	9.01	39.6	241	17.8	11.81	9.81
28	10	8.5	11	5.82	7.82	9.81	13.41	54.56	197	15.81	11.81	9.81
29	10	8.5	11	4.27	5.82	11.81	23	55.24	328.6	15.81	12.61	9.81
30	11		11	4.27	5.42	12.61	50.48	45.72	453.6	16.61	14.61	9.81
31	9.5		11		5.02		94.6	34.84		17.4		9.81
Total	9.58	9.24	10.13	6.2	6.02	10.34	18.24	27.02	231.28	71.56	13.12	10.57

Table 30 Daily Discharge (m3/s) at KGT9 station in 2013

Day	Jan	Feb	Mar	Apr	May	Jun	Jul	Aug	Sep	Oct	Nov	Dec
1	9.81	9.81	9.81	4.1	6.2	6.55	13.4	70.3	27.8	256.5	17.45	13.4
2	9.81	9.81	9.81	4.1	6.2	9.7	12.95	76.15	25.1	261.5	14.75	12.5
3	9.81	9.81	9.81	4.1	6.2	10.75	11.45	277	20.15	240	13.4	11.45
4	9.81	9.81	9.81	4.1	4.45	16.1	11.8	94.6	22.85	318.8	13.85	10.75
5	9.81	9.81	9.81	4.1	4.45	23.3	15.65	69.65	21.95	516.2	14.3	10.75
6	9.81	9.81	9.81	4.1	3.75	23.75	17.45	43.5	22.85	782	12.95	10.75
7	9.81	9.81	9.41	4.1	3.75	17	22.85	30.95	22.85	706.8	13.85	10.75
8	9.81	9.81	4.52	4.1	11.45	18.8	22.85	32.3	41.5	609.4	32.75	10.75
9	9.81	9.81	4.52	4.1	13.4	14.75	20.15	57	110	487.4	102.3	10.75
10	9.81	9.81	4.77	4.1	9.7	12.15	20.15	41	91.1	245.2	159.9	10.75
11	9.81	9.81	4.77	3.75	13.4	13.4	19.25	45.6	51	49.8	206	10.4
12	9.81	10.61	4.52	3.75	9.7	14.75	19.25	75.5	87.6	39	26.9	10.4
13	9.81	10.21	4.52	3.75	7.95	21.05	19.25	77.45	69	32.3	20.15	10.05
14	9.81	10.21	4.52	3.75	6.2	41.5	17	129.2	89.7	29.6	26	10.05
15	9.81	10.21	4.52	3.75	6.2	56.4	13.4	256.5	80.05	26	37	9.7

Table 30 Daily Discharge (m3/s) at KGT9 station in 2013 (Cons.)

Day	Jan	Feb	Mar	Apr	May	Jun	Jul	Aug	Sep	Oct	Nov	Dec
16	9.81	9.81	4.52	3.75	4.45	38.5	12.5	54.6	73.55	108.6	24.2	9.7
17	9.81	9.81	4.52	3.75	4.45	27.8	11.1	56.4	69.65	289.4	20.15	9.7
18	9.81	9.81	4.52	3.75	4.45	27.8	11.1	27.35	44	320.6	20.15	9.7
19	9.81	9.81	4.27	3.75	4.45	21.95	10.4	20.6	54	337.2	18.8	9.35
20	9.81	9.81	4.27	3.75	6.2	19.7	9.7	32.75	269.5	384.3	14.75	9
21	9.81	9.41	4.27	3.75	6.2	18.35	10.4	38.5	469.6	321.2	13.4	8.65
22	9.81	9.41	4.27	4.1	6.2	20.15	13.4	18.35	479	177	13.4	7.95
23	9.41	9.41	4.27	6.2	5.15	23.3	22.4	17.45	278.5	48.6	13.4	7.95
24	9.01	9.41	4.27	6.2	4.45	36.5	100.2	20.15	58.8	35	12.5	7.6
25	9.01	9.41	4.27	6.2	4.45	44	172	28.25	49.2	29.15	14.3	7.6
26	9.01	9.41	4.52	6.2	5.15	45	52.2	49.8	49.8	26.45	16.55	7.25
27	9.41	9.41	4.52	6.2	5.15	35.5	32.3	31.4	64.8	21.5	14.75	7.25
28	9.81	9.41	4.52	6.2	4.45	35.5	34.1	22.85	122	20.15	14.3	7.25
29	9.81		4.77	6.2	4.45	28.25	70.3	22.85	211.3	18.8	13.85	6.9
30	9.81		4.77	6.2	4.45	23.75	64.8	22.4	137.2	15.65	15.2	6.9
31	9.81		4.77		4.45		64.2	54.6		15.65		6.55
Total	9.71	9.77	5.69	4.53	6.18	24.87	30.58	61.13	107.15	218.38	31.71	9.44

Table 31 Daily Discharge (m3/s) at KGT9 station in 2014

Day	Jan	Feb	Mar	Apr	May	Jun	Jul	Aug	Sep	Oct	Nov	Dec
1	6.9	4.45	4.45	3	3.4	4.4	8.8	10.96	74.6	217.2	36.2	25.88
2	6.9	4.45	4.45	3	3.4	4.4	8	16.88	86.6	218.8	32.7	11.44
3	6.9	4.45	4.45	2.8	3.6	4.6	6.8	32.7	179.5	118.2	32	11.44
4	6.9	4.45	4.1	2.8	3.8	4.8	7.6	36.9	165	43.9	27.24	11.92
5	6.9	3.75	4.1	2.8	3.8	5	11.44	14.8	84.4	39	32.7	13.36
6	6.55	3.75	4.1	2.8	3.8	5.2	10.48	54.8	46	35.5	36.2	13.36
7	6.55	3.75	4.1	3	3.6	5	6.4	53.9	53.9	29.96	28.6	13.36
8	6.55	4.45	4.1	3	3.6	4.6	5.6	23.12	59.3	32.7	22.6	12.88
9	6.55	4.45	4.45	3.4	3.8	4.2	6.4	18.96	33.4	140.5	20.52	12.4
10	6.55	4.45	4.45	3.4	3.8	3.8	6.4	14.8	24.16	93.2	18.44	11.92
11	6.55	4.45	4.45	3.4	3.8	3.4	4.8	8.4	33.4	70.1	17.4	11.92
12	6.55	4.45	4.1	3.4	4	3.2	4.2	6.4	42.5	149.5	16.88	11.44
13	6.55	4.45	4.1	3.4	5	3.6	5.8	5.8	47.4	103.1	16.88	10.96
14	6.55	3.75	4.1	3.2	4.4	4.6	11.44	6	61.1	47.4	16.36	10.96
15	6.55	3.75	4.1	3.2	4.4	6.8	15.84	5.8	157.2	34.8	15.84	10.96

Table 31 Daily Discharge (m3/s) at KGT9 station in 2014 (Cons.)

Day	Jan	Feb	Mar	Apr	May	Jun	Jul	Aug	Sep	Oct	Nov	Dec
16	6.2	3.75	4.1	3.2	4.4	5.8	11.44	4.8	158.7	29.28	15.32	10.96
17	6.2	3.75	4.1	3.2	4.4	4.4	9.2	8.4	78.2	24.68	15.32	10.96
18	6.2	3.4	4.1	3.2	4.2	4.4	9.2	5.8	52.3	22.6	13.84	10.96
19	6.2	3.4	3.75	3	4.2	5.4	7.6	4.4	42.5	21.56	13.36	10.96
20	6.2	3.4	3.75	3	4	8.4	10.48	4.2	36.2	34.1	10.48	10.48
21	6.2	2.7	3.75	3	4	7.2	25.88	5.6	28.6	32	10.48	10.96
22	6.2	2.7	3.75	3.2	4	6	18.96	8	29.96	25.2	10.48	10.48
23	5.5	3.4	3.75	3.2	4	5.4	16.88	12.88	30.64	25.88	10.96	10.48
24	5.5	3.4	3.75	3.2	4.4	5.4	12.4	16.36	40.4	26.56	11.44	10.48
25	5.5	3.75	3.75	3.4	4	8.4	9.6	12.4	75.5	23.12	11.44	10.48
26	4.45	4.45	3.75	3.4	3.4	25.2	9.6	21.56	68.3	41.8	11.44	10.48
27	4.45	4.8	3.75	3.4	4	21.56	8.4	70.1	50.2	47.4	11.92	10
28	4.45	5.15	3.4	3.4	4.8	17.4	7.2	94.3	43.9	53.9	11.92	9.2
29	4.45		3.4	3.4	4.4	11.92	6.4	85.5	88.8	65.6	13.36	10.48
30	4.45		3.4	3.4	4	10.96	13.36	218.8	115.6	81.1	15.84	9.6
31	4.45		3.4		4		21.56	176.6		43.9		8.4
Total	6.02	3.98	3.98	3.17	4.01	7.18	10.26	34.19	69.61	63.63	18.61	11.6

Table 32 Daily Discharge (m3/s) at KGT9 station in 2015

Day	Jan	Feb	Mar	Apr	May	Jun	Jul	Aug	Sep	Oct	Nov	Dec
1	4.2	4	4	2.4	0	3	5.1	6.3	17	50	5.4	3.6
2	3.8	3.6	3.8	2.2	0	2.6	3.6	10.5	15	56.07	4.8	3.3
3	4.8	3.6	3.6	2.2	0	2.4	3.3	9.5	16	56.23	4.8	3
4	4.2	3.4	3.6	2.2	0	2.4	3.9	23.2	11.5	56.29	5.1	2.6
5	4.2	3.4	3.6	2	0	2.2	3	10	9.5	56.56	5.4	2.4
6	4.2	3.4	3.6	2	0	2	3	9	10	56.55	4.2	2.4
7	4.2	3.4	3.6	1.8	0	2	2.4	11	8.7	56.36	4.8	2.4
8	4.2	3.2	3.4	1.8	0	2	2.2	8.7	7.5	56.13	4.8	2.4
9	4.2	3.2	3.6	2	0	2	2.2	23.2	7.2	56.32	5.4	2.4
10	4.2	3.2	3.4	2	0	2.2	2.2	16.5	8.4	139.24	4.8	2.4
11	4.2	3.2	3.6	2	0	2.6	2.8	16.5	16.5	56.29	4.8	2.4
12	4	3.2	3.6	1.8	0	2.2	2.2	56.05	16.5	56.18	3.9	2.4
13	4	3.2	3.4	1.8	0	2	2.2	25.3	56	56.02	5.1	2.4
14	4	3.4	3.4	1.6	0	2.6	2.6	15	56.05	31.6	5.1	2.6
15	4	3.6	3.4	1.4	0	5.4	2.4	10.5	56.15	20.4	5.1	3.3

Table 32 Daily Discharge (m3/s) at KGT9 station in 2015 (Cons.)

Day	Jan	Feb	Mar	Apr	May	Jun	Jul	Aug	Sep	Oct	Nov	Dec
16	3.8	3.6	3.2	1.4	0	4.2	2.4	9	56.31	16	5.4	3.3
17	3.6	3.6	3.2	1.4	0	3.6	2.8	10	165.77	17	5.1	2.6
18	4.2	3.6	3.2	1.2	0	6.6	2.4	10.5	297.52	18	6.3	2.4
19	4	3.6	3.2	1.2	0.8	6.6	2.4	7.5	389.38	15.5	5.4	2.4
20	3.8	3.6	3.2	1	3.6	6.9	2.8	8.1	391.37	13	5.1	2.4
21	3.4	3.6	3.2	1	3.9	4.2	2.8	7.2	236	11	4.5	2.4
22	3.8	3.6	3	0.9	4.5	4.2	2.4	6.3	34.1	9.5	4.2	2.4
23	4.2	3.6	3	0.8	3	4.2	2.4	5.1	30.2	8.7	4.2	2.4
24	3.8	3.6	3	0.9	2.8	4.2	2.2	4.5	56.02	8.1	4.2	2.4
25	3.8	3.6	3.2	1	3.3	6.9	3	4.5	54.8	7.5	4.2	2.4
26	3.8	3.6	3.2	1	2.8	6.9	2.8	5.1	47.6	6.9	3.9	2.4
27	4.2	3.6	3.2	1.2	2.6	8.7	2.4	5.7	45.2	5.7	3.9	3.9
28	5	3.8	3.2	1.4	2.8	7.5	2.4	11	45.2	5.4	3.9	3.9
29	8.4		3.2	0.9	2.8	6.9	2.8	17.5	52.4	5.1	3.9	4.2
30	9.2		3	0.3	2.8	6	3.9	16	52.4	4.2	3.9	4.2
31	10.96		3.2		3		4.8	23.9		5.7		4.2
Total	4.59	3.5	3.35	1.49	1.25	4.17	2.83	13	75.54	32.82	4.72	2.84

Table 33 Daily Discharge (m3/s) at KGT9 station in 2016

Day	Jan	Feb	Mar	Apr	May	Jun	Jul	Aug	Sep	Oct	Nov	Dec
1	4.2	6.9	6.3	2.5	2.5	1.9	5.1	31.2	24.8	63	45.4	2.6
2	4.2	6.9	5.4	2.6	2.3	1.9	14.2	29.6	21.2	72.9	55.3	2.3
3	3.9	6.6	5.1	2.6	2.3	1.9	6	24.8	21.2	92.7	44.3	2.8
4	4.2	6.6	5.1	3	2.2	1.9	8	25.6	19.1	152.2	34.7	3
5	4.2	6.6	5.1	2.8	2.2	1.9	13.5	57.5	17	275	23.3	5.7
6	4.2	6.6	5.1	2.7	2.2	1.9	45.4	92.7	14.2	186.5	18.4	4.2
7	4.2	6.9	5.1	2.7	2.2	2	69.6	79.5	10.7	101.5	17.7	6.8
8	4.2	6.6	5.1	2.6	2.3	1.9	113.5	83.9	10	61.9	14.2	9.2
9	4.2	6.9	5.1	2.6	2.2	1.9	63	65.2	10	44.3	24	6.8
10	4.2	6.9	4.8	2.6	2.1	2	26.4	50.9	10	80.6	29.6	6
11	4.2	6.9	4.8	2.6	2.1	2	12.8	50.9	9.6	64.1	48.7	7.2
12	4.2	6.9	4.8	2.6	2.1	1.9	29.6	91.6	9.2	58.6	49.8	8
13	4.5	6.9	4.8	2.5	2.4	1.9	42.1	66.3	9.6	78.4	34.7	9.2
14	4.5	6.3	4.8	2.5	2.3	1.9	102.6	40.1	11.4	107.1	25.6	6
15	5.7	6.6	4.8	2.6	2.2	2	70.7	32	12.1	48.7	19.1	7.2

Table 33 Daily Discharge (m3/s) at KGT9 station in 2016 (Cons.)

Day	Jan	Feb	Mar	Apr	May	Jun	Jul	Aug	Sep	Oct	Nov	Dec
16	6.6	6.9	4.8	2.5	2.1	2.1	68.5	27.2	10.7	33.8	16.3	6.8
17	6.9	6.6	4.8	2.5	2.3	2	33.8	28.8	12.1	69.6	17	5.7
18	7.2	6.6	4.8	2.5	2.4	1.9	14.9	25.6	21.9	94.9	14.2	6.8
19	6.3	6.6	4.8	2.4	2.3	1.9	12.8	25.6	27.2	43.2	14.9	5.4
20	7.2	6.6	4.8	2.5	2.4	2	18.4	20.5	61.9	26.4	13.5	3
21	6.9	6.6	4.8	2.6	2.7	2.5	24.8	19.1	89.4	21.9	19.8	6.4
22	6.9	6.6	4.8	2.3	2.6	2.2	18.4	18.4	28.8	21.2	24.8	5.7
23	6.9	6.6	4.8	2.5	2.2	2.1	12.1	17	34.7	17.7	18.4	8
24	6.9	6.6	4.8	2.5	1.9	2.1	11.4	19.8	99.3	17	13.5	6.4
25	6.9	6.3	4.8	2.5	2	2	11.4	43.2	107.9	20.5	9.6	5.7
26	6.9	6.3	4.8	2.5	2.1	2.1	9.2	45.4	59.7	28.8	7.6	5.7
27	6.9	6.3	4.8	2.5	2.2	2.4	11.4	40.1	53.1	22.6	5.1	4.5
28	6.9	6.3	4.8	2.4	2.3	2.8	12.8	31.2	109.75	25.6	5.4	4.5
29	6.9	6.3	4.8	2.5	2	2.5	17.7	26.4	119.4	24.8	4.2	4.8
30	6.9		4.8	2.5	2	2.3	20.5	24.8	103.7	26.4	3.3	4.5
31	6.9		4.5		2		19.1	24		37.4		4.2
Total	5.64	6.63	4.93	2.56	2.23	2.06	30.31	40.61	38.32	65.14	22.41	5.65

Table 34 Daily Discharge (m3/s) at KGT9 station in 2017

Day	Jan	Feb	Mar	Apr	May	Jun	Jul	Aug	Sep	Oct	Nov	Dec
1	4.5	3.3	2.7	5	3.5	73	17.5	27.2	36.8	15.5	2.5	6
2	4.5	3	2.7	5.5	3	38.4	15	31.2	33.6	19	1.5	5
3	4.5	3.3	2.7	5.5	3	35.2	14	32	21.6	26.4	4.5	5
4	4.8	3	2.7	8	3	43.2	80	65	15.5	152.3	3.5	4.5
5	4.8	3	2.7	6	3	87.28	112.88	50	12	128.24	2	4
6	4.8	2.9	2.7	6.5	3	71	97.52	43.2	11.5	46	2.5	3.5
7	4.8	3.9	2.5	7	3.5	49	105.2	49	11.5	39.2	9	2
8	4.8	3.9	2	7.5	3.5	91.12	45	67	11.5	32.8	9	1
9	4.8	3.3	2.2	7.5	4	105.2	28	54	11.5	37.6	6.5	3.5
10	4.8	3.3	2.7	6	4.5	72	25.6	52	20.8	25.6	3	3
11	4.5	3	2.7	2	5	55	21.6	38.4	46	38.4	0.5	3.5
12	4.5	3	2.6	3.5	4	43.2	28	42.4	29.6	56	0	1.5
13	4.5	3	2.5	3	5	32.8	27.2	41.6	17	34.4	6.5	1
14	4.8	3	2.3	4.5	10.5	31.2	25.6	29.6	13.5	70	11	5
15	4.8	3	2.6	6.5	10	34.4	39.2	22.4	16.5	133.36	9	5.5

Table 34 Daily Discharge (m3/s) at KGT9 station in 2017 (Cons.)

Day	Jan	Feb	Mar	Apr	May	Jun	Jul	Aug	Sep	Oct	Nov	Dec
16	4.8	3	2.9	6	9	27.2	28	15.5	12	50	6	6
17	4.8	3	2.7	3	15	22.4	17.5	16.5	11	20	5	5.5
18	4.5	3	2.5	5.5	24.8	19.5	20	14.5	10.5	47	4	5.5
19	4.2	3	2.7	4.5	16.5	18.5	37.6	15	10	75.2	4	5.5
20	3.9	3	2.7	4	16	18.5	36	19.5	10	25.6	5.5	5.5
21	3.6	3	2.7	3.5	19.5	16.5	49	28.8	15.5	19	6.5	5
22	3.3	3	2.5	3.5	18	14	105.2	17	19	17	7.5	1.5
23	3	3	2.3	3.5	14	13.5	129.52	12.5	26.4	20	7.5	0.5
24	2.9	2.9	2.8	4	18.5	11	57	8.5	152.3	28.8	7.5	0
25	2.7	2.8	3	3.5	17.5	10.5	30.4	7.5	128.24	19.5	8	3
26	2.7	2.7	3	3.5	17	14.5	33.6	18.5	46	17	7	5.5
27	2.7	2.7	3	3.5	18	34.4	119.28	41.6	39.2	12	8	5.5
28	3	2.7	3	3.5	76.4	105.2	124.4	24.8	32.8	8	6.5	4
29	4.2		3	3.5	150.05	63	61	42.4	37.6	6.5	3	3.5
30	4.2		3	3	73	32	58	64	25.6	5	7	3
31	3.9		3		48		39.2	41.6		5		3.5
Total	4.15	3.06	2.68	4.73	19.99	42.76	52.52	33.33	29.5	39.69	5.47	3.77

Table 35 Daily Discharge (m3/s) at KGT9 station in 2018

Day	Jan	Feb	Mar	Apr	May	Jun	Jul	Aug	Sep	Oct	Nov	Dec
1	3.5	1.5	1.5	7.5	42.4	57	17.4	144.8	27.6	46.4	10.5	8.1
2	3	1	1	9	36.8	46.4	16.2	86	22.2	63	10.8	7.5
3	3	1	0.5	9	31.2	51.2	16.2	56	19.2	39.2	12	8.4
4	3	1	0.5	9	28.8	34.8	19.8	50.4	134	36	12	8.7
5	3	1	0.5	9.3	36.8	35.4	30.6	48.8	171.6	98	9.9	7.8
6	3	0.5	1	11.4	48	40.8	34.2	63	89	108.8	7.5	8.7
7	4	1	0.5	13.2	49.6	31.2	29.4	55	43.2	54	8.1	8.4
8	3.5	1	0	21	37.6	31.2	24.6	110	46.4	41.6	9	7.8
9	3	0.5	1.5	13.8	30.6	30.6	20.4	150	99.2	51.2	10.5	9.6
10	4	1	1	10.5	27	30.6	29.4	129.2	104	35.4	11.1	9
11	4	1	0.5	9.6	24	30	55	79	66	21	11.1	8.4
12	6.5	1	0.5	8.7	28.2	30	53	62	75	14.4	11.4	10.2
13	6	1	0.5	9.6	27.6	26.4	41.6	52	80	13.8	11.4	8.1
14	5	1	0.5	10.2	25.8	24.6	30.6	52	116	13.2	11.4	9.3
15	4	1	0.5	9.9	27.6	25.2	40	90	248.9	14.4	11.1	8.7

Table 35 Daily Discharge (m3/s) at KGT9 station in 2018 (Cons.)

Day	Jan	Feb	Mar	Apr	May	Jun	Jul	Aug	Sep	Oct	Nov	Dec
16	4	0.5	0	9.9	24.6	29.4	36.8	187.6	203.8	16.2	11.1	8.4
17	3.5	0.5	0	10.8	22.8	38.4	41.6	152.4	76	15.6	10.8	9
18	3.5	1	1.5	69	24	36.8	92	86	56	11.7	10.8	7.2
19	3	1	1	72	33	30.6	92	68	41.6	141.2	10.8	9
20	3	1	1	22.2	39.2	29.4	53	64	35.4	136.4	16.2	7.5
21	2	1	0.5	24	35.4	25.8	36	90	41.6	65	10.8	19.2
22	1	1	0.5	13.2	71	23.4	27	160	37.6	92	6.9	9
23	1	2	0.5	11.7	91	24	27	155.2	32.4	49.6	6.9	8.4
24	1	2.5	0.5	11.4	57	21	69	94.4	33.6	30	6.6	6.6
25	1	2.5	0.5	10.8	70	19.2	58	59	71	27.6	5.4	5.4
26	1	1.5	0.5	9.6	62	14.4	57	44.8	46.4	24	6.9	7.5
27	1	1.5	0.5	11.1	54	17.4	47.2	66	34.2	22.8	6.9	5.7
28	1.5	2.5	0.5	20.4	44.8	21	76	152	29.4	19.2	8.1	7.8
29	1.5		0.5	122	43.2	24	101.6	130.4	20.4	14.4	7.2	7.2
30	1		0.5	92	82	19.8	105.2	61	24.6	12.6	7.2	6.9
31	1		0.5		83		151.6	35.4		11.4		8.4
Total	2.85	1.18	0.63	22.39	43.19	30	49.34	91.43	70.88	43.23	9.68	8.45